

# Amortised and provably-robust simulation-based inference

Ayush Bharti<sup>1,\*</sup> Charita Dellaporta<sup>2,\*</sup> Yuga Hikida<sup>1</sup> François-Xavier Briol<sup>2</sup>

<sup>1</sup>Department of Computer Science, Aalto University, Finland

<sup>2</sup>Department of Statistical Science, University College London, UK

Corresponding author: [ayush.bharti@aalto.fi](mailto:ayush.bharti@aalto.fi)

## Abstract

Complex simulator-based models are now routinely used to perform inference across the sciences and engineering, but existing inference methods are often unable to account for outliers and other extreme values in data which occur due to faulty measurement instruments or human error. In this paper, we introduce a novel approach to simulation-based inference grounded in generalised Bayesian inference and a neural approximation of a weighted score-matching loss. This leads to a method that is both amortised and provably robust to outliers, a combination not achieved by existing approaches. Furthermore, through a carefully chosen conditional density model, we demonstrate that inference can be further simplified and performed without the need for Markov chain Monte Carlo sampling, thereby offering significant computational advantages, with complexity that is only a small fraction of that of current state-of-the-art approaches.

## 1 Introduction

Simulation-based inference (SBI, [Cranmer et al. \(2020\)](#)) has emerged as a powerful framework for addressing complex Bayesian inference problems where likelihood functions are intractable but simulation is feasible. Its flexibility and scalability have led to widespread adoption in domains such as particle physics ([Brehmer, 2021](#)), epidemiology ([Kypraios et al., 2017](#)), wireless communications ([Bharti et al., 2022a](#)), and cosmology ([Alsing et al., 2018; Jeffrey et al., 2021](#)). In particular, recent advances have focused on conditional density estimation, often enabling amortised inference where a model trained once can be reused for multiple observations ([Zammit-Mangion et al., 2025](#)).

Despite these successes, a major challenge remains: SBI methods often lack robustness to model misspecification ([Cannon et al., 2022; Nott et al., 2024; Kelly et al., 2025](#)), which can arise from corrupted or incomplete data, outliers, or inadequacies in the simulator. The recent review of [Martin et al. \(2024\)](#) identifies misspecification as one of the most urgent open problems in Bayesian computation, while [Hermans et al. \(2022\)](#) caution that over-confident posteriors, an issue amplified by misspecification, are at risk of precipitating a broader crisis of trust in SBI. Such is the current interest in this open challenge that [Dellaporta et al. \(2022\)](#) were awarded the Best Paper Award at AISTATS 2022 for making concrete progress toward its resolution.

Unfortunately, whilst various approaches have been proposed, they either *lack formal robustness guarantees* ([Ward et al., 2022; Bharti et al., 2022b; Huang et al., 2023; Gloeckler et al., 2023; Gao et al., 2023; Quera-Bofarull et al., 2023; Dyer et al., 2023; Wehenkel et al., 2025; Kelly et al., 2024; Wu et al., 2024; Swierc et al., 2024; Mishra et al., 2025; Verma et al., 2025; Senouf et al., 2025; O’Callaghan et al., 2025; Ruhlmann et al., 2025; Sadasivan et al., 2025; Elsemüller et al., 2025; Mao et al., 2025; Sun et al., 2026](#)), *are incompatible with amortised inference* ([Briol](#)

---

\*Equal contribution.

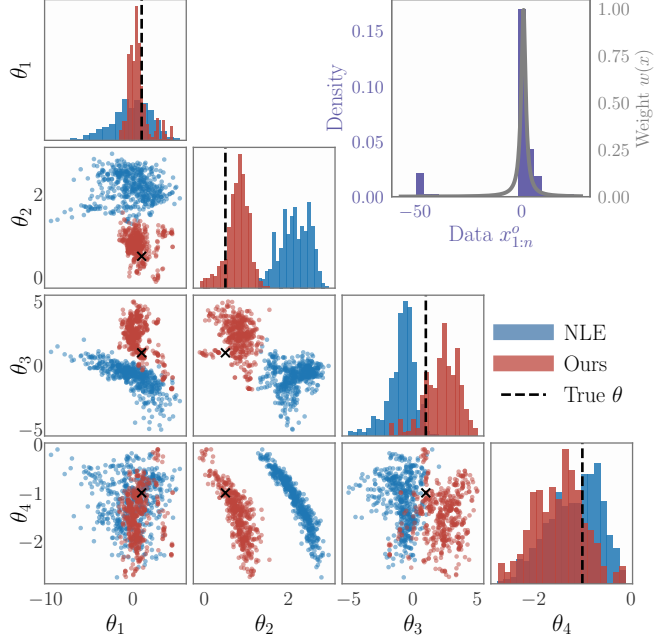


Figure 1: **Amortised SBI in the presence of outliers.** With a few one-sided outliers (10%) in the observed data (■), shown in the top-right plot, the neural likelihood estimation (NLE ■) posterior of the g-and-k distribution is significantly impacted, specifically parameters  $\theta_2$  and  $\theta_3$  that govern the scale and skewness of the distribution (details in Section 5.1). In contrast, our proposed method, named neural score-matching Bayes (■), is robust as we use the function  $w(x)$  (■) to down-weight the effect of the outliers.

et al., 2019; Kisamori et al., 2020; Frazier et al., 2020; Fujisawa et al., 2021; Dellaporta et al., 2022; Frazier et al., 2025; Thomas et al., 2025; Pacchiardi et al., 2024; Legramanti et al., 2022), or both. Apart from lacking robustness guarantees, some of these existing methods also require side information in the form of additional data to achieve robustness (Wehenkel et al., 2025; Senouf et al., 2025; Mishra et al., 2025), and therefore have more limited applicability.

We introduce a method that addresses these shortcomings and is specialised for robustness to outliers. Our method is centred around the score-matching objective of Hyvärinen (2006) and resembles the two-step approach of neural likelihood estimation (NLE, Papamakarios et al. (2019)). The first step consists of training a *neural* conditional density model using simulated data, typically implemented via a flexible architecture such as a normalising flow (Papamakarios et al., 2021) or an energy-based model. The second step corresponds to updating prior beliefs using generalised Bayesian inference (Bissiri et al., 2016) with a weighted score-matching (SM) loss (Altamirano et al., 2023) evaluated on the observed data and approximated with the aforementioned neural surrogate. This results in *neural score-matching Bayes* (NSM-Bayes), a method that is both amortised and provably-robust to outliers. This is illustrated in Figure 1 for a g-and-k simulator, where the NLE posterior is severely biased in the presence of outliers, whilst NSM-Bayes remains centred around the correct parameter value.

We propose two versions of our approach. The first version (Section 3.1) is the most general, wherein any flexible conditional density model and prior can be used, akin to NLE. The second version is a conjugate special case of NSM-Bayes, termed *NSM-Bayes-conj* (Section 3.2). NSM-Bayes-conj considers Gaussian priors and restricts the flexibility of the conditional density model to a specific form of energy-based model, resulting in substantial reductions in the computational cost of inference. In Section 4, we present theoretical guarantees that these two methods are robust to outliers, providing the first such guarantees for amortised SBI methods. In Section 5, we then consider simulators from epidemiology and telecommunications engineering and demonstrate

that our methods provide reliable inference under the presence of outliers, with NSM-Bayes-conj simultaneously leading to significant computational cost savings at inference time.

## 2 Background

Let  $\mathcal{X} = \mathbb{R}^{d_X}$  be some domain and  $\mathcal{P}(\mathcal{X})$  be the space of probability distributions on  $\mathcal{X}$ . We consider Bayesian inference for some parameter  $\theta \in \Theta \subseteq \mathbb{R}^{d_\Theta}$  of a model  $\{\mathbb{P}_\theta\}_{\theta \in \Theta} \subset \mathcal{P}(\mathcal{X})$  with (typically unknown) density  $p(\cdot|\theta)$ , based on some independent and identically distributed (iid) observed data  $x_{1:n}^o = \{x_1^o, \dots, x_n^o\} \in \mathcal{X}^n$  obtained from the (unknown) data-generating process  $\mathbb{P}_0 \in \mathcal{P}(\mathcal{X})$  with density  $p_0$ , which we assume for now to be uncorrupted. Assuming a prior density  $\pi(\theta)$ , the posterior density is

$$\pi(\theta|x_{1:n}^o) \propto \prod_{i=1}^n p(x_i^o|\theta) \pi(\theta). \quad (1)$$

We now briefly review approximate Bayesian (Section 2.1) and generalised Bayesian (Section 2.2) inference methods for simulators, with an emphasis on amortisation and robustness.

### 2.1 Approximate Bayesian Inference for Simulators

In simulation-based inference (SBI; also called likelihood-free inference), performing exact Bayesian inference is not feasible since the density  $p(\cdot|\theta)$  (or equivalently, the likelihood) is intractable, typically due to unobserved latent variables or the computational cost of evaluation. Instead, we assume one can simulate data from this model for any parameter value through a simulator, and we then use such simulations to construct an approximate posterior. The most established SBI approach is approximate Bayesian computation (ABC, [Beaumont \(2019\)](#)), which can be made robust; see [Kisamori et al. \(2020\)](#); [Frazier et al. \(2020\)](#); [Fujisawa et al. \(2021\)](#); [Legramanti et al. \(2022\)](#). Another approach is Bayesian synthetic likelihood ([Price et al., 2018](#)), whose robustness has been extensively studied in the works of [Frazier and Drovandi \(2021\)](#); [Frazier et al. \(2025\)](#). Finally, [Dellaporta et al. \(2022\)](#) proposed to use the posterior bootstrap of [Lyddon et al. \(2018\)](#); [Fong et al. \(2019\)](#) with the minimum distance estimator from [Briol et al. \(2019\)](#) to get a robust non-parametric posterior which is highly parallelisable. Although most of these approaches are provably-robust to outliers, they unfortunately *do not permit amortisation*; i.e. given new observations, the entire method needs to be re-run to obtain an approximate posterior, which can be extremely computationally demanding.

Neural likelihood estimation (NLE, [Papamakarios et al. \(2019\)](#); [Lueckmann et al. \(2019\)](#); [Boelts et al. \(2022\)](#); [Radev et al. \(2023\)](#)) is an alternative approach to SBI. It consists of (i) using a conditional density model based on some parametric class  $\{q_\phi(\cdot|\theta)\}_{\phi \in \Phi}$  with  $\Phi \subseteq \mathbb{R}^{d_\Phi}$  (typically based on a neural network; e.g. a mixture density network or normalising flow) to estimate  $p(\cdot|\theta)$  for any  $\theta \in \Theta$ , then (ii) replacing the unknown likelihood with the fitted model to perform Bayesian inference. Step (i) is performed by obtaining samples  $\{(\theta_i, x_i)\}_{i=1}^m$  through simulating parameter values from the prior  $\theta_i \sim \pi$ , then simulating data from the simulator  $x_i \sim \mathbb{P}_{\theta_i}$ . Given these simulations, the optimal value  $\phi \in \Phi$  is usually obtained by minimising the empirical negative log-likelihood loss:

$$\hat{\phi}_m := \arg \min_{\phi \in \Phi} -\frac{1}{m} \sum_{i=1}^m \log q_\phi(x_i|\theta_i). \quad (2)$$

Given  $\hat{\phi}_m$ , step (ii) consists of replacing  $p(\cdot|\theta)$  by  $q_{\hat{\phi}_m}(\cdot|\theta)$  in Equation (1) and approximating this posterior, denoted  $\pi_{\text{NLE}}(\theta|x_{1:n}^o, \hat{\phi}_m)$ , typically through Markov chain Monte Carlo (MCMC, [Robert and Casella \(2000\)](#)). NLE is often called *partially amortised* since inference on a new set of observations only requires the MCMC step (i.e. step (ii)), without the need to re-train  $q_\phi$ .

from scratch (i.e. we do not have to repeat step (i)). Moreover, a new observation  $x_{n+1}^o \in \mathcal{X}$  can be included simply by adding a term  $q_{\hat{\phi}_m}(x_{n+1}^o | \theta)$  in step (ii), which again requires no additional simulation. Alternatively, neural posterior estimation (NPE, (Papamakarios and Murray, 2016; Lueckmann et al., 2017; Greenberg et al., 2019; Radev et al., 2022)) approximates the posterior directly using conditional density models, and is thus called *fully amortised* as it does not require any MCMC post-training.

Several neural SBI methods have been shown *empirically* to provide robustness to model misspecification. These are based on explicit modelling of the misspecification (Ward et al., 2022; Kelly et al., 2024; Verma et al., 2025; O’Callaghan et al., 2025), penalisation of the learning objectives (Huang et al., 2023; Gloeckler et al., 2023), or side information (Wehenkel et al., 2025; Mishra et al., 2025; Krouglova et al., 2025; Hikida et al., 2025). Unfortunately, *none of these methods have theoretical guarantees of robustness to outliers* or other forms of model misspecification.

Although less directly relevant to our paper, we note that an interesting complementary line of work has investigated diagnostics for prior or simulator misspecification, including formal tests (Key et al., 2021; Ramírez-Hassan and Frazier, 2024) and empirical checks (Leclercq, 2022; Elsemüller et al., 2024; Schmitt et al., 2024; Anau Montel et al., 2025; Yuyan et al., 2025).

## 2.2 Generalised Bayesian Inference for Simulators

An alternative to Bayesian inference which can provide robustness is generalised Bayesian Inference (GBI) (Bissiri et al., 2016; Knoblauch et al., 2022). This consists of updating beliefs through an empirical loss function  $\mathcal{L} : \Theta \times \mathcal{X}^n \rightarrow \mathbb{R}$  computed for the observed data  $x_{1:n}^o$ :

$$\pi_{\mathcal{L}}(\theta | x_{1:n}^o) \propto \exp(-\beta n \mathcal{L}(\theta; x_{1:n}^o)) \pi(\theta), \quad (3)$$

where  $\beta > 0$  is a temperature/learning rate parameter (Wu and Martin, 2023) which weights the relative importance of the loss and the prior. Several special cases are of interest:  $\mathcal{L}_{\text{Bayes}}(\theta; x_{1:n}^o) := -\frac{1}{n} \sum_{i=1}^n \log p(x_i^o | \theta)$  and  $\beta = 1$  recovers standard Bayesian inference as given in Equation (1),  $\mathcal{L}_{\text{NLE}}(\theta; x_{1:n}^o, \hat{\phi}_m) := -\frac{1}{n} \sum_{i=1}^n \log q_{\hat{\phi}_m}(x_i^o | \theta)$  with  $\beta = 1$  recovers NLE (as well as Bayesian synthetic likelihoods, which can be viewed as a special case), and Schmon et al. (2020) showed how to recover ABC by marginalising a generalised posterior on an extended space.

However, none of these losses provide robustness to model misspecification, and alternative robust losses that have been proposed for SBI have significant limitations. Matsubara et al. (2022, 2024) showed that loss functions based on score-based discrepancies are well-suited to performing GBI with intractable likelihoods, but their approach still requires access to an unnormalised expression of the likelihood. Pacchiardi et al. (2024) showed that kernel-based scoring-rule losses give posteriors akin to the maximum mean discrepancy (MMD) Bayes posterior of Chérief-Abdellatif and Alquier (2020) and can resolve this limitation. Unfortunately, their approach requires the use of advanced Monte Carlo methods which can be hard to tune, and it is also not amortised. Gao et al. (2023) proposed a method that amortises MMD-Bayes across different observed datasets available during training, but their method has no formal robustness guarantees. Concurrently to the present paper, Sun et al. (2026) proposed a power-posterior version of NPE, but power-posteriors are not provably robust to outliers and have the downside that they equally downweight corrupted and uncorrupted observations. These limitations leave open the question of how to construct an amortised SBI method which is provably robust.

## 3 Methodology

We now present our novel approach, called neural score-matching Bayes (NSM-Bayes). A key tool used for this is the score matching (SM) divergence, which was popularised for parameter estimation by Hyvärinen (2006), and further extended by Hyvärinen (2007); Lyu (2009); Barp

et al. (2019); Yu et al. (2019, 2022); Xu et al. (2022). We use the weighted (or ‘diffusion’) SM divergence of Barp et al. (2019) as the weights will give us the additional flexibility needed to achieve robustness. For two densities  $p, q$  on  $\mathcal{X} = \mathbb{R}^{d_X}$  and an invertible matrix-valued weight function  $W : \mathcal{X} \rightarrow \mathbb{R}^{d_X \times d_X}$ , this is given by:

$$\text{SM}_W(p||q) := \mathbb{E}_{X \sim p} \left[ \left\| W(X)^\top (\nabla_x \log q(X) - \nabla_x \log p(X)) \right\|_2^2 \right]. \quad (4)$$

This divergence is well-defined when  $p$  and  $q$  are positive and continuously differentiable,  $\nabla_x \log p - \nabla_x \log q \in L^2(q)$ , and the weight  $W$  is bounded and continuously differentiable. Although we operate on  $\mathbb{R}^{d_X}$  throughout, these conditions can be extended to bounded domains (see Altamirano et al., 2023, Appendix B.5). Under certain regularity conditions on  $p$  and  $q$  (Barp et al., 2019) and using integration-by-parts, the SM divergence can be expressed as:

$$\text{SM}_W(p||q) = \mathbb{E}_{X \sim p} \left[ \left\| W(X)^\top \nabla_x \log q(X) \right\|_2^2 + 2 \nabla_x \cdot (W(X) W(X)^\top \nabla_x \log q(X)) \right] + C_p, \quad (5)$$

where  $C_p \in \mathbb{R}$  is a constant with respect to  $q$ . This expression of the SM divergence forms the basis of our NSM-Bayes (Section 3.1) and NSM-Bayes-conj (Section 3.2) method. In Section 3.3, we discuss how to select the hyperparameters of our method.

### 3.1 Neural Score-matching Bayes for Simulation-based Inference

We first present the most general case of our method, and assume the observed data  $x_{1:n}^o \sim \mathbb{P}_0$  may contain outliers which can arbitrarily bias the standard Bayes posterior. One way to obtain robustness is through a specific form of GBI called weighted SM-Bayes (Altamirano et al., 2023, 2024; Reimann, 2024; Laplante et al., 2025a; Rooijakkers et al., 2025; Ezzerg et al., 2025), which is inspired by the score-based approach to generalised Bayes of Matsubara et al. (2022, 2024):

$$\pi_{\text{SM}}(\theta | x_{1:n}^o) \propto \exp(-\beta n \mathcal{L}_{\text{SM}}(\theta; x_{1:n}^o)) \pi(\theta). \quad (6)$$

Here, the loss function  $\mathcal{L}_{\text{SM}}(\theta; x_{1:n}^o)$  can be expressed as:

$$\mathcal{L}_{\text{SM}}(\theta; x_{1:n}^o) := \frac{1}{n} \sum_{i=1}^n \left\| W(x_i^o)^\top \nabla_x \log p(x_i^o | \theta) \right\|_2^2 + 2 \nabla_x \cdot (W(x_i^o) W(x_i^o)^\top \nabla_x \log p(x_i^o | \theta)). \quad (7)$$

This corresponds to a Monte Carlo estimator of  $\text{SM}_W(p_0 || p(\cdot | \theta))$ , based on Equation (5), up to the additive constant which can be dropped from the loss term since it can be incorporated into the normalisation constant of the SM-Bayes posterior. Throughout this paper, we will assume the following about the matrix-valued weight function  $W$ :

**Assumption A1.**  $W(x) := w(x) I_{d_X}$  for some  $w : \mathcal{X} \rightarrow \mathbb{R}_+$  and  $d_X$ -dimensional identity matrix  $I_{d_X}$ ,  $\sup_{x \in \mathcal{X}} w(x) < \infty$  and  $\sup_{x \in \mathcal{X}} \|\nabla_x w(x)\|_2 < \infty$ .

The diagonal form of  $W$  is the most common choice in practice (Altamirano et al., 2024), and the boundedness of  $w$  and  $\nabla w$  are mild regularity conditions necessary to guarantee robustness, as formalised in Section 4. Though we recommend a specific  $W$  satisfying A1 later in the section, we keep the presentation general. In SBI, the exact SM loss is intractable since  $p(\cdot | \theta)$  is itself intractable. However, assuming we have a surrogate  $q_{\hat{\phi}_m}(\cdot | \theta)$  satisfying certain regularity conditions, this loss can be easily approximated.

**Assumption A2.** For all  $\phi \in \Phi$ ,  $q_\phi(\cdot | \theta)$  is a twice-differentiable density and  $p_0(\cdot) w(\cdot)^2 \nabla_x \log q_\phi(\cdot | \theta), \nabla_x \cdot (p_0(\cdot) w(\cdot)^2 \nabla_x \log q_\phi(\cdot | \theta))$  are integrable on  $\mathbb{R}^{d_X}$ .

Under [A1](#) and [A2](#), we call this approximation the *neural SM* (NSM) loss, and it is given by

$$\begin{aligned}\mathcal{L}_{\text{NSM}}(\theta; x_{1:n}^o, \hat{\phi}_m) := & \frac{1}{n} \sum_{i=1}^n w(x_i^o)^2 \left\| \nabla_x \log q_{\hat{\phi}_m}(x_i^o | \theta) \right\|_2^2 + 2 \left( \nabla_x w(x_i^o)^2 \right)^\top \nabla_x \log q_{\hat{\phi}_m}(x_i^o | \theta) \\ & + 2w(x_i^o)^2 \text{Tr} \left( \nabla_x^2 \log q_{\hat{\phi}_m}(x_i^o | \theta) \right).\end{aligned}\quad (8)$$

Doing GBI with  $\mathcal{L}_{\text{NSM}}$  results in our neural-surrogate approximation of SM-Bayes, called *NSM-Bayes*:

$$\pi_{\text{NSM}}(\theta | x_{1:n}^o, \hat{\phi}_m) \propto \exp \left( -\beta n \mathcal{L}_{\text{NSM}}(\theta; x_{1:n}^o, \hat{\phi}_m) \right) \pi(\theta) \quad (9)$$

Thus, similarly to NLE, our NSM-Bayes approach proceeds in two steps: we first train a conditional density model  $q_\phi$  using simulated data  $\{(\theta_i, x_i)\}_{i=1}^m$ , and then update prior beliefs using the NSM loss in Equation (9). Importantly, we do not put any restrictions on how  $q_\phi$  is selected or how  $\hat{\phi}_m$  has been obtained. In our experiments,  $q_\phi$  will either be a mixture density network (MDN) ([Bishop, 1994](#)) or a normalising flow, e.g. a masked autoregressive flow (MAF) ([Papamakarios et al., 2017](#)) trained through Equation (2), but any alternative model where the score function is available could be used. Note that NSM-Bayes is partially amortised; once  $\hat{\phi}_m$  is estimated by training the neural surrogate, we can directly use  $q_{\hat{\phi}_m}$  to add additional observations or perform inference on a new dataset, without ever needing to run additional simulations.

### 3.2 Conjugate Neural Score-matching Bayes

We now consider a special case of the framework above. assume, without loss of generality, that our model is based on an unnormalised family; i.e.  $q_\phi(x|\theta) = \tilde{q}_\phi(x|\theta)/C(\theta, \phi)$ , where  $\tilde{q}_\phi(x|\theta)$  can be evaluated in closed-form, but  $C(\theta, \phi) > 0$  is a (possibly intractable) normalisation constant. In particular, we consider models which are (natural) exponential families in  $\theta$ .

**Assumption A3.** *Let  $q_\phi(x|\theta) \propto \exp(T_\phi(x)^\top \theta + b_\phi(x))$ , where the statistic  $T_\phi : \mathcal{X} \rightarrow \mathbb{R}^{d_\Theta}$  and  $b_\phi : \mathcal{X} \rightarrow \mathbb{R}$  are both twice-differentiable and such that  $q_\phi$  satisfies [A2](#).*

Examples include energy-based models which are linear in  $\theta$ , as well as certain instances of [Arbel and Gretton \(2018\)](#); [Sasaki and Hyvärinen \(2018\)](#); [Pacchiardi and Dutta \(2022\)](#). This form is restrictive in  $\theta$ , but  $T_\phi$  and  $b_\phi$  can be flexible non-linear maps, such as neural networks with smooth activation functions (e.g. tanh, softplus, and GELU).

Since the model in [A3](#) is unnormalised, we will not be able to use  $\mathcal{L}_{\text{NLE}}$  in **step (i)**. Instead, we utilise score-matching to train  $\phi$  since scores do not require any knowledge of the normalisation constant:  $\nabla_x \log q_\phi(x|\theta) = \nabla_x \log \tilde{q}_\phi(x|\theta)$ . As  $q_\phi$  is trained on simulated data  $\{(\theta_i, x_i)\}_{i=1}^m$  which does not contain any outliers, we use the unweighted SM objective for conditional densities due to [Altamirano et al. \(2024\)](#) as the loss function  $J(\phi) := \mathbb{E}_{\theta \sim \pi} [\text{SM}(p(\cdot|\theta) || q_\phi(\cdot|\theta))]$ , and estimate the parameters of our conditional density estimator as  $\hat{\phi}_m := \arg \min_{\phi \in \Phi} J_m(\phi)$ , where  $J_m(\phi)$  is a Monte Carlo estimate of  $J(\phi)$  obtained through the simulated data, with the additive constant dropped and simplified:

$$J_m(\phi) = \frac{1}{m} \sum_{i=1}^m \left\| \nabla_x \log q_\phi(x_i | \theta_i) \right\|_2^2 + 2 \text{Tr} \left( \nabla_x^2 \log q_\phi(x_i | \theta_i) \right). \quad (10)$$

This approach is similar to other score-based methods already proposed in the SBI literature ([Pacchiardi and Dutta, 2022](#); [Geffner et al., 2023](#); [Simons et al., 2023](#); [Linhart et al., 2024](#); [Sharrock et al., 2024](#); [Gloeckler et al., 2024](#); [Khoo et al., 2025](#); [Nautiyal et al., 2025](#); [Jiang et al., 2025](#)). In particular, [Pacchiardi and Dutta \(2022\)](#) also propose learning a neural exponential

family surrogate via score-matching. However, they use MCMC to sample from the Bayes posterior instead of using GBI, and their method is therefore not robust.

The advantage of A3 is that **step (ii)** of obtaining the NSM-Bayes posterior can now be performed in a fully conjugate manner leading to the so-called NSM-Bayes-conj posterior.

**Proposition 1.** *Suppose A3 holds,  $\pi(\theta) \propto \mathcal{N}(\theta; \mu, \Sigma)$ , and  $W(x) = I_{d_X} w(x)$  for some  $w : \mathcal{X} \rightarrow \mathbb{R}$ . Then  $\pi_{NSM}(\theta | x_{1:n}^o, \hat{\phi}_m) \propto \mathcal{N}(\theta; \mu_{n,m}, \Sigma_{n,m})$  where:*

$$\begin{aligned}\mu_{n,m} &:= \Sigma_{n,m} \left( \Sigma^{-1} \mu - 2\beta \left( \sum_{i=1}^n w(x_i^o)^2 \nabla_x T_{\hat{\phi}_m}(x_i^o) \nabla_x b_{\hat{\phi}_m}(x_i^o) - \nabla_x \cdot (w(x_i^o)^2 \nabla_x T_{\hat{\phi}_m}(x_i^o)^\top)^\top \right) \right), \\ \Sigma_{n,m}^{-1} &:= \Sigma^{-1} + 2\beta \sum_{i=1}^n w(x_i^o)^2 \nabla_x T_{\hat{\phi}_m}(x_i^o) \nabla_x T_{\hat{\phi}_m}(x_i^o)^\top.\end{aligned}$$

Here we use the convention:  $\nabla_x T_{\hat{\phi}_m}(x_i^o) \in \mathbb{R}^{d_\Theta \times d_X}$ . This result is a direct application of Proposition 3.1 in Altamirano et al. (2023) with a diagonal weight function and surrogate likelihood, see Section A.1 for the proof. This result makes our approach fully amortised; once the model is trained in step (i), we can introduce new observed data points and/or change the (Gaussian-like) prior, and we directly obtain an expression for the NSM-Bayes posterior without the need for MCMC, which may have tuning parameters that are difficult to select. NSM-Bayes-conj also amortises over the choice of the weight function and the learning rate, allowing the method to be adapted for robustness according to the specific needs of the observed dataset. This computational advantage comes at the cost of restrictions on the choice of surrogate  $q_\phi$  and the prior  $\pi$ , though we found that this did not have a large impact on performance in our numerical experiments.

### 3.3 Hyperparameter Selection

We select the weight as  $W(x) := w(x) I_{d_X}$  so as to induce robustness, following the suggestions in Barp et al. (2019); Altamirano et al. (2023, 2024); Duran-Martin et al. (2024); Liu and Briol (2025). In particular, we take  $w : \mathcal{X} \rightarrow \mathbb{R}$  to be the inverse multi-quadratic (IMQ) function:

$$w_\zeta(x) := \left( 1 + \|x - \hat{\nu}_n\|_{\hat{\Xi}_n^{-1}}^2 \right)^{-\frac{1}{\zeta}} \quad (11)$$

for some  $\zeta > 0$ , since this choice satisfies A1. Here,  $\hat{\nu}_n, \hat{\Xi}_n$  are robust estimators of the mean and covariance (Rousseeuw and Driesssen, 1999) of  $\mathbb{P}_0$  based on  $x_{1:n}^o$ , and robustness of these estimators is essential since we expect outliers. The function  $w_\zeta$  down-weights the outlying data points that are far from  $\hat{\nu}_n$  (since  $w_\zeta(x) \rightarrow 0$  as  $x \rightarrow \pm\infty$ ), thereby reducing their impact on the generalised posterior. The strength of this down-weighting is controlled by  $\zeta$ , with most existing work fixing  $\zeta = 2$ . However, the extra flexibility provided by  $\zeta$  will be essential in our case, with  $0 < \zeta \leq 1$  guaranteeing outlier-robustness when using masked autoregressive flows for  $q_\phi$ , as we will see theoretically in Section 4 and empirically in Section 5.

We select the temperature/learning rate  $\beta > 0$  with a focus on calibration. This is important since Hermans et al. (2022) have highlighted issues with the calibration of SBI methods. To do so, we can rely on prior work by Lyddon et al. (2019); Syring and Martin (2019); Wu and Martin (2023); Matsubara et al. (2024). Specifically, we use the method of Syring and Martin (2019) and select  $\beta$  such that the  $100(1 - \alpha)\%$  credible region of our generalised posterior has empirical frequentist coverage close to  $1 - \alpha$ ; see Algorithm 1. We made this choice because it is one of the most widespread in the GBI literature, but we note that our approach could also be used with some of the other calibration approaches. Following Syring and Martin (2019), we first solve  $\hat{\theta}_n = \arg \min_{\theta} \mathcal{L}_{NSM}(\theta; x_{1:n}^o, \hat{\phi}_m)$  and then define a stochastic approximation procedure over  $\beta$  using estimates of the credible region and empirical coverage from bootstrapped samples of  $x_{1:n}^o$ .

---

**Algorithm 1** Learning Rate Calibration

---

**Require:** Data  $x_{1:n}^o$ , GBI loss  $\mathcal{L}$ , initial learning rate  $\beta_0$ , iterations  $T$ , number of bootstrap samples  $B$ , step-size  $\kappa_t$ , target coverage  $1 - \alpha$

- 1: Compute  $\hat{\theta}_n = \arg \min_{\theta \in \Theta} \mathcal{L}(\theta; x_{1:n}^o)$  for any GBI loss  $\mathcal{L}$ .
- 2: **for**  $t = 1$  **to**  $T$  **do**
- 3:     Draw  $B$  bootstrap datasets  $x_{1:n}^{*(b)}$  by resampling from  $x_{1:n}^o$  with replacement.
- 4:     **for**  $b = 1$  **to**  $B$  **do**
- 5:         Estimate the GBI posterior mean  $\hat{\mu}_{\beta_t}^{(b)}$  and covariance  $\hat{\Sigma}_{\beta_t}^{(b)}$ .
- 6:         Form the credible region using the  $1 - \alpha$  quantile  $\chi_{1-\alpha, d_\Theta}^2$  of a chi-squared distribution:

$$C_{\alpha, \beta_t}(x_{1:n}^{*(b)}) = \left\{ \theta : \left( \theta - \hat{\mu}_{\beta_t}^{(b)} \right)^\top \left( \hat{\Sigma}_{\beta_t}^{(b)} \right)^{-1} \left( \theta - \hat{\mu}_{\beta_t}^{(b)} \right) \leq \chi_{1-\alpha, d_\Theta}^2 \right\}.$$

- 7:     **end for**
- 8:     Estimate the coverage:  $\hat{c}(\beta_t) = \frac{1}{B} \sum_{b=1}^B \mathbb{I} \left\{ \hat{\theta}_n \in C_{\alpha, \beta_t}(x_{1:n}^{*(b)}) \right\}$ .
- 9:     Update  $\beta$ :  $\beta_{t+1} = \beta_t + \kappa_t (\hat{c}(\beta_t) - (1 - \alpha))$ .
- 10: **end for**
- 11: **return**  $\beta_T$

---

and  $\hat{\theta}_n$ . At each iteration, we increase  $\beta$  if the empirical coverage exceeds  $1 - \alpha$ , and decrease  $\beta$  otherwise. Note that  $\hat{\theta}_n$  can be obtained in closed-form for NSM-Bayes-conj (Laplante et al., 2025b), while for NSM-Bayes, we estimate  $\hat{\theta}_n$  using the Adam optimiser (Kingma, 2014). As repeated posterior inference for different bootstrapped data sample is computationally intensive for NSM-Bayes, we run MCMC once for an initial  $\beta$  value and then adopt an importance sampling strategy to estimate the posterior at other  $\beta$  values (Syring and Martin, 2019). As large updates to  $\beta$  can make this procedure unstable, we rerun MCMC to refresh the samples at the current  $\beta$  if the effective sample size falls below a preset threshold. Once  $\beta$  is selected, we sample again from  $\pi_{\text{NSM}}(\theta | x_{1:n}^o, \hat{\phi}_m)$ . Thus, NSM-Bayes requires (at least) two MCMC runs to calibrate  $\beta$  and perform inference; see Section B.1 for further details.

## 4 Robustness

We are now ready to provide our formal results on robustness. We first prove that the NLE posterior is *not* robust to outliers under standard assumptions (Theorem 1) and then provide two robustness results for our method; a general result for NSM-Bayes (Theorem 2), and a more refined result for the special case of NSM-Bayes-conj (Theorem 3).

### 4.1 Lack of Robustness of Neural Likelihood Estimation

To do so, we consider the classical framework of Huber and Ronchetti (1981), where given a data distribution  $\mathbb{P}_0 \in \mathcal{P}(\mathcal{X})$ , we consider its  $\epsilon$ -contaminated counterpart  $\mathbb{P}_{\epsilon, x^c} = (1 - \epsilon)\mathbb{P}_0 + \epsilon\delta_{x^c}$ , where  $\delta_{x^c}$  denotes the Dirac measure at some point  $x^c \in \mathbb{R}^{d_x}$  and  $\epsilon \in [0, 1]$  denotes the contamination degree. Our data-generating process is therefore denoted  $\mathbb{P}_{\epsilon, x^c}$ , and the uncorrupted process  $\mathbb{P}_0$  is now the distribution we are hoping to recover through inference. To this end, for any  $\mathbb{P} \in \mathcal{P}(\mathcal{X})$  and loss  $\mathcal{L}$ , we define the GBI posterior given  $\mathbb{P}$  as

$$\pi_{\mathcal{L}}(\theta | \mathbb{P}) \propto \exp(-\beta n \mathcal{L}(\theta; \mathbb{P})) \pi(\theta), \quad (12)$$

where  $\mathcal{L}(\theta; \mathbb{P})$  is now an expected loss instead of an empirical loss. Using this notation, the GBI posterior in Equation (3) satisfies  $\pi_{\mathcal{L}}(\theta | x_{1:n}^o) = \pi_{\mathcal{L}}(\theta | \mathbb{P}_n)$  where  $\mathbb{P}_n := \frac{1}{n} \sum_{i=1}^n \delta_{x_i^o}$  is the empirical measure of the observations. Robustness is then defined through studying the behaviour of

a *posterior influence function (PIF)*, a quantity well-studied in GBI (Ghosh and Basu, 2016; Matsubara et al., 2022; Altamirano et al., 2023; Duran-Martin et al., 2024; Altamirano et al., 2024; Laplante et al., 2025a; Rooijakkers et al., 2025) which measures the influence of a contamination on  $\pi_{\mathcal{L}}$ . Following Ghosh and Basu (2016); Altamirano et al. (2023); Matsubara et al. (2022), we first define:

$$\text{PIF}_{\Delta}(x^c, \theta, \mathbb{P}_0, \mathcal{L}) := \frac{d}{d\epsilon} \pi_{\mathcal{L}}(\theta \mid \mathbb{P}_{\epsilon, x^c}) \Big|_{\epsilon=0}. \quad (13)$$

We say that  $\pi_{\mathcal{L}}(\theta \mid \mathbb{P}_n)$  is *globally-bias robust* if and only if  $\sup_{\theta \in \Theta, x^c \in \mathcal{X}} \text{PIF}_{\Delta}(x^c, \theta, \mathbb{P}_n, \mathcal{L}) < \infty$ , i.e., a GBI posterior is globally bias-robust if an infinitesimal contamination cannot impact it arbitrarily badly. We first show that the NLE posterior is *not* globally-bias robust.

**Theorem 1.** *Assume  $\max_i \mathbb{E}_{\theta \sim \pi_{NLE}(\cdot \mid x_{1:n}^o, \hat{\phi}_m)} [\log q_{\hat{\phi}_m}(x_i^o \mid \theta)] < \infty$ . Then, the NLE posterior is not globally-bias robust; i.e.  $\sup_{\theta \in \Theta, x^c \in \mathcal{X}} \text{PIF}_{\Delta}(x^c, \theta, \mathbb{P}_n, \mathcal{L}_{NLE}) = \infty$ .*

The proof is provided in Appendix A.2. The assumption of Theorem 1 is very mild and simply guarantees that  $\text{PIF}_{\Delta}$  is well-defined and that the NLE posterior does not concentrate on parameter values that assign vanishing likelihood to the observed data. Despite ample experimental results demonstrating that NLE is not robust, this is the first theoretical justification of this claim.

## 4.2 Robustness of Neural Score-matching Bayes

In contrast with the previous result, the following theorem shows that NSM-Bayes is globally-bias robust under mild conditions. We denote by  $L^q(\pi)$  the Lebesgue space of functions  $f : \Theta \rightarrow \mathbb{R}$  such that  $\int_{\Theta} |f(\theta)|^q \pi(\theta) d\theta < \infty$ .

**Assumption A4.** *Suppose that  $\sup_{\theta \in \Theta} \pi(\theta) < \infty$  and  $\exists f : \Theta \rightarrow \mathbb{R}_+$ ,  $g : \Theta \rightarrow \mathbb{R}_+$  such that  $f \in L^2(\pi)$ ,  $g \in L^1(\pi)$ ,  $\sup_{\theta \in \Theta} (f(\theta)^2 + f(\theta) + g(\theta)) \pi(\theta) < \infty$  and  $\forall x \in \mathcal{X}$ :*

$$\begin{aligned} \|\nabla_x \log q_{\hat{\phi}_m}(x \mid \theta)\|_2 &\leq f(\theta) \min\{w(x)^{-1}, \|\nabla_x w(x)^2\|_2^{-1}\}, \\ |\text{Tr} \nabla_x^2 \log q_{\hat{\phi}_m}(x \mid \theta)| &\leq g(\theta) w(x)^{-2}. \end{aligned}$$

**Theorem 2.** *Suppose that A1, A2 and A4 hold. Then,  $\pi_{NSM}(\theta \mid x_{1:n}^o, \hat{\phi}_m)$  is globally-bias robust, i.e.  $\sup_{\theta \in \Theta, x^c \in \mathcal{X}} \text{PIF}_{\Delta}(x^c, \theta, \mathbb{P}_n, \mathcal{L}_{NSM}) < \infty$ .*

The proof is in Section A.3. The intuition behind these assumptions is that the weight function  $w$  and the prior  $\pi$  must counter-balance any growth of  $\|\nabla_x \log q_{\hat{\phi}_m}(x \mid \theta)\|_2$  and  $|\text{Tr} \nabla_x^2 \log q_{\hat{\phi}_m}(x \mid \theta)|$  towards infinity in  $x$  and  $\theta$ , respectively. This is achieved by ensuring that the first two derivatives of  $\log q_{\hat{\phi}_m}(x \mid \theta)$  are bounded pointwise by functions  $f(\theta)$  and  $g(\theta)$ , whose growth is integrable under the prior, and offset by  $w(x)$  in the data space. Hence, any increase in likelihood sensitivity with respect to  $x$  or  $\theta$  is sufficiently controlled to keep the posterior influence function uniformly bounded. These are very mild assumptions as  $f, g$  can usually be found by inspecting the specific form of  $q_{\phi}$ , as will be shown below. A strength of this theorem is that it is applicable for a broad class of weights, including the IMQ weights used in this paper and a large part of the literature (Altamirano et al., 2023, 2024; Reimann, 2024; Laplante et al., 2025a; Rooijakkers et al., 2025), but also for the squared-exponential weights in Altamirano et al. (2024) and the plateau-IMQ weights of Ezzerg et al. (2025). However, when restricting ourselves to IMQ weights and sub-exponential priors with light tails, the assumptions can be significantly simplified.

**Assumption A4'.** *Suppose that we take the IMQ weight  $w_{\zeta}$  defined as in Equation (11) and a sub-exponential prior (Wainwright, 2019, Definition 2.7) such that  $\pi(\theta) \leq C \exp(-c\|\theta\|)$  for*

all  $\|\theta\| \geq R$ , and for some constants,  $C, c, R > 0$ . Assume further that there exist constants  $0 < K_1, K_2 < \infty$  and  $k_1, k_2 \geq 0$  such that for all  $x \in \mathcal{X}$ :

$$\begin{aligned} \left\| \nabla_x \log q_{\hat{\phi}_m}(x|\theta) \right\|_2 &\leq K_1 \left( 1 + \|\theta\|^{k_1} \right) \left( 1 + \|x\|_2^{\frac{2}{\zeta}} \right) \\ \left| \text{Tr} \nabla_x^2 \log q_{\hat{\phi}_m}(x|\theta) \right| &\leq K_2 \left( 1 + \|\theta\|^{k_2} \right) \left( 1 + \|x\|_2^{\frac{4}{\zeta}} \right). \end{aligned}$$

**Corollary 1.** Suppose Assumptions A2 and A4' hold, then the statement of Theorem 2 holds, i.e.  $\sup_{\theta \in \Theta, x \in \mathcal{X}} \text{PIF}_{\Delta}(x^c, \theta, \mathbb{P}_n, \mathcal{L}_{NSM}) < \infty$ .

A proof is provided in Appendix A.4.1. We note that these simplified assumptions are much easier to check; it suffices to check the growth of the score and trace terms in terms of powers of  $\theta$  and  $x$ . The assumption on  $\pi$  is very mild and includes most widely used priors with sufficiently light tails such as Gaussian, Laplace, logistic and log-concave exponential-family priors.

### 4.3 Robustness with Mixture Density Networks and Normalising Flows

Next, we show that the assumptions on  $q_{\phi}$  hold for MDNs (Bishop, 1994) and MAFs (Papamakarios et al., 2017). These results therefore guarantee robustness for NSM-Bayes and NSM-Bayes across all our experiments in Section 5. Importantly, the assumptions concern only the fitted neural network architecture obtained in step (i): once  $\hat{\phi}_m$  is specified, they can be verified directly before running NSM-Bayes in step (ii).

**Mixture density network.** An MDN (Bishop, 1994) represents a conditional density using a finite mixture of simple parametric distributions, typically Gaussians, with weights  $\{\omega_k(\cdot; \phi)\}_{k=1}^K$  that sum to 1, mean vectors  $\{\vartheta_k(\cdot; \phi)\}_{k=1}^K$ , and covariance matrices  $\{\Omega_k(\cdot; \phi)\}_{k=1}^K$ , all parameterised by neural networks. Here  $\phi$  is the vector of parameters of these networks. Thus, an MDN made of Gaussian distributions takes the form:

$$q_{\phi}(x|\theta) = \sum_{k=1}^K \omega_k(\theta; \phi) \mathcal{N}(x; \vartheta_k(\theta; \phi), \Omega_k(\theta; \phi)). \quad (14)$$

where  $K$  is the number of mixture components. In the following result, we show that for certain values of the IMQ weight hyperparameter  $\zeta$ , MDNs satisfy Assumption A4', and hence the statement of Corollary 1 holds in these cases.

**Proposition 2.** Suppose  $q_{\hat{\phi}_m}$  is a Gaussian mixture-density network as in (14) such that:

- The neural networks are continuous in  $\theta$ ; i.e.  $\omega_k(\cdot; \hat{\phi}_m), \vartheta_k(\cdot; \hat{\phi}_m), \Omega_k(\cdot; \hat{\phi}_m) \in C(\Theta)$ .
- $\vartheta_k(\cdot; \hat{\phi}_m)$  has at most polynomial growth, i.e.  $\exists r > 0, C \geq 0$  such that  $\max_k \|\vartheta_k(\theta, \hat{\phi}_m)\| \leq C(1 + \|\theta\|^r)$ .
- The covariance functions  $\Omega_k(\theta, \hat{\phi}_m)$  satisfy uniform eigenvalue bounds, i.e.  $0 < \lambda_{\min} \leq \lambda_{\min}(\Omega_k(\theta, \hat{\phi}_m)) \leq \lambda_{\max}(\Omega_k(\theta, \hat{\phi}_m)) \leq \lambda_{\max} < \infty$  for all  $k \in \{1, \dots, K\}, \theta \in \Theta$ .

Then, Assumption A4' is satisfied for any  $0 < \zeta \leq 2$ .

The proof is provided in Appendix A.4.2. This means that under standard assumptions on the networks of an MDN, robustness is guaranteed for a large range of IMQ weights, including the commonly used choice of  $\zeta = 2$ . We now move on to showing a similar result for a class of normalising flows.

**Masked autoregressive flows.** An MAF (Papamakarios et al., 2017) is a conditional normalising flow defined by an invertible transformation  $\varrho_\phi(\cdot; \theta) : \mathbb{R}^{d_x} \rightarrow \mathbb{R}^{d_x}$  that maps a simple  $d_x$ -dimensional base random variable  $z \sim p_z(z) = \mathcal{N}(0, I_{d_x})$  to our target variable  $x$  conditioned on  $\theta$  such that  $x = \varrho_\phi(z; \theta)$  and  $z = \varrho_\phi^{-1}(x; \theta)$ . By change of variables, we can express  $q_\phi(x|\theta)$  as  $q_\phi(x|\theta) = p_z(\varrho_\phi^{-1}(x; \theta)) |\det \partial \varrho_\phi^{-1}(x; \theta) / \partial x|$ . In practice,  $\varrho_\phi^{-1}$  is composed of  $L$  autoregressive layers  $\varrho_\phi^{-1} = \varrho_L^{-1} \circ \dots \circ \varrho_1^{-1}$  with intermediate states  $h_0 = x$ ,  $h_l = \varrho_l^{-1}(h_{l-1}; \theta)$ , and  $z = h_L$ :

$$\log q_\phi(x|\theta) = \log p_z(z) + \sum_{l=1}^L \log \left| \det \frac{\partial \varrho_l^{-1}(h_{l-1}; \theta)}{\partial h_{l-1}} \right|,$$

where  $h_0 = x$ ,  $h_l = \varrho_l^{-1}(h_{l-1}; \theta)$ ,  $z = h_L$ , and  $\phi$  constitutes the combined parameters of  $\varrho_1^{-1}, \dots, \varrho_L^{-1}$ . In each layer, the invertible map  $\varrho_\phi^{-1}$  is an autoregressive affine transformation of the form (scaling and shifting operation):

$$z_i = (\varrho_\phi^{-1}(x; \theta))_i = \frac{x_i - \mu_{\phi,i}(x_{<i}, \theta)}{\sigma_{\phi,i}(x_{<i}, \theta)} \quad i = 1, \dots, d_x, \quad (15)$$

where  $\mu_{\phi,i}$  and  $\sigma_{\phi,i} > 0$  are outputs of masked multi-layer perceptrons (MLPs), parameterised by  $\phi$ , that ensure the autoregressive dependency structure, i.e. the  $i^{\text{th}}$  output only depends on  $x_{<i} := (x_1, x_2, \dots, x_{i-1})^\top \in \mathbb{R}^{i-1}$ ,  $i \in \{1, \dots, d_x\}$ . The conditioning on  $\theta$  is included in every layer. The corresponding Jacobian is a lower triangular matrix, hence  $\log |\det \partial z / \partial x| = -\sum_{i=1}^{d_x} \log \sigma_{\phi,i}(x_{<i}, \theta)$ , and therefore the log-density becomes:

$$\log q_\phi(x|\theta) = \log p_z(z) - \sum_{i=1}^{d_x} \log \sigma_{\phi,i}(x_{<i}, \theta), \quad (16)$$

where  $z_i$  (with components  $z_i$ ) given by Equation (15). Similarly to MDNs, when  $q_\phi$  is an MAF, robustness holds for certain values of  $\zeta$  under standard network conditions.

**Proposition 3.** *Suppose  $q_{\hat{\phi}_m}$  is a masked autoregressive flow as in Equation (16) such that*

- *The networks computing  $\mu_{\hat{\phi}_m,i}$  and  $\sigma_{\hat{\phi}_m,i}$  are MLPs built from affine layers with  $\tanh$  activation functions.*
- *An additional softplus activation is applied to the final output of  $\sigma_{\hat{\phi}_m,i}$ .*

*Then Assumption A4' is satisfied for any  $0 < \zeta \leq 1$ .*

The proof is provided in Appendix A.4.3. Note that the network assumptions in Proposition 3 follow the default implementation of MAF provided by the SBI library (Tejero-Cantero et al., 2020). Most notably, this result guarantees that the examples considered in Section 5 will be robust. Interestingly, it shows that the choice of  $\zeta = 2$ , which is prevalent in the literature on SM-Bayes, may not be a good one for NSM-Bayes based on normalising flows.

#### 4.4 Robustness of Conjugate Neural Score-matching Bayes

We now move to NSM-Bayes-conj, where we can build on Theorem 2, but also study robustness under an alternative form of PIF suggested by Altamirano et al. (2024). This alternative is preferable, as it is divergence-based and offers a more interpretable measure of robustness. It is not as widely used as it is often challenging to compute, but it is tractable for the special case of NSM-Bayes-conj. Consider the case where a single observation  $x_j^o$ , for some  $j \in \{1, \dots, n\}$ , is replaced by an arbitrary contamination datum  $x_j^c$ , and denote the set of observed data as  $x_{1:n}^o$  and the contamination dataset as  $x_{1:n}^c := (x_{1:n}^o \setminus x_j^o) \cup x_j^c$ . The PIF of Altamirano et al. (2024) is defined by examining the influence of this contamination, measured using the Kullback-Leibler

divergence between the posterior based on the original dataset  $x_{1:n}^o$  and that based on the contaminated dataset  $x_{1:n}^c$ :

$$\text{PIF}_{\text{KL}}(x_j^c, \mathbb{P}_n, \mathcal{L}) := \text{KL}(\pi_{\mathcal{L}}(\theta|x_{1:n}^o) \parallel \pi_{\mathcal{L}}(\theta|x_{1:n}^c)).$$

Similarly to before,  $\pi_{\mathcal{L}}$  is called robust if  $\text{PIF}_{\text{KL}}$  is bounded as a function of  $x_j^c$ . For any  $n \times m$  matrix  $A$ , we write  $\|A\|_F := (\sum_{i=1}^m \sum_{j=1}^n |A_{ij}|^2)^{\frac{1}{2}}$  for the Frobenius norm.

**Assumption A5.** *Suppose  $\exists C, C' < \infty$  such that  $\forall x \in \mathcal{X}$ :*

$$\begin{aligned} \max \left\{ \left( \left\| \nabla_x T_{\hat{\phi}_m}(x) \right\|_F \left\| \nabla_x b_{\hat{\phi}_m}(x) \right\|_2 \right)^{\frac{1}{2}}, \left\| \nabla_x^2 T_{\hat{\phi}_m}(x) \right\|_F^{\frac{1}{2}}, \left\| \nabla_x T_{\hat{\phi}_m}(x) \right\|_F \right\} &\leq C w(x)^{-1}, \\ \left\| \nabla_x T_{\hat{\phi}_m}(x) \right\|_F &\leq C' \left\| \nabla_x w(x)^2 \right\|_2^{-1}. \end{aligned}$$

**Theorem 3.** *Suppose A1, A3 and A5 hold. Then, the NSM-Bayes-conj is outlier-robust; i.e.  $\sup_{x_j^c \in \mathbb{R}^{d_{\mathcal{X}}}} \text{PIF}_{\text{KL}}(x_j^c, \mathbb{P}_n, \mathcal{L}_{\text{NSM}}) < \infty$ .*

See Section A.4.4 for the proof. Assumption A5 ensures that the first- and second-order derivatives of  $T_{\hat{\phi}_m}$  and  $b_{\hat{\phi}_m}$  grow at most at a rate that is offset by  $w$  and  $\nabla w$ , so that extreme observations cannot induce unbounded posterior influence. Note that if Assumption A5 is satisfied, then under mild additional assumptions, Assumption A4 is satisfied as well. Consequently, robustness is guaranteed under both PIF definitions (see Appendix A.4.5 for a proof). This time, we do not have additional assumptions on the prior since this must be Gaussian to ensure conjugacy. Here, the constants  $C$  and  $C'$  act very similarly to  $f, g$  in Assumptions A4 and A4', with the difference being that they do not depend on  $\theta$ .

We emphasise that a key strength of all robustness results in Section 4 is that they depend only on Assumptions about the fitted density  $q_{\hat{\phi}_m}$  rather than the entire model class  $\{q_{\phi} : \phi \in \Phi\}$ . Consequently, step (i) can be carried out independently to obtain  $\hat{\phi}_m$ , after which the weight  $w$  can be selected such that the required Assumptions are satisfied.

## 5 Experiments

We demonstrate the performance of our methods against NLE and other robust SBI baselines. Given the significant interest in the problem, an exhaustive comparison is infeasible. We therefore benchmark against five competitors representative of the literature: (i) the robust sequential NLE (RSNLE) method of Kelly et al. (2024), (ii) the MMD posterior bootstrap (NPL-MMD) method of Dellaporta et al. (2022), (iii) the NPE with robust statistics (NPE-RS) method of Huang et al. (2023), (iv) the amortised cost estimation (ACE) method of Gao et al. (2023), and (v) the GBI scoring rule (GBI-SR) method of Pacchiardi et al. (2024). We exclude comparison with methods that require additional data for robustness as they are not as widely applicable.

We use two metrics to evaluate performance. The first is the MMD<sup>2</sup> (Gretton et al., 2006) between posterior samples and a reference NLE posterior obtained from uncorrupted data (denoted as MMD<sub>ref</sub><sup>2</sup>). The second is the mean squared error  $\text{MSE} = \mathbb{E}[\|\theta - \theta^*\|_2^2]$  estimated using posterior samples, which measures whether the posteriors are centred around  $\theta^*$ . Note that MSE can be computed in closed-form for NSM-Bayes-conj. We also report the time to perform inference on a single dataset. For partially amortised methods where the density estimator need not be re-trained for new observations, training and inference times are reported separately. For NSM-Bayes, NSM-Bayes-conj, GBI-SR and ACE, inference time also includes tuning the learning rate  $\beta$ . As ACE and GBI-SR do not provide a method to tune  $\beta$ , we set it using the same approach as NSM-Bayes; see Section B.1 for further details.

For a fair comparison, we fix the simulation budget  $m$  and the number of posterior samples for all methods. We use the same default conditional density estimator from the sbi library

Table 1: **Benchmarking robust SBI methods on g-and-k distribution.** Standard deviation for the metrics across 20 runs are reported in the parenthesis.

Method	MMD <sub>ref</sub> <sup>2</sup>	MSE	Empirical Coverage	Training time [s]	Inference time [s]	Amortised	Robustness guarantee
NLE	0.54 (0.03)	15.0 (1.8)	0%	93 (37)	36 (19)	✓(Partially)	✗
NPL-MMD	0.69 (0.21)	37.2 (9.4)	30%	-	0.6 (0.1)	✗	✓
RSNLE	0.49 (0.08)	3.8 (1.6)	0%	-	38 (4)	✗	✗
NPE-RS	0.36 (0.15)	8.0 (4.9)	15%	-	41 (19)	✗	✗
ACE	0.24 (0.15)	4.6 (1.5)	85%	376 (80)	390 (5)	✓(Partially)	✗
GBI-SR	0.24 (0.15)	4.1 (5.4)	80%	-	415 (8)	✗	✓
NSM-Bayes	0.13 (0.09)	5.5 (2.4)	100%	93 (37)	163 (2)	✓(Partially)	✓
NSM-Bayes-conj	0.20 (0.14)	6.1 (2.9)	100%	176 (53)	5.1 (0.1)	✓(Fully)	✓

(Tejero-Cantero et al., 2020) for both NLE and NSM-Bayes, which is an MAF for the g-and-k (Section 5.1) and SIR experiments (Section 5.2), and an MDN for the radio propagation experiment (Section 5.3). We set  $\zeta = 1$  in Equation (11) to ensure that our theory is satisfied for both MDNs and MAFs. A slice sampler is used to obtain 500 samples (with 500 warm-up steps) from the NLE and the NSM-Bayes posterior in the g-and-k and SIR experiments. For the radio propagation experiment, we sample 1000 posterior samples. For simplicity, we compare all the runtimes on CPU (Apple M4, 16GB), but some methods may benefit from parallelisation (e.g. NPL-MMD). Further implementation details and explanation of the baselines are in Section B. The code to reproduce the experiments is available at <https://github.com/bharti-ayush/nsm-bayes>.

## 5.1 Benchmarking on the g-and-k distribution

Our first example is the g-and-k (Prangle, 2020): a flexible parametric family of univariate distributions which does not have a closed-form likelihood but is easy to simulate from. This is a popular example in the SBI literature (Fearnhead and Prangle, 2012; Price et al., 2018; Wang et al., 2022; Bharti et al., 2022b; Chen et al., 2023), which has been used to benchmark robustness (Dellaporta et al., 2022). The distribution has four parameters  $(\theta_1, \theta_2, \theta_3, \theta_4)$ , and sampling can be done by simulating  $u \sim \mathcal{N}(0, 1)$  and substituting it in the following generator:

$$G_\theta(u) = \theta_1 + \theta_2 \left( 1 + 0.8 \left( \frac{1 - \exp(-\theta_3 u)}{1 + \exp(-\theta_3 u)} \right) \right) (1 + u^2)^{\theta_4} u, \quad u \sim \mathcal{N}(0, 1).$$

For stability, we log-transform the scale and kurtosis parameters  $(\theta_2, \theta_4)$ . We then place a Gaussian prior on  $(\theta_1, \log \theta_2, \theta_3, \log \theta_4)$  with mean  $[0.0, 0.7, 0.0, -1.5]^\top$  and a diagonal covariance matrix where the diagonal entries are  $[5.0, 0.5, 4.0, 0.25]^\top$ .

We generate observed data  $x_{1:n}^o$  with one-sided outliers by sampling  $n = 100$  points from a Huber contamination model where 90% of observations are drawn from some g-and-k distribution  $\mathbb{P}_{\theta^*}$  with  $\theta^* = [1, 0.5, 1, -1]^\top$ , and the remainder from some corrupted distribution  $\mathbb{Q} = \mathbb{P}_{\theta^*} - 50$ . We fix the simulation budget to be  $m = 10^5$  samples and repeat the experiment 20 times. Results are reported in Table 1 and the marginal posterior densities are in Figure 2. We also report the empirical coverage for each method, which measures how often  $\theta^*$  was included in the 95% credible region of their posterior.

NLE is most affected by the one-sided contamination in the scale parameter  $\theta_2$ , leading to inflated scale and reduced skewness  $\theta_3$  estimates. Correspondingly, it achieves 0% empirical coverage and exhibits large MMD and MSE values. NPE-RS is fast at inference but fails to provide robust posteriors, with low coverage, and poor performance. Similarly, RSNLE is fast but achieves large MMD and 0% coverage, despite having the lowest MSE. NPL-MMD is the fastest method but performs poorly in this setting. This is because it places a non-informative

prior on  $\mathbb{P}_0$  rather than the informative prior all other methods use for  $\theta$ , and therefore would require a much larger simulation budget to improve performance; as shown in Section B.5. ACE attains a relatively good coverage and competitive MMD/MSE values, but has large training and inference times. GBI-SR also achieves competitive performance and maintains good coverage, but its performance is more variable across runs, particularly for  $\theta_3$ , and it has the largest inference time.

In contrast with these benchmark methods, NSM-Bayes and NSM-Bayes-conj achieve 100% empirical coverage and the lowest  $MMD_{ref}^2$  values. Both methods also perform well in MSE, and NSM-Bayes-conj takes just a few seconds for inference, which is primarily spent on calibrating  $\beta$ . Training NSM-Bayes-conj is slower than NLE since it minimises an (unweighted) score-matching objective, and NSM-Bayes is typically  $2 - 3 \times$  slower than NLE due to the score and Hessian computation required for  $\mathcal{L}_{NSM}$ . Overall, NSM-Bayes and NSM-Bayes-conj are the only methods in this benchmark that are simultaneously amortised and provably robust, while achieving strong empirical robustness, reasonable coverage, and competitive inference times.

## 5.2 A Susceptible-Infectious-Recovered model with under-reporting of cases

Next, we consider a stochastic, discrete-time Susceptible-Infectious-Recovered (SIR) model (Tuckwell and Williams, 2007; Allen, 2017) which is a set of stochastic recurrence relations that determine how many people in a given population  $N$  are susceptible, infectious, and recovered over a given time period. Let a population of size  $N$  be divided into three compartments: Susceptible ( $S_t$ ), Infectious ( $I_t$ ), and Recovered ( $R_t$ ),  $t = 0, \dots, T$ . Given a time step  $\Delta t$ , the dynamics are governed by a set of stochastic recurrence relations. The transition of individuals between compartments at each time step  $t \rightarrow t + \Delta t$  is modelled using Binomial distributions, which account for the discrete nature of the population and the inherent randomness of transmission and recovery processes:  $\Delta I_t \sim \text{Binomial}(S_t, 1 - \exp(-\theta_1 \frac{I_t}{N} \Delta t))$ , and  $\Delta R_t \sim \text{Binomial}(I_t, 1 - \exp(-\theta_2 \Delta t))$ , where  $\theta_1$  is the transmission rate and  $\theta_2$  is the recovery rate. The binomial transitions arise from assuming independent infection and recovery events over the interval  $[t, t + \Delta t]$ . The state variables are then updated as:  $S_{t+1} = S_t - \Delta I_t$ ,  $I_{t+1} = I_t + \Delta I_t - \Delta R_t$ ,  $R_{t+1} = R_t + \Delta R_t$ . This formulation corresponds to a discrete-time approximation of the continuous-time SIR process, with binomial transitions capturing demographic stochasticity. The system is initialized with  $\theta_4$  infected individuals and  $S_0 = N - \theta_4$  susceptible individuals, where  $N$  is assumed known.

Let  $y_t$  denote the observed number of reported new infections at time  $t$ . The expected reported cases are  $\theta_3 \cdot \Delta I_t$ , where  $\theta_3 \in [0, 1]$  is the reporting rate. We consider the Poisson observation model for  $y_t$ :  $y_t \sim \text{Poisson}(\theta_3 \Delta I_t)$ . As only partial observations are available, inference relies on low-dimensional summary statistics rather than the full latent trajectory. From a single observed epidemic trajectory  $y_{1:T}$ , we compute three summary statistics commonly used to characterise epidemic severity (House et al., 2013; Meyer et al., 2025): (i) the attack rate:  $x_1 = \frac{1}{N} \sum_{t=1}^T y_t$ , (ii) the normalised peak timing:  $x_2 = \frac{1}{T-1} \arg \max_{t \in \{1, \dots, T\}} y_t$ , and (iii) the normalised peak height:  $x_3 = \frac{1}{N} \max_t y_t$ . Thus,  $x = [x_1, x_2, x_3]^\top \in \mathbb{R}^3$  is the summary statistics vector. We transform the parameters to the unconstrained real space via the transformation:  $\theta = [\log \theta_1, \log \theta_2, \text{logit} \theta_3, \log \theta_4]^\top$ , and place Gaussian prior with mean  $[\log 0.5, \log 0.2, \text{logit} 0.5, \log 20]^\top$  and a diagonal covariance matrix with diagonal elements  $[0.5^2, 0.5^2, 1.0, 0.7^2]^\top$ . We set  $\theta^* = [\log 0.6, \log 0.15, \text{logit} 0.6, \log 20]^\top$ ,  $N = 1000$  and  $T = 150$ .

Outlier robustness is particularly relevant in epidemiology due to the common practical problem of undercounting infectious cases, which leads to one-sided contamination in the data (Gibbons et al., 2014; Li et al., 2020). To model the systematic under-reporting or undercounting of cases, we introduce a one-sided contamination mechanism on the observed epidemic trajectories. Let  $y^{(i)} = (y_1^{(i)}, \dots, y_T^{(i)})$  denote the reported new infections for the  $i^{\text{th}}$  trajectory,  $i = 1, \dots, n$ , generated from the model with true parameter  $\theta^*$ . We assume that a

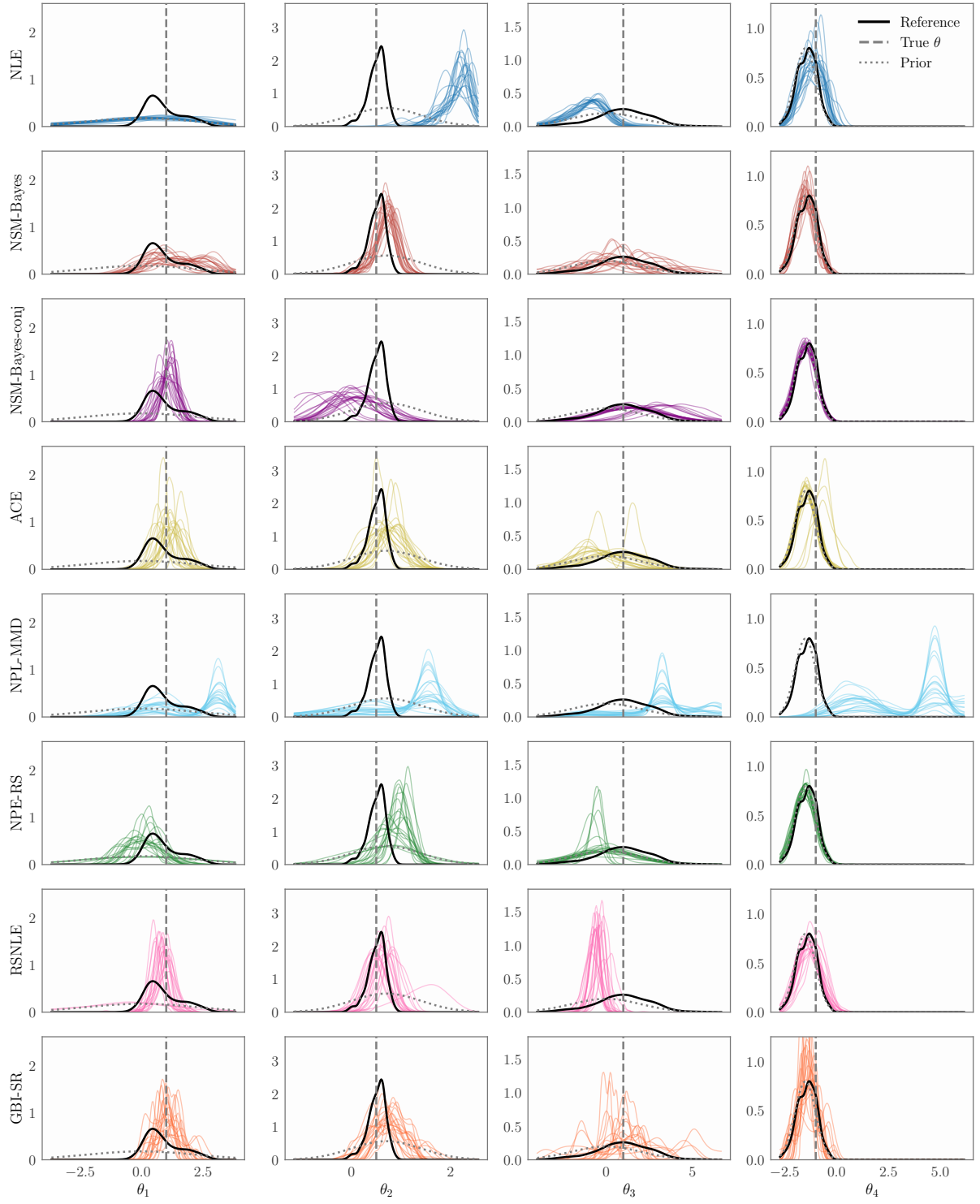


**Figure 2: The g-and-k distribution.** Kernel density estimates of the marginal posterior distributions from NLE (■), NSM-Bayes (■), NSM-Bayes-conj (■), ACE (■), NPL-MMD (■), NPE-RS (■), RSNL (■), and GBI-SR (■) from 500 samples, along with the reference NLE posterior (■) given uncorrupted data. The dashed and dotted gray lines denote the true parameter value and the prior distribution, respectively.

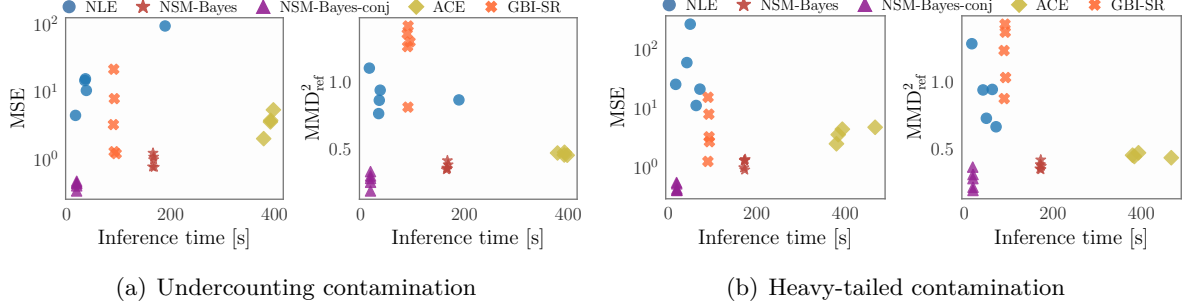


Figure 4: **SIR model.** Performance vs. posterior inference time for NLE (■), NSM-Bayes (■), NSM-Bayes-conj (■), GBI-SR (■), and ACE (■) under both undercounting and heavy-tailed contamination. In both cases, NSM-Bayes-conj performs the best whilst incurring the least time.

fraction  $\epsilon \in (0, 1)$  of observed trajectories are affected by undercounting. For each trajectory  $i$ , we draw an independent contamination random variable  $U_i \sim \text{Bernoulli}(\epsilon)$  which indicates whether trajectory  $i$  is undercounted or not. If  $U_i = 1$ , the entire trajectory is subject to one-sided undercounting, modelled via binomial thinning:

$$\tilde{y}_t^{(i)} | y_t^{(i)} \sim \text{Binomial}(y_t^{(i)}, r), \quad t = 1, \dots, T,$$

where  $r \in (0, 1)$  is a *retention probability*. Smaller values of  $r$  correspond to more severe undercounting. Thus, the marginal distribution of observed trajectories follows the mixture model  $\tilde{y}^{(i)} \sim (1 - \epsilon)\mathbb{P}_{\theta^*} + \epsilon\mathbb{P}_{\theta^*, r}^{\text{under}}$ , where  $\mathbb{P}_{\theta^*, r}^{\text{under}}$  denotes the distribution induced by the binomial thinning of trajectories drawn from  $\mathbb{P}_{\theta^*}$ . Figure 3 shows an example of an observed dataset with both uncorrupted and undercounted trajectories. Out of  $n = 100$  observed time-series recordings, we set  $\epsilon = 5\%$  of them to be undercounted by  $r = 50\%$  to simulate outliers. We also simulate **heavy-tailed contamination** by adding Cauchy distributed noise to  $\epsilon = 10\%$  of the data samples.

In Figure 4, we plot both the metrics against inference time for NLE, NSM-Bayes, and NSM-Bayes-conj using just  $m = 5 \times 10^4$  samples to measure their sample-efficiency. We also include GBI-SR and ACE: the best-performing baselines from Table 1. However, we cannot use the stochastic gradient version of GBI-SR (which we used in Section 5.1) as the SIR simulator is non-differentiable. We therefore use pseudo-marginal MCMC (Andrieu and Roberts, 2009) version of GBI-SR instead, which performs poorly here, primarily because the simulation budget is not large enough. We actually find that the method requires orders of magnitude more simulations to become competitive; see Section B.5. ACE performs better than NLE and GBI-SR, but requires large inference time and also fails to include the true parameter in its posteriors, as seen from the posterior plots in Section B.4. NSM-Bayes-conj performs the best whilst requiring the least inference time, followed by NSM-Bayes. This shows that our methods can provide robust inferences whilst being sample-efficient, unlike methods like GBI-SR which require advanced MCMC samplers.

### 5.3 A radio propagation model with corrupted receiver

Finally, we consider a model that simulates the behaviour of radio signals at a receiving antenna (Turin et al., 1972; Pedersen, 2019), and is used to design and test wireless communication

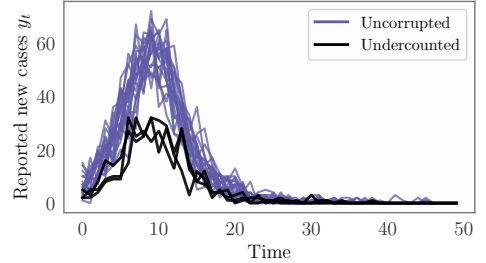


Figure 3: Observed uncorrupted (■) and undercounted (■) trajectories of incidence from the SIR model with  $\epsilon = 5\%$  and  $50\%$  retention probability.

systems in different propagation environments. The model simulates the scenario where channel transfer function data is being measured at  $K$  equidistant points within a frequency bandwidth  $B$ , resulting in a frequency separation of  $\Delta f = B/(K - 1)$ . Assuming additive white Gaussian measurement noise, the measured data  $Y_k$  at the  $k^{\text{th}}$  point can be written as  $Y_k = H_k + Z_k$ ,  $k = 0, 1, \dots, K - 1$ , where  $H_k$  is the transfer function at the  $k^{\text{th}}$  point and  $Z_k \sim \mathcal{CN}(0, \sigma_Z^2)$  is the zero-mean complex circular symmetric Gaussian noise. The transfer function is modelled as  $H_k = \sum_l \alpha_l \exp(-j2\pi\Delta f k \tau_l)$ , where  $\tau_l$  is the time-delay and  $\alpha_l$  is the complex-valued gain of the  $l^{\text{th}}$  signal component. The arrival time of the delays is modelled as a one-dimensional homogeneous Poisson point process  $\tau_l \sim \text{PPP}(\mathbb{R}_+, \lambda)$ , with  $\lambda > 0$  being the arrival rate parameter. The complex-valued gains  $\alpha_l$  are conditioned on the delays, and are modelled as iid zero-mean complex Gaussian random variables with conditional variance  $\mathbb{E}[|\alpha_l|^2 | \tau_l] = G_0 \exp(-\tau_l/T)/\lambda$ . Here,  $G_0$  is the parameter that governs the starting value of the variance, and the parameter  $T$  controls its rate of decay. Since all the parameters are non-negative, we parameterise the model using their log values, i.e., the parameter vector becomes  $\theta = [\log G_0, \log T, \log \nu, \log \sigma_Z^2]^\top$ . We convert the frequency-domain signal into a time-domain signal  $y(t)$  by taking the inverse Fourier transform as  $y(t) = \frac{1}{K} \sum_{k=0}^{K-1} Y_k \exp(j2\pi k \Delta f t)$ . We then summarise the time-domain signal using their log temporal moments (Bharti et al., 2021), which are computed as  $x_j = \log \int y(t) t^j dt$ ,  $j = 0, 1, \dots, J$ . We set  $J = 2$ ,  $B = 4$  GHz, and  $K = 801$  similar to Huang et al. (2023), and place independent Gaussian priors on the log of all the parameters with mean vector  $[-19.0, -19.0, 22.0, -22.0]^\top$  and an identity covariance matrix.

The need for outlier-robust methods has long been recognised in this field (Savic et al., 2015). Typical causes of outliers are faulty or unstable measurements (Quimby, 2020) or destructive interference (Schneckenburger et al., 2018). We simulate a scenario where we observe  $n = 100$  time-series data of which  $\epsilon = 10\%$  record only noise due to faulty antennas. Example of an uncorrupted and an outlying time-series is in Figure 5.

We simulate  $m = 50,000$  samples from the Gaussian prior, and use an MDN for NLE and NSM-Bayes in this example. The pairwise bivariate scatter plots of the posterior samples from NLE, NSM-Bayes, and ACE is shown in Figure 6, along with the bivariate posterior densities from NSM-Bayes-conj. Again, this simulator is non-differentiable, and the pseudo-marginal MCMC version of GBI-SR does not work well for this problem so we exclude it. We see that the NLE posterior is severely biased, grossly underestimating  $\theta_3$  under the presence of outliers. In contrast, the posteriors for NSM-Bayes and NSM-Bayes-conj are robust and centred around the true parameter value. The posterior from ACE is also robust for  $\theta_3$ , however, it yields a diffuse, and slightly biased marginal posterior for  $\theta_2$ . The inference times are reported in Section B.4. Thus, NSM-Bayes and NSM-Bayes-conj yield robust posteriors under outlier contamination even for non-differentiable simulators whilst being well-calibrated, demonstrating that our approach can deliver reliable uncertainty quantification.

## 6 Conclusion

We proposed a novel SBI method based on a neural approximation to SM-Bayes which is provably robust to outliers and applies to arbitrary neural likelihood surrogates and prior distributions. Restricting this flexibility to a specific form of energy-based model with a Gaussian prior yields conjugate posterior updates, enabling fully amortised inference.

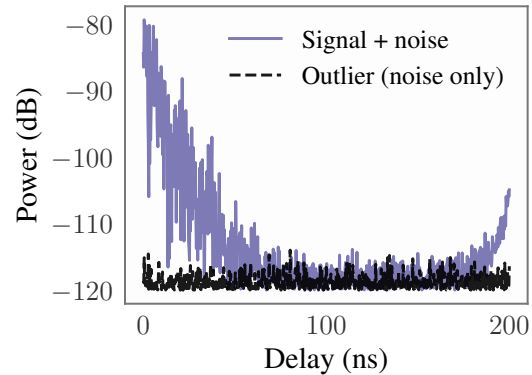


Figure 5: A valid (■) and an outlying (■) time series from the radio propagation model.

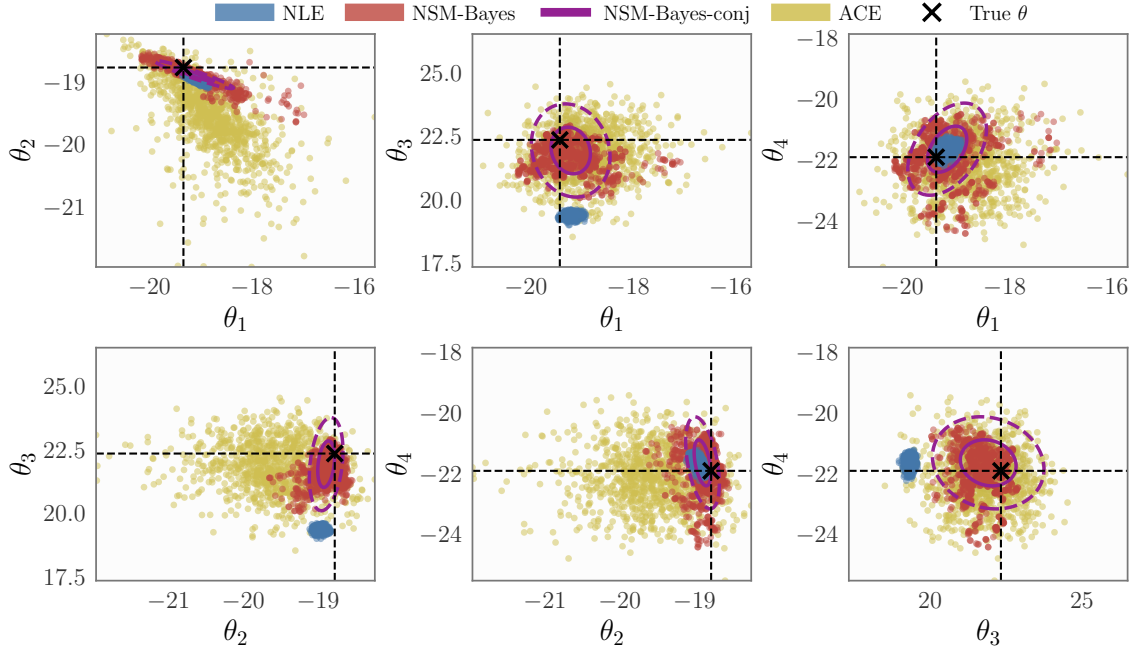


Figure 6: **Radio propagation model.** Pairwise scatter plots of approximate posterior samples from NLE (■), NSM-Bayes (■), and ACE (■) for the radio propagation model under 10% outliers, along with the NSM-Bayes-conj (■) posterior density. The NLE posterior is severely biased, while the NSM-Bayes and the NSM-Bayes-conj posteriors are around the true parameter, and therefore robust to outliers. ACE yields biased posterior for  $\theta_2$ , but works well for  $\theta_3$  and  $\theta_4$ . ACE also yields fairly robust posterior, but with increased uncertainty, especially for  $\theta_2$ .

As with all score-based methods, our approach is ill-suited to inference problems with highly multimodal, well-separated likelihoods (Wenliang, 2020; Zhang et al., 2022). In such cases, the GBI update may miss the full posterior structure, and can also affect training of the neural surrogate in the conjugate setting. Moreover, our formulation assumes continuous data and does not directly handle discrete or structured data. Extensions of score-matching to such settings exist (Hyvärinen, 2007; Lyu, 2009; Matsubara et al., 2024), including some permitting conjugacy (Laplante et al., 2025b). Integrating these within SBI remains future work. Finally, we focused on outlier robustness, whereas other forms of misspecification, such as distributional shifts or misspecified dependence structures, may also be relevant and warrant investigation.

## Acknowledgements

The authors thank Conor Hassan for tips on implementation and William Laplante for helpful feedback on a draft. AB and YH were supported by the Research Council of Finland grant no. 362534. CD and FXB were supported by the EPSRC grant [EP/Y022300/1] and CD was additionally supported by the project ‘Reliable insights from scientific simulations’ funded from the EPSRC grant [UKRI3030].

## References

Allen, L. J. (2017). A primer on stochastic epidemic models: Formulation, numerical simulation, and analysis. *Infectious Disease Modelling*, 2(2):128–142. 14

Alsing, J., Wandelt, B., and Feeney, S. (2018). Massive optimal data compression and density

estimation for scalable, likelihood-free inference in cosmology. *Monthly Notices of the Royal Astronomical Society*, 477(3):2874–2885. 1

Altamirano, M., Briol, F.-X., and Knoblauch, J. (2023). Robust and scalable Bayesian online changepoint detection. In *International Conference on Machine Learning*, pages 642–663. 2, 5, 7, 9, 29, 31

Altamirano, M., Briol, F.-X., and Knoblauch, J. (2024). Robust and conjugate Gaussian process regression. In *International Conference on Machine Learning*, pages 1155–1185. 5, 6, 7, 9, 11

Anau Montel, N., Alvey, J., and Weniger, C. (2025). Tests for model misspecification in simulation-based inference: From local distortions to global model checks. *Physical Review D*, 111:083013. 4

Andrieu, C. and Roberts, G. O. (2009). The pseudo-marginal approach for efficient monte carlo computations. *The Annals of Statistics*, 37(2):697–725. 16, 42

Arbel, M. and Gretton, A. (2018). Kernel conditional exponential family. In *International Conference on Artificial Intelligence and Statistics*, pages 1337–1346. 6

Barp, A., Briol, F.-X., Duncan, A. B., Girolami, M., and Mackey, L. (2019). Minimum Stein discrepancy estimators. In *Neural Information Processing Systems*, pages 12964–12976. 4, 5, 7

Beaumont, M. A. (2019). Approximate Bayesian computation. *Annual Review of Statistics and Its Application*, 6(1):379–403. 3

Bharti, A., Adeogun, R., Cai, X., Fan, W., Briol, F.-X., Clavier, L., and Pedersen, T. (2021). Joint modeling of received power, mean delay, and delay spread for wideband radio channels. *IEEE Transactions on Antennas and Propagation*, 69(8):4871–4882. 17

Bharti, A., Briol, F.-X., and Pedersen, T. (2022a). A general method for calibrating stochastic radio channel models with kernels. *IEEE Transactions on Antennas and Propagation*, 70(6):3986–4001. 1

Bharti, A., Filstroff, L., and Kaski, S. (2022b). Approximate Bayesian computation with domain expert in the loop. In *International Conference on Machine Learning*, pages 1893–1905. 1, 13

Bishop, C. M. (1994). Mixture density networks. Technical Report NCRG/94/004, Neural Computing Research Group, Department of Computer Science and Applied Mathematics, Aston University. 6, 10

Bissiri, P. G., Holmes, C. C., and Walker, S. G. (2016). A general framework for updating belief distributions. *Journal of the Royal Statistical Society: Series B (Statistical Methodology)*, 78(5):1103–1130. 2, 4

Boelts, J., Lueckmann, J.-M., Gao, R., and Macke, J. H. (2022). Flexible and efficient simulation-based inference for models of decision-making. *Elife*, 11:e77220. 3

Brehmer, J. (2021). Simulation-based inference in particle physics. *Nature Reviews Physics*, 3(5):305–305. 1

Briol, F.-X., Barp, A., Duncan, A. B., and Girolami, M. (2019). Statistical inference for generative models with maximum mean discrepancy. *arXiv:1906.05944*. 1, 3

Cannon, P., Ward, D., and Schmon, S. M. (2022). Investigating the impact of model misspecification in neural simulation-based Inference. *arXiv:2209.01845*. 1

Chen, Y., Gutmann, M. U., and Weller, A. (2023). Is learning summary statistics necessary for likelihood-free inference? In *International Conference on Machine Learning*, pages 4529–4544. [13](#)

Chérif-Abdellatif, B.-E. and Alquier, P. (2020). MMD-Bayes: robust Bayesian estimation via maximum mean discrepancy. In *2nd Symposium on Advances in Approximate Bayesian Inference*, pages 1–19. [4](#), [42](#)

Cranmer, K., Brehmer, J., and Louppe, G. (2020). The frontier of simulation-based inference. *Proceedings of the National Academy of Sciences of the United States of America*, 117(48). [1](#)

Dellaporta, C., Knoblauch, J., Damoulas, T., and Briol, F.-X. (2022). Robust Bayesian inference for simulator-based models via the MMD posterior bootstrap. In *International Conference on Artificial Intelligence and Statistics*, pages 943–970. [1](#), [2](#), [3](#), [12](#), [13](#), [42](#)

Duran-Martin, G., Altamirano, M., Shestopaloff, A. Y., Knoblauch, J., Jones, M., Briol, F.-X., and Murphy, K. (2024). Outlier-robust Kalman filtering through generalised Bayes. In *International Conference on Machine Learning*, pages 12138–12171. [7](#), [9](#)

Dyer, J., Quera-Bofarull, A., Chopra, A., Farmer, J. D., Calinescu, A., and Wooldridge, M. (2023). Gradient-assisted calibration for financial agent-based models. In *Proceedings of the Fourth ACM International Conference on AI in Finance*, pages 288–296. [1](#)

Elsemüller, L., Olischläger, H., Schmitt, M., Bürkner, P.-C., Köthe, U., and Radev, S. T. (2024). Sensitivity-aware amortized Bayesian inference. *Transactions in Machine Learning Research*. [4](#)

Elsemüller, L., Pratz, V., von Krause, M., Voss, A., Bürkner, P.-C., and Radev, S. T. (2025). Does unsupervised domain adaptation improve the robustness of amortized bayesian inference? a systematic evaluation. *Transactions on Machine Learning Research*. [1](#)

Ezzerg, A., Bogunovic, I., and Knoblauch, J. (2025). Robust Bayesian optimisation with unbounded corruptions. *arXiv:2511.15315v1*. [5](#), [9](#)

Fearnhead, P. and Prangle, D. (2012). Constructing summary statistics for approximate Bayesian computation: semi-automatic approximate bayesian computation. *Journal of the Royal Statistical Society. Series B (Statistical Methodology)*, 74(3):419–474. [13](#)

Fong, E., Lyddon, S., and Holmes, C. (2019). Scalable nonparametric sampling from multimodal posteriors with the posterior bootstrap. In *International Conference on Machine Learning*, pages 3443–3464. [3](#)

Frazier, D. T. and Drovandi, C. (2021). Robust approximate Bayesian inference with synthetic likelihood. *Journal of Computational and Graphical Statistics*, 30(4):958–976. [3](#)

Frazier, D. T., Nott, D. J., and Drovandi, C. (2025). Synthetic likelihood in misspecified models. *Journal of the American Statistical Association*, 120(550):884–895. [2](#), [3](#)

Frazier, D. T., Robert, C. P., and Rousseau, J. (2020). Model misspecification in ABC: consequences and diagnostics. *Journal of the Royal Statistical Society B: Statistical Methodology*, 82(2):421–444. [2](#), [3](#)

Fujisawa, M., Teshima, T., Sato, I., and Sugiyama, M. (2021).  $\gamma$ -abc: Outlier-robust approximate Bayesian computation based on a robust divergence estimator. In *International Conference on Artificial Intelligence and Statistics*, volume 130, pages 1783–1791. [2](#), [3](#)

Gao, R., Deistler, M., and Macke, J. H. (2023). Generalized Bayesian inference for scientific simulators via amortized cost estimation. *Advances in Neural Information Processing Systems*, 36. [1](#), [4](#), [12](#), [39](#), [42](#)

Geffner, T., Papamakarios, G., and Mnih, A. (2023). Compositional score modeling for simulation-based inference. In *International Conference on Machine Learning*, volume 202, pages 11098–11116. [6](#)

Ghosh, A. and Basu, A. (2016). Robust Bayes estimation using the density power divergence. *Annals of the Institute of Statistical Mathematics*, 68(2):413–437. [9](#), [28](#)

Gibbons, C. L., Mangen, M.-J. J., Plass, D., Havelaar, A. H., Brooke, R. J., Kramarz, P., Peterson, K. L., Stuurman, A. L., Cassini, A., Fèvre, E. M., et al. (2014). Measuring underreporting and under-ascertainment in infectious disease datasets: a comparison of methods. *BMC public health*, 14(1):147. [14](#)

Gloeckler, M., Deistler, M., and Macke, J. H. (2023). Adversarial robustness of amortized Bayesian inference. *International Conference on Machine Learning*, pages 11493–11524. [1](#), [4](#)

Gloeckler, M., Deistler, M., Weilbach, C. D., Wood, F., and Macke, J. H. (2024). All-in-one simulation-based inference. In *International Conference on Machine Learning*, volume 235, pages 15735–15766. [6](#)

Greenberg, D., Nonnenmacher, M., and Macke, J. (2019). Automatic posterior transformation for likelihood-free inference. In *International Conference on Machine Learning*, volume 97, pages 2404–2414. [4](#)

Gretton, A., Borgwardt, K., Rasch, M., Schölkopf, B., and Smola, A. (2006). A kernel method for the two-sample-problem. In *Advances in Neural Information Processing Systems*, volume 19. [12](#)

Hermans, J., Delaunoy, A., Rozet, F., Wehenkel, A., Begy, V., and Louppe, G. (2022). A trust crisis in simulation-based inference? Your posterior approximations can be unfaithful. *Transactions in Machine Learning Research*. [1](#), [7](#)

Hikida, Y., Bharti, A., Jeffrey, N., and Briol, F.-X. (2025). Multilevel neural simulation-based inference. In *Conference on Neural Information Processing Systems*. [4](#)

Horn, R. A. and Johnson, C. R. (2012). *Matrix analysis*. Cambridge university press. [30](#), [35](#)

House, T., Ross, J. V., and Sirl, D. (2013). How big is an outbreak likely to be? methods for epidemic final-size calculation. *Proceedings of the Royal Society A: Mathematical, Physical and Engineering Sciences*, 469(2150). [14](#)

Huang, D., Bharti, A., Souza, A. H., Acerbi, L., and Kaski, S. (2023). Learning robust statistics for simulation-based inference under model misspecification. In *Conference on Neural Information Processing Systems*. [1](#), [4](#), [12](#), [17](#), [41](#)

Huber, P. J. and Ronchetti, E. M. (1981). Robust statistics, ser. *Wiley Ser Probab Math Stat New York, NY, USA Wiley-IEEE*, 52:54. [8](#)

Hyvärinen, A. (2006). Estimation of non-normalized statistical models by score matching. *Journal of Machine Learning Research*, 6:695–708. [2](#), [4](#)

Hyvärinen, A. (2007). Some extensions of score matching. *Computational Statistics and Data Analysis*, 51(5):2499–2512. [4](#), [18](#)

Jeffrey, N., Alsing, J., and Lanusse, F. (2021). Likelihood-free inference with neural compression of DES SV weak lensing map statistics. *Monthly Notices of the Royal Astronomical Society*, 501(1):954–969. [1](#)

Jiang, H., Wang, Y., and Yang, Y. (2025). Simulation-based inference via langevin dynamics with score matching. *arXiv:2509.03853*. [6](#)

Jones, A. and Leimkuhler, B. (2011). Adaptive stochastic methods for sampling driven molecular systems. *The Journal of chemical physics*, 135(8). [42](#)

Kelly, R. P., Nott, D. J., Frazier, D. T., Warne, D. J., and Drovandi, C. (2024). Misspecification-robust sequential neural likelihood for simulation-based inference. *Transactions on Machine Learning Research*. [1](#), [4](#), [12](#), [41](#)

Kelly, R. P., Warne, D. J., Frazier, D. T., Nott, D. J., Gutmann, M. U., and Drovandi, C. (2025). Simulation-based Bayesian inference under model misspecification. *arXiv:2503.12315*. [1](#)

Key, O., Fernandez, T., Gretton, A., and Briol, F.-X. (2021). Composite goodness-of-fit tests with kernels. In *NeurIPS 2021 Workshop Your Model Is Wrong: Robustness and Misspecification in Probabilistic Modeling*. [4](#)

Khoo, S., Wang, Y., Liu, S., and Beaumont, M. (2025). Direct fisher score estimation for likelihood maximization. In *Conference on Neural Information Processing Systems*. [6](#)

Kingma, D. P. (2014). Adam: A method for stochastic optimization. *arXiv:1412.6980*. [8](#)

Kisamori, K., Kanagawa, M., and Yamazaki, K. (2020). Simulator calibration under covariate shift with kernels. In *International Conference on Artificial Intelligence and Statistics*, pages 1244–1253. [2](#), [3](#)

Knoblauch, J., Jewson, J., and Damoulas, T. (2022). An optimization-centric view on Bayes' rule: reviewing and generalizing variational inference. *Journal of Machine Learning Research*, 23(132):1–109. [4](#)

Krouglova, A. N., Johnson, H. R., Confavreux, B., Deistler, M., and Gonçalves, P. J. (2025). Multi-fidelity simulation-based inference for computationally expensive simulators. *arXiv:2502.08416*. [4](#)

Kypraios, T., Neal, P., and Prangle, D. (2017). A tutorial introduction to Bayesian inference for stochastic epidemic models using approximate Bayesian computation. *Mathematical Biosciences*, 287:42–53. [1](#)

Laplante, W., Altamirano, M., Duncan, A. B., Knoblauch, J., and Briol, F.-X. (2025a). Robust and conjugate spatio-temporal Gaussian processes. In *International Conference on Machine Learning*. [5](#), [9](#)

Laplante, W., Altamirano, M., Knoblauch, J., Duncan, A., and Briol, F.-X. (2025b). Conjugate generalised Bayesian inference for discrete doubly intractable problems. *arxiv:2511.23275*. [8](#), [18](#)

Leclercq, F. (2022). Simulation-based inference of Bayesian hierarchical models while checking for model misspecification. *Physical Sciences Forum*, 5(4):4. [4](#)

Legramanti, S., Durante, D., and Alquier, P. (2022). Concentration and robustness of discrepancy-based ABC via Rademacher complexity. *arXiv:2206.06991*. [2](#), [3](#)

Li, R., Pei, S., Chen, B., Song, Y., Zhang, T., Yang, W., and Shaman, J. (2020). Substantial undocumented infection facilitates the rapid dissemination of novel coronavirus (sars-cov-2). *Science*, 368(6490):489–493. [14](#)

Linhart, J., Cardoso, G. V., Gramfort, A., Corff, S. L., and Rodrigues, P. L. (2024). Diffusion posterior sampling for simulation-based inference in tall data settings. *arXiv:2404.07593*. [6](#)

Liu, X. and Briol, F.-X. (2025). On the robustness of kernel goodness-of-fit tests. *Journal of Machine Learning Research*, 26(262):1–72. [7](#)

Lueckmann, J.-M., Bassetto, G., Karaletsos, T., and Macke, J. H. (2019). Likelihood-free inference with emulator networks. In *Advances in Approximate Bayesian Inference*, pages 32–53. [3](#)

Lueckmann, J.-M., Gonçalves, P. J., Bassetto, G., Öcal, K., Nonnenmacher, M., and Macke, J. H. (2017). Flexible statistical inference for mechanistic models of neural dynamics. In *Advances in Neural Information Processing Systems*, page 1289–1299. [4](#)

Lyddon, S., Walker, S., and Holmes, C. (2018). Nonparametric learning from Bayesian models with randomized objective functions. In *Conference on Neural Information Processing Systems*, page 2075–2085. [3](#)

Lyddon, S. P., Holmes, C. C., and Walker, S. G. (2019). General Bayesian updating and the loss-likelihood bootstrap. *Biometrika*, 106(2):465–478. [7](#)

Lyu, S. (2009). Interpretation and generalization of score matching. In *Conference on Uncertainty in Artificial Intelligence*, pages 359–366. [4, 18](#)

Mao, R., Lee, J. E., and Edwards, M. C. (2025). Robust and scalable simulation-based inference for gravitational wave signals with gaps. *arXiv:2512.18290*. [1](#)

Martin, G. M., Frazier, D. T., and Robert, C. P. (2024). Approximating Bayes in the 21st Century. *Statistical Science*, 39(1):20–45. [1](#)

Matsubara, T., Knoblauch, J., Briol, F.-X., and Oates, C. J. (2022). Robust generalised Bayesian inference for intractable likelihoods. *Journal of the Royal Statistical Society: Series B: (Statistical Methodology)*, 84(3):997–1022. [4, 5, 9](#)

Matsubara, T., Knoblauch, J., Briol, F.-X., and Oates, C. J. (2024). Generalized bayesian inference for discrete intractable likelihood. *Journal of the American Statistical Association*, 119(547):2345–2355. [4, 5, 7, 18](#)

Meyer, A. D., Guerrero, S. M., Dean, N. E., Anderson, K. B., Stoddard, S. T., and Perkins, T. A. (2025). Predictability of infectious disease outbreak severity: Chikungunya as a case study. *Science Advances*, 11(40):eadt5419. [14](#)

Mishra, A., Habermann, D., Schmitt, M., Radev, S. T., and Bürkner, P.-C. (2025). Robust amortized Bayesian inference with self-consistency losses on unlabeled data. *arxiv:2501.13483*. [1, 2, 4](#)

Nautiyal, M., Hellander, A., and Singh, P. (2025). Condisim: Conditional diffusion models for simulation based inference. *arXiv:2505.08403*. [6](#)

Nott, D. J., Drovandi, C., and Frazier, D. T. (2024). Bayesian inference for misspecified generative models. *Annual Review of Statistics and Its Application*, 11:179–202. [1](#)

O’Callaghan, M., Mandel, K. S., and Gilmore, G. (2025). Robust variational neural posterior estimation for simulation-based inference. *arXiv:2509.05724*. [1, 4](#)

Pacchiardi, L. and Dutta, R. (2022). Score matched neural exponential families for likelihood-free inference. *Journal of Machine Learning Research*, 23(38):1–71. [6](#)

Pacchiardi, L., Khoo, S., and Dutta, R. (2024). Generalized Bayesian likelihood-free inference. *Electronic Journal of Statistics*, 18:3628–3686. [2](#), [4](#), [12](#), [39](#), [42](#), [45](#)

Papamakarios, G. and Murray, I. (2016). Fast  $\epsilon$ -free inference of simulation models with Bayesian conditional density estimation. In *Advances in Neural Information Processing Systems*, pages 1036–1044. [4](#)

Papamakarios, G., Nalisnick, E., Rezende, D. J., Mohamed, S., and Lakshminarayanan, B. (2021). Normalizing flows for probabilistic modeling and inference. *Journal of Machine Learning Research*, 22(57):1–64. [2](#)

Papamakarios, G., Pavlakou, T., and Murray, I. (2017). Masked autoregressive flow for density estimation. In *Advances in Neural Information Processing Systems*, volume 30. [6](#), [10](#), [11](#)

Papamakarios, G., Sterratt, D., and Murray, I. (2019). Sequential neural likelihood: Fast likelihood-free inference with autoregressive flows. In *International Conference on Artificial Intelligence and Statistics*, volume 89, pages 837–848. [2](#), [3](#)

Pedersen, T. (2019). Stochastic multipath model for the in-room radio channel based on room electromagnetics. *IEEE Transactions on Antennas and Propagation*, 67(4):2591–2603. [16](#)

Prangle, D. (2020). gk: An R Package for the g-and-k and generalised g-and-h distributions. *The R Journal*, 12(1):7. [13](#)

Price, L. F., Drovandi, C. C., Lee, A., and Nott, D. J. (2018). Bayesian Synthetic Likelihood. *Journal of Computational and Graphical Statistics*, 27(1):1–11. [3](#), [13](#)

Quera-Bofarull, A., Chopra, A., Calinescu, A., Wooldridge, M., and Dyer, J. (2023). Bayesian calibration of differentiable agent-based models. *arXiv:2305.15340*. [1](#)

Quimby, J. (2020). Channel sounder measurement verification: Conducted tests. Technical report, Institute for Telecommunication Sciences. [17](#)

Radev, S. T., Mertens, U. K., Voss, A., Ardizzone, L., and Köthe, U. (2022). Bayesflow: Learning complex stochastic models with invertible neural networks. *IEEE Transactions on Neural Networks and Learning Systems*, 33(4):1452–1466. [4](#)

Radev, S. T., Schmitt, M., Pratz, V., Picchini, U., Köthe, U., and Bürkner, P.-C. (2023). Jana: Jointly amortized neural approximation of complex bayesian models. In *Conference on Uncertainty in Artificial Intelligence*, pages 1695–1706. [3](#)

Ramírez-Hassan, A. and Frazier, D. T. (2024). Testing model specification in approximate Bayesian computation using asymptotic properties. *Journal of Computational and Graphical Statistics*, 33(3):1122–1128. [4](#)

Reimann, H. (2024). *Towards robust inference for Bayesian filtering of linear Gaussian dynamical systems subject to additive change*. Masters thesis, University of Potsdam. [5](#), [9](#)

Robert, C. P. and Casella, G. (2000). *Monte Carlo Statistical Methods*. Springer. [3](#)

Rooijakkers, J., Ronneberg, L., Briol, F.-X., Knoblauch, J., and Altamirano, M. (2025). Multi-output robust and conjugate Gaussian processes. *arXiv:2510.26401*. [5](#), [9](#)

Rousseeuw, P. J. and Driessen, K. V. (1999). A fast algorithm for the minimum covariance determinant estimator. *Technometrics*, 41(3):212–223. [7](#)

Ruhlmann, P.-L., Rodrigues, P. L., Arbel, M., and Forbes, F. (2025). Flow matching for robust simulation-based inference under model misspecification. *arXiv:2509.23385*. [1](#)

Sadasivan, D., Cordero, I., Graham, A., Marsh, C., Kupcho, D., Mourad, M., and Mai, M. (2025). Deep neural network driven simulation based inference method for pole position estimation under model misspecification. *arXiv:2507.18824*. [1](#)

Sasaki, H. and Hyvärinen, A. (2018). Neural-kernelized conditional density estimation. *arXiv:1806.01754*. [6](#)

Savic, V., Ferrer-Coll, J., Ängskog, P., Chilo, J., Stenumgaard, P., and Larsson, E. G. (2015). Measurement analysis and channel modeling for toa-based ranging in tunnels. *IEEE Transactions on Wireless Communications*, 14(1):456–467. [17](#)

Schmitt, M., Bürkner, P.-C., Köthe, U., and Radev, S. T. (2024). Detecting model misspecification in amortized Bayesian inference with neural networks: An extended investigation. *arXiv:2406.03154*. [4](#)

Schmon, S. M., Cannon, P. W., and Knoblauch, J. (2020). Generalized posteriors in Approximate Bayesian Computation. In *Advances in Approximate Bayesian Inference*, pages 1–11. [4](#)

Schneckenburger, N., Fiebig, U.-C., Lo, S., Enge, P., and Lilley, R. (2018). Characterization and mitigation of multipath for terrestrial based aviation radionavigation. *Navigation: Journal of The Institute of Navigation*, 65(2):143–156. [17](#)

Senouf, O., Wehenkel, A., Vincent-Cuaz, C., Abbe, E., and Frossard, P. (2025). Inductive domain transfer in misspecified simulation-based inference. In *Conference on Neural Information Processing Systems*. [1](#), [2](#)

Sharrock, L., Simons, J., Liu, S., and Beaumont, M. (2024). Sequential neural score estimation: Likelihood-free inference with conditional score based diffusion models. In *International Conference on Machine Learning*, volume 235, pages 44565–44602. [6](#)

Simons, J., Sharrock, L., Liu, S., and Beaumont, M. (2023). Neural score estimation: Likelihood-free inference with conditional score based diffusion models. In *Advances in Approximate Bayesian Inference*. [6](#)

Sun, S., Nicholls, G. K., and Lee, J. E. (2026). Amortized simulation-based inference in generalized Bayes via neural posterior estimation. *arxiv:2601.22367*. [1](#), [4](#)

Swierc, P., Tamargo-Arizmendi, M., Ćiprijanović, A., and Nord, B. D. (2024). Domain-adaptive neural posterior estimation for strong gravitational lens analysis. *arXiv:2410.16347*. [1](#)

Syring, N. and Martin, R. (2019). Calibrating general posterior credible regions. *Biometrika*, 106(2):479–486. [7](#), [8](#), [38](#), [40](#)

Tejero-Cantero, A., Boelts, J., Deistler, M., Lueckmann, J.-M., Durkan, C., Gonçalves, P. J., Greenberg, D. S., and Macke, J. H. (2020). sbi: A toolkit for simulation-based inference. *Journal of Open Source Software*, 5(52):2505. [11](#), [13](#)

Thomas, O., Sá-Leão, R., de Lencastre, H., Kaski, S., Corander, J., and Pesonen, H. (2025). Misspecification-robust likelihood-free inference in high dimensions. *Computational Statistics*, pages 1–41. [2](#)

Tuckwell, H. C. and Williams, R. J. (2007). Some properties of a simple stochastic epidemic model of SIR type. *Mathematical biosciences*, 208(1):76–97. [14](#)

Turin, G. L., Clapp, F. D., Johnston, T. L., Fine, S. B., and Lavry, D. (1972). A statistical model of urban multipath propagation. *IEEE Transactions on Vehicular Technology*, 21(1):1–9. [16](#)

Verma, Y., Bharti, A., and Garg, V. (2025). Robust simulation-based inference under missing data via neural processes. In *International Conference on Learning Representation*. [1](#), [4](#)

Wainwright, M. J. (2019). *High-dimensional statistics: A non-asymptotic viewpoint*, volume 48. Cambridge university press. [9](#)

Wang, Y., Kaji, T., and Rockova, V. (2022). Approximate Bayesian computation via classification. *Journal of Machine Learning Research*, 23(350):1–49. [13](#)

Ward, D., Cannon, P., Beaumont, M., Fasiolo, M., and Schmon, S. M. (2022). Robust neural posterior estimation and statistical model criticism. In *Advances in Neural Information Processing Systems*, pages 33845–33859. [1](#), [4](#)

Wehenkel, A., Gamella, J. L., Sener, O., Behrmann, J., Sapiro, G., Jacobsen, J.-H., and Cuturi, M. (2025). Addressing misspecification in simulation-based inference through data-driven calibration. In *International Conference on Machine Learning*. [1](#), [2](#), [4](#)

Wenliang, L. K. (2020). Blindness of score-based methods to isolated components and mixing proportions. *arXiv:2008.10087*. [18](#)

Wu, P.-S. and Martin, R. (2023). A comparison of learning rate selection methods in generalized Bayesian inference. *Bayesian Analysis*, 18(1):105–132. [4](#), [7](#)

Wu, Y., Radev, S., and Tuerlinckx, F. (2024). Testing and improving the robustness of amortized Bayesian inference for cognitive models. *arXiv:2412.20586*. [1](#)

Xu, J., Scealy, J. L., Wood, A. T. A., and Zou, T. (2022). Generalized score matching for regression. *arXiv:2203.09864*, pages 1–35. [5](#)

Yu, S., Drton, M., and Shojaie, A. (2019). Generalized score matching for non-negative data. *Journal of Machine Learning Research*, 20:1–70. [5](#)

Yu, S., Drton, M., and Shojaie, A. (2022). Generalized score matching for general domains. *Information and Inference: A Journal of the IMA*, 11(2):739–780. [5](#)

Yuyan, W., Evans, M., and Nott, D. J. (2025). Robust Bayesian methods using amortized simulation-based inference. *arXiv:2504.09475*. [4](#)

Zaheer, M., Kottur, S., Ravanbakhsh, S., Poczos, B., Salakhutdinov, R. R., and Smola, A. J. (2017). Deep sets. *Advances in Neural Information Processing Systems*, 30. [42](#)

Zammit-Mangion, A., Sainsbury-Dale, M., and Huser, R. (2025). Neural methods for amortized inference. *Annual Review of Statistics and Its Application*, 12(1):311–335. [1](#)

Zhang, M., Key, O., Hayes, P., Barber, D., Paige, B., and Briol, F.-X. (2022). Towards healing the blindness of score matching. In *NeurIPS 2022 Workshop on Score-Based Methods*. [18](#)

Zhang, Y., Pan, J., Li, L. K., Liu, W., Chen, Z., Liu, X., and Wang, J. (2023). On the properties of Kullback-Leibler divergence between multivariate Gaussian distributions. *Advances in Neural Information Processing Systems*, 36:58152–58165. [34](#)

## Supplementary Materials

Section A contains the proofs of our theoretical results, and Section B consists of the implementation details and additional results for the experiments in Section 5.

### A Proofs

We now present our proofs. Section A.1 proves conjugacy for NSM-Bayes-conj. Section A.2 proves that NLE is not globally-bias robust, whereas Section A.3 proves robustness of NSM-Bayes in the general setting. Finally, A.4 contains proofs of all results associated with the IMQ weight and sub-exponential or Gaussian priors.

#### A.1 Proof of Proposition 1

*Proof.* We aim to derive the conjugate form of  $\pi_{\text{NSM}}(\theta|x_{1:n}^o)$  given in Proposition 1. Recall that:

$$\mathcal{L}_{\text{NSM}}(\theta; x_{1:n}^o, \hat{\phi}_m) := \frac{1}{n} \sum_{i=1}^n \left\| W(x_i^o)^\top \nabla_x \log q_{\hat{\phi}_m}(x_i^o|\theta) \right\|_2^2 + 2\nabla_x \cdot W(x_i^o) W(x_i^o)^\top \nabla_x \log q_{\hat{\phi}_m}(x_i^o|\theta).$$

Substituting  $W(x) := w(x)I_{d_x}$  and setting  $q_\phi(x|\theta) \propto \exp(T_\phi(x)^\top \theta + b_\phi(x))$ , we get

$$\begin{aligned} \mathcal{L}_{\text{NSM}}(\theta; x_{1:n}^o, \hat{\phi}_m) &= \frac{1}{n} \sum_{i=1}^n \left\| w(x_i^o)^\top \left( \nabla_x T_{\hat{\phi}_m}(x_i^o)^\top \theta + \nabla_x b_{\hat{\phi}_m}(x_i^o) \right) \right\|_2^2 + 2\nabla_x \cdot \left( w(x_i^o)^2 \nabla_x b_{\hat{\phi}_m}(x_i^o)^\top \right) \\ &\quad + 2\nabla_x \cdot \left( w(x_i^o)^2 \nabla_x T_{\hat{\phi}_m}(x_i^o)^\top \right) \theta \end{aligned}$$

We can then express this loss as a quadratic objective in  $\theta$ :

$$\mathcal{L}_{\text{NSM}}(\theta; x_{1:n}^o, \hat{\phi}_m) = \theta^\top M_1(x_i^o) \theta + 2\theta^\top \ell_1(x_i^o) + \ell_2(x_i^o) + 2\theta^\top M_2(x_i^o) + 2\ell_3(x_i^o), \quad \text{where}$$

$$\begin{aligned} M_1(x_{1:n}^o) &= \frac{1}{n} \sum_{i=1}^n w(x_i^o)^2 \nabla_x T_{\hat{\phi}_m}(x_i^o) \nabla_x T_{\hat{\phi}_m}(x_i^o)^\top, \quad \ell_1(x_{1:n}^o) = \frac{1}{n} \sum_{i=1}^n w(x_i^o)^2 \nabla_x T_{\hat{\phi}_m}(x_i^o) \nabla_x b_{\hat{\phi}_m}(x_i^o) \\ \ell_2(x_{1:n}^o) &= \frac{1}{n} \sum_{i=1}^n w(x_i^o)^2 \nabla_x b_{\hat{\phi}_m}(x_i^o)^\top \nabla_x b_{\hat{\phi}_m}(x_i^o), \quad M_2(x_{1:n}^o) = \frac{1}{n} \sum_{i=1}^n \nabla_x \cdot \left( w(x_i^o)^2 \nabla_x T_{\hat{\phi}_m}(x_i^o)^\top \right)^\top \\ \ell_3(x_{1:n}^o) &= \frac{1}{n} \sum_{i=1}^n \nabla_x \cdot \left( w(x_i^o)^2 \nabla_x b_{\hat{\phi}_m}(x_i^o)^\top \right)^\top. \end{aligned}$$

For the Gaussian-like prior  $\pi(\theta) \propto \exp(\frac{1}{2}(\theta - \mu)^\top \Sigma^{-1}(\theta - \mu))$ , we then obtain the conjugate expression for the NSM-Bayes posterior  $\pi_{\text{NSM}}(\theta|x_{1:n}^o, \hat{\phi}_m) \propto \mathcal{N}(\mu_{n,m}, \Sigma_{n,m})$  by completing the square:

$$\begin{aligned} \log \pi_{\text{NSM}}(\theta|x_{1:n}^o, \hat{\phi}_m) &= \log \pi(\theta) - \beta n \mathcal{L}_{\text{NSM}}(\theta; x_{1:n}^o, \hat{\phi}_m) + C \\ &= -\frac{1}{2}(\theta - \mu)^\top \Sigma^{-1}(\theta - \mu) - \beta n \left[ \theta^\top M_1(x_{1:n}^o) \theta + 2\theta^\top (\ell_1(x_{1:n}^o) + M_2(x_{1:n}^o)) \right] + C' \\ &= -\frac{1}{2}(\theta^\top \Sigma^{-1} \theta - 2\theta^\top \Sigma^{-1} \mu) - \beta n \theta^\top M_1(x_{1:n}^o) \theta - 2\beta n \theta^\top (\ell_1(x_{1:n}^o) + M_2(x_{1:n}^o)) + C'' \\ &= -\frac{1}{2} \left[ \theta^\top (\Sigma^{-1} + 2\beta n M_1(x_{1:n}^o)) \theta - 2\theta^\top (\Sigma^{-1} \mu - 2\beta n (\ell_1(x_{1:n}^o) + M_2(x_{1:n}^o))) \right] + C'' \\ &= -\frac{1}{2} \left[ \theta^\top \Sigma_{n,m}^{-1} \theta - 2\theta^\top \mu_{n,m} \right] + C''. \end{aligned}$$

Here  $C, C', C''$  are constants in  $\theta$ , and

$$\Sigma_{n,m}^{-1} := \Sigma^{-1} + 2\beta n M_1(x_{1:n}^o) = \Sigma^{-1} + 2\beta \sum_{i=1}^n w(x_i^o)^2 \nabla_x T_{\hat{\phi}_m}(x_i^o) \nabla_x T_{\hat{\phi}_m}(x_i^o)^\top, \quad (17)$$

$$\mu_{n,m} := \Sigma_{n,m} [\Sigma^{-1} \mu - 2\beta n M_2(x_{1:n}^o) - 2\beta n \ell_1(x_{1:n}^o)] \quad (18)$$

$$= \Sigma_{n,m} \left[ \Sigma^{-1} \mu - 2\beta \sum_{i=1}^n \left( \nabla_x \cdot \left( w(x_i^o)^2 \nabla_x T_{\hat{\phi}_m}(x_i^o)^\top \right)^\top + w(x_i^o)^2 \nabla_x T_{\hat{\phi}_m}(x_i^o) \nabla_x b_{\hat{\phi}_m}(x_i^o) \right) \right].$$

This completes the proof.  $\square$

## A.2 Proof of Theorem 1

*Proof.* Recall the PIF for the NLE posterior:

$$\text{PIF}_\Delta(x^c, \theta, \mathbb{P}_0, \mathcal{L}_{\text{NLE}}) := \left. \frac{d}{d\epsilon} \pi_{\text{NLE}}(\theta | \mathbb{P}_{\epsilon, x^c}, \hat{\phi}_m) \right|_{\epsilon=0}.$$

From (17) of Ghosh and Basu (2016), we have for the NLE posterior that:

$$\begin{aligned} & \sup_{\theta \in \Theta, x^c \in \mathcal{X}} |\text{PIF}_\Delta(x^c, \theta; \mathbb{P}_n, \mathcal{L}_{\text{NLE}})| \\ &= \beta n \times \sup_{\theta \in \Theta, x^c \in \mathcal{X}} \pi_{\text{NLE}}(\theta | x_{1:n}^o, \hat{\phi}_m) \times \left| -D\mathcal{L}_{\text{NLE}}(x^c; \theta, \mathbb{P}_n) + \int D\mathcal{L}_{\text{NLE}}(x^c; \theta', \mathbb{P}_n) \pi_{\text{NLE}}(\theta' | x_{1:n}^o, \hat{\phi}_m) d\theta' \right| \end{aligned}$$

where

$$\begin{aligned} D\mathcal{L}_{\text{NLE}}(x^c; \theta, \mathbb{P}_n) &:= \left. \frac{d}{d\epsilon} (-\mathcal{L}_{\text{NLE}}(\theta; \mathbb{P}_{\epsilon, x^c})) \right|_{\epsilon=0} \\ &= \left. \frac{d}{d\epsilon} \left( (1-\epsilon) \left( \frac{1}{n} \sum_{i=1}^n \log q_{\hat{\phi}_m}(x_i^o | \theta) \right) + \epsilon \left( \log q_{\hat{\phi}_m}(x^c | \theta) \right) \right) \right|_{\epsilon=0} \\ &= \log q_{\hat{\phi}_m}(x^c | \theta) - \frac{1}{n} \sum_{i=1}^n \log q_{\hat{\phi}_m}(x_i^o | \theta). \end{aligned}$$

Instead of considering the supremum over all possible  $\theta$  values, we consider the lower bound obtained by fixing  $\theta = \theta_{\text{MAP}}$ , the maximum *a posteriori* (MAP) estimate of the NLE posterior:

$$\begin{aligned} & \sup_{\theta \in \Theta, x^c \in \mathcal{X}} |\text{PIF}_\Delta(x^c, \theta, \mathbb{P}_n, \mathcal{L}_{\text{NLE}})| \\ & \geq C_1 \sup_{x^c \in \mathcal{X}} \left| -D\mathcal{L}_{\text{NLE}}(x^c; \theta_{\text{MAP}}, \mathbb{P}_n) + \int D\mathcal{L}_{\text{NLE}}(x^c; \theta', \mathbb{P}_n) \pi_{\text{NLE}}(\theta' | x_{1:n}^o, \hat{\phi}_m) d\theta' \right| \\ & \geq C_1 \left[ \sup_{x^c \in \mathcal{X}} \int D\mathcal{L}_{\text{NLE}}(x^c; \theta', \mathbb{P}_n) \pi_{\text{NLE}}(\theta' | x_{1:n}^o, \hat{\phi}_m) d\theta' - \inf_{x^c \in \mathcal{X}} D\mathcal{L}_{\text{NLE}}(x^c; \theta_{\text{MAP}}, \mathbb{P}_n) \right], \end{aligned}$$

where the constant  $C_1 = \beta n \times \pi_{\text{NLE}}(\theta_{\text{MAP}} | x_{1:n}^o, \hat{\phi}_m) = \beta n \times \frac{1}{Z} \prod_{i=1}^n q_{\hat{\phi}_m}(x_i^o | \theta_{\text{MAP}}) \pi(\theta_{\text{MAP}}) > 0$  (this must be strictly greater than zero since  $\theta_{\text{MAP}}$  lies in the support of the posterior), and the second inequality uses  $\sup |f(x) - g(x)| \geq \sup f(x) - \inf g(x)$ .

Now we note that we can lower bound this supremum by replacing  $x^c$  by  $x_n^o$ :

$$\begin{aligned} & \sup_{x^c \in \mathcal{X}} \int D\mathcal{L}_{\text{NLE}}(x^c; \theta', \mathbb{P}_n) \pi_{\text{NLE}}(\theta' | x_{1:n}^o, \hat{\phi}_m) d\theta' \\ &= \sup_{x^c \in \mathcal{X}} \int \left( \log q_{\hat{\phi}_m}(x^c | \theta') - \frac{1}{n} \sum_{i=1}^n \log q_{\hat{\phi}_m}(x_i^o | \theta') \right) \pi_{\text{NLE}}(\theta' | x_{1:n}^o, \hat{\phi}_m) d\theta' \\ &\geq \int \left( \log q_{\hat{\phi}_m}(x_n^o | \theta') - \frac{1}{n} \sum_{i=1}^n \log q_{\hat{\phi}_m}(x_i^o | \theta') \right) \pi_{\text{NLE}}(\theta' | x_{1:n}^o, \hat{\phi}_m) d\theta' \\ &\geq \left( 1 - \frac{1}{n} \right) \int \log q_{\hat{\phi}_m}(x_n^o | \theta') \pi_{\text{NLE}}(\theta' | x_{1:n}^o, \hat{\phi}_m) d\theta' - \frac{1}{n} \sum_{i=1}^{n-1} \int \log q_{\hat{\phi}_m}(x_i^o | \theta') \pi_{\text{NLE}}(\theta' | x_{1:n}^o, \hat{\phi}_m) d\theta' \\ &> -\infty \end{aligned}$$

where the final step follows from the fact that based on the assumptions the posterior expectations are finite, i.e.  $\int |\log q_{\hat{\phi}_m}(x_i^o | \theta')| \pi_{\text{NLE}}(\theta' | x_{1:n}^o, \hat{\phi}_m) d\theta' < \infty$  for  $i = 1, \dots, n$ . Finally, we have

$$-\inf_{x^c \in \mathcal{X}} D\mathcal{L}_{\text{NLE}}(x^c, \theta_{\text{MAP}}, \mathbb{P}_n) = -\inf_{x^c \in \mathcal{X}} \log q_{\hat{\phi}_m}(x^c | \theta_{\text{MAP}}) + \frac{1}{n} \sum_{i=1}^n \log q_{\hat{\phi}_m}(x_i^o | \theta_{\text{MAP}}) \rightarrow \infty$$

since we assumed that  $q_{\hat{\phi}_m}$  is a normalised density in  $\mathbb{R}^d$  and hence  $\inf_{x \in \mathcal{X}} q_{\hat{\phi}_m}(x | \theta_{\text{MAP}}) = 0$ . Thus,  $-\inf_{x \in \mathcal{X}} \log q_{\hat{\phi}_m}(x | \theta_{\text{MAP}}) = \infty$  and hence  $\sup_{\theta \in \Theta, x^c \in \mathcal{X}} |\text{PIF}_\Delta(x^c, \theta, \mathbb{P}_n, \mathcal{L}_{\text{NLE}})| = \infty$ .  $\square$

### A.3 Proof of Theorem 2

*Proof.* By Proposition B.1 of Altamirano et al. (2023), we need to show there exists  $\gamma : \Theta \rightarrow \mathbb{R}$  such that: (1)  $\sup_{x \in \mathcal{X}} \mathcal{L}_{\text{NSM}}(\theta; x, \hat{\phi}_m) \leq \gamma(\theta)$ , (2)  $\sup_{\theta \in \Theta} \gamma(\theta)\pi(\theta) < \infty$ , and (3)

$\int_{\Theta} \gamma(\theta)\pi(\theta)d\theta < \infty$ . Let  $S_{\theta}(x) := \|\nabla_x \log q_{\hat{\phi}_m}(x|\theta)\|_2$  and  $H_{\theta}(x) := |\text{Tr}(\nabla_x^2 \log q_{\hat{\phi}_m}(x|\theta))|$ , then:

$$\mathcal{L}_{\text{NSM}}(\theta; x, \hat{\phi}_m) = w(x)^2 S_{\theta}(x)^2 + 2 \left( \nabla_x w(x)^2 \right)^{\top} \nabla_x \log q_{\hat{\phi}_m}(x|\theta) + 2w(x)^2 H_{\theta}(x).$$

Therefore, under the assumptions of the theorem, we have:

$$\begin{aligned} \mathcal{L}_{\text{NSM}}(\theta; x, \hat{\phi}_m) &= w(x)^2 S_{\theta}(x)^2 + 2 \left( \nabla_x w(x)^2 \right)^{\top} \nabla_x \log q_{\hat{\phi}_m}(x|\theta) + 2w(x)^2 H_{\theta}(x) \\ &\leq f(\theta)^2 + 2 \left\| \nabla_x w(x)^2 \right\|_2 S_{\theta}(x) + 2g(\theta) \\ &\leq f(\theta)^2 + 2f(\theta) + 2g(\theta) \end{aligned}$$

where we used the Cauchy-Schwarz inequality in the first inequality. Therefore, it follows from Assumption A4 that

$$\sup_x \mathcal{L}_{\text{NSM}}(\theta; x, \hat{\phi}_m) \leq f(\theta)^2 + 2f(\theta) + 2g(\theta) < \infty$$

and therefore conditions 2 and 3 above hold with  $\gamma(\theta) := f(\theta)^2 + 2f(\theta) + 2g(\theta)$ . The result then follows from Proposition B.1. of Altamirano et al. (2023).  $\square$

### A.4 Robustness with the IMQ weights and sub-exponential priors

In this section, we prove that under the simplified Assumption A4', global-bias robustness holds and verify that these assumptions hold in the cases of mixture density models and masked autoregressive flows.

#### A.4.1 Proof of Corollary 1

*Proof.* Similarly to the proof of Theorem 2, we prove the result using Proposition B.1 of Altamirano et al. (2023). Following this result, it is sufficient to show that there exists a function  $\gamma : \Theta \rightarrow \mathbb{R}$  such that: (1)  $\sup_{x \in \mathcal{X}} \mathcal{L}_{\text{NSM}}(\theta; x, \hat{\phi}_m) \leq \gamma(\theta)$ , (2)  $\sup_{\theta \in \Theta} \gamma(\theta)\pi(\theta) < \infty$ , (3)  $\int_{\Theta} \gamma(\theta)\pi(\theta)d\theta < \infty$ .

For simplicity let  $S_{\theta}(x) := \|\nabla_x \log q_{\hat{\phi}_m}(x|\theta)\|_2$  and  $H_{\theta}(x) := |\text{Tr}(\nabla_x^2 \log q_{\hat{\phi}_m}(x|\theta))|$ . Then using the Cauchy-Schwarz inequality we have:

$$\begin{aligned} \mathcal{L}_{\text{NSM}}(\theta; x, \hat{\phi}_m) &= w_{\zeta}(x)^2 S_{\theta}(x)^2 + 2 \left( \nabla_x w_{\zeta}(x)^2 \right)^{\top} \nabla_x \log q_{\hat{\phi}_m}(x|\theta) + 2w_{\zeta}(x)^2 H_{\theta}(x) \\ &\leq w_{\zeta}(x)^2 S_{\theta}(x)^2 + 2 \left\| \nabla_x w_{\zeta}(x)^2 \right\|_2 S_{\theta}(x) + 2w_{\zeta}(x)^2 H_{\theta}(x). \end{aligned} \quad (19)$$

We first make use of the specific form of the IMQ weight to bound all terms relating to  $w_{\zeta}(x)$  in terms of a function of  $\|x\|_2$ . We start with bounding the  $\|\nabla_x w_{\zeta}(x)^2\|_2$  term. Recall that  $w_{\zeta}(x) = (1 + r(x)^2)^{-1/\zeta}$  for  $\zeta > 0$  where  $r(x)^2 = \|x - \hat{\nu}_n\|_{\hat{\Xi}_n^{-1}}^2$ . Then

$$\nabla_x w_{\zeta}(x)^2 = -\frac{2}{\zeta} (1 + r(x)^2)^{-\frac{2}{\zeta}-1} \nabla_x (r(x)^2) = -\frac{4}{\zeta} (1 + r(x)^2)^{-\frac{2}{\zeta}-1} \hat{\Xi}_n^{-1}(x - \hat{\nu}_n)$$

and hence by letting  $\lambda_{\max}(\hat{\Xi}_n^{-1})$  denote the largest eigenvalue of  $\hat{\Xi}_n^{-1}$  (which is positive since  $\hat{\Xi}_n^{-1}$  is positive-definite) we obtain:

$$\begin{aligned} \|\nabla_x w_{\zeta}(x)^2\|_2 &\leq \frac{4}{\zeta} (1 + r(x)^2)^{-\frac{2}{\zeta}-1} \left\| \hat{\Xi}_n^{-1}(x - \hat{\nu}_n) \right\|_2 \leq \frac{4}{\zeta} (1 + r(x)^2)^{-\frac{2}{\zeta}-1} \left\| \hat{\Xi}_n^{-1} \right\|_{\text{op}} \|x - \hat{\nu}_n\|_2 \\ &\leq \frac{4}{\zeta} (1 + r(x)^2)^{-\frac{2}{\zeta}-1} \lambda_{\max}(\hat{\Xi}_n^{-1}) \|x - \hat{\nu}_n\|_2 \\ &= \frac{4}{\zeta} w_{\zeta}(x)^{2+\zeta} \lambda_{\max}(\hat{\Xi}_n^{-1}) \|x - \hat{\nu}_n\|_2 \end{aligned} \quad (20)$$

where the second inequality follows from the definition of the operator norm, the third inequality follows from the fact that  $\hat{\Xi}_n^{-1}$  is a symmetric, positive definite matrix and the last equality follows from the fact that

$$(1 + r(x)^2)^{-\frac{2}{\zeta}-1} = (w_\zeta(x)^{-\zeta})^{-\frac{2}{\zeta}-1} = w_\zeta(x)^{2+\zeta}.$$

Now by the Rayleigh quotient bounds (Horn and Johnson, 2012, Theorem 4.2.2) it follows that  $r(x)^2 = \|x - \hat{\nu}_n\|_{\hat{\Xi}_n^{-1}}^2 = (x - \hat{\nu}_n)^\top \hat{\Xi}_n^{-1} (x - \hat{\nu}_n) \geq \lambda_{\min}(\hat{\Xi}_n^{-1}) \|x - \hat{\nu}_n\|_2^2$  and hence  $\|x - \hat{\nu}_n\|_2 \leq r(x)/(\lambda_{\min}(\hat{\Xi}_n^{-1}))^{1/2}$  where  $\lambda_{\min}(\hat{\Xi}_n^{-1})$  denotes the smallest eigenvalue of  $\hat{\Xi}_n^{-1}$  which satisfies  $\lambda_{\min}(\hat{\Xi}_n^{-1}) > 0$  since  $\hat{\Xi}_n^{-1}$  is positive definite. Therefore, by using this in Equation (20) we obtain:

$$\|\nabla_x w_\zeta(x)^2\|_2 \leq 4 \frac{\lambda_{\max}(\hat{\Xi}_n^{-1})}{\sqrt{\lambda_{\min}(\hat{\Xi}_n^{-1})}} r(x) w_\zeta(x)^{2+\zeta} \leq \underbrace{4 \frac{\lambda_{\max}(\hat{\Xi}_n^{-1})}{\sqrt{\lambda_{\min}(\hat{\Xi}_n^{-1})}}}_{:=C(\hat{\Xi}_n^{-1}) < \infty} w_\zeta(x)^{2+\frac{\zeta}{2}}$$

since  $r(x) = (w_\zeta(x)^{-\zeta} - 1)^{1/2} \leq (w_\zeta(x)^{-\zeta})^{1/2} = w_\zeta(x)^{\zeta/2}$ . Substituting in (19) we obtain:

$$\mathcal{L}_{\text{NSM}}(\theta; x, \hat{\phi}_m) \leq w_\zeta(x)^2 S_\theta(x)^2 + 4C(\hat{\Xi}_n^{-1}) w_\zeta(x)^{2+\frac{\zeta}{2}} S_\theta(x) + 2w_\zeta(x)^2 H_\theta(x). \quad (21)$$

We now proceed by bounding the terms in (21) involving  $w_\zeta(x)^2$ . Under Assumption A4', we have that:  $S_\theta(x) \leq K_1(1 + \|\theta\|^{k_1})(1 + \|x\|_2^{2/\zeta})$  and  $H_\theta(x) \leq K_2(1 + \|\theta\|^{k_2})(1 + \|x\|_2^{4/\zeta})$  hence we aim to bound  $1 + \|x\|_2^{2/\zeta}$  and  $1 + \|x\|_2^{4/\zeta}$  in terms of  $w_\zeta(x)$ . To achieve this, we study the behaviour of  $w_\zeta(x) = (1 + r(x)^2)^{-1/\zeta}$  relative to  $\|x\|_2$  separately when  $\|x\|_2 \leq 1$  and  $\|x\|_2 \geq 1$ .

First consider the case  $\|x\|_2 \geq 1$ . As previously stated, since  $\hat{\Xi}_n^{-1}$  is positive definite, its eigenvalues satisfy  $0 < \lambda_{\min}(\hat{\Xi}_n^{-1}) \leq \lambda_{\max}(\hat{\Xi}_n^{-1})$ . Therefore, for any  $x \in \mathbb{R}^{d_x}$  we have:

$$\|x\|_{\hat{\Xi}_n^{-1}}^2 = x^\top \hat{\Xi}_n^{-1} x \leq \lambda_{\max}(\hat{\Xi}_n^{-1}) \|x\|_2^2 \quad \text{and hence,} \quad r(x)^2 \leq \lambda_{\max}(\hat{\Xi}_n^{-1}) \|x - \hat{\nu}_n\|_2^2. \quad (22)$$

From (22) and using the triangle inequality we have:

$$\begin{aligned} r(x)^2 &\leq \lambda_{\max}(\hat{\Xi}_n^{-1}) \|x - \hat{\nu}_n\|_2^2 \leq \lambda_{\max}(\hat{\Xi}_n^{-1}) (\|x\|_2^2 + \|\hat{\nu}_n\|_2^2) \leq \lambda_{\max}(\hat{\Xi}_n^{-1}) (\|x\|_2^2 + \|\hat{\nu}_n\|_2^2 \|x\|_2^2) \\ &:= C_1 \|x\|_2^2 \end{aligned}$$

where  $C_1 := \lambda_{\max}(\hat{\Xi}_n^{-1}) (1 + \|\hat{\nu}_n\|_2^2) < \infty$ . Substituting this into the definition of  $w_\zeta$  we have:

$$w_\zeta(x) = (1 + r(x)^2)^{-\frac{1}{\zeta}} \leq (r(x)^2)^{-\frac{1}{\zeta}} \leq C_1^{-\frac{1}{\zeta}} \|x\|_2^{-\frac{2}{\zeta}}$$

which yields:

$$1 + \|x\|_2^{\frac{2}{\zeta}} \leq C_1^{-\frac{1}{\zeta}} w_\zeta(x)^{-1} + 1, \quad 1 + \|x\|_2^{\frac{4}{\zeta}} \leq C_1^{-\frac{2}{\zeta}} w_\zeta(x)^{-2} + 1. \quad (23)$$

Now consider the case  $\|x\|_2 \leq 1$ . Since  $w(x) \leq 1$  we have:

$$1 + \|x\|_2^{\frac{2}{\zeta}} \leq 2 \leq w_\zeta(x)^{-1} + 1, \quad 1 + \|x\|_2^{\frac{4}{\zeta}} \leq 2 \leq w_\zeta(x)^{-2} + 1. \quad (24)$$

By letting  $C_2 := \max\{1, C_1^{-1/\zeta}\}$  and  $C_3 := \max\{1, C_1^{-2/\zeta}\}$  and using (23) and (24), we have that for all  $x \in \mathbb{R}^{d_x}$ :

$$1 + \|x\|_2^{\frac{2}{\zeta}} \leq C_2 w_\zeta(x)^{-1} + 1, \quad \|x\|_2^{\frac{4}{\zeta}} \leq C_3 w_\zeta(x)^{-2} + 1. \quad (25)$$

Substituting (25) in (21) and using Assumption A4' we obtain:

$$\begin{aligned}
\mathcal{L}_{\text{NSM}}(\theta; x, \hat{\phi}_m) &\leq w_\zeta(x)^2 S_\theta(x)^2 + 4C(\hat{\Xi}_n^{-1}) w_\zeta(x)^{2+\frac{\zeta}{2}} S_\theta(x) + 2w_\zeta(x)^2 H_\theta(x) \\
&\leq w_\zeta(x)^2 K_1^2 \left(1 + \|\theta\|^{2k_1}\right) \left(1 + \|x\|_2^{\frac{4}{\zeta}}\right) + 4C(\hat{\Xi}_n^{-1}) w_\zeta(x)^{2+\frac{\zeta}{2}} K_1 \left(1 + \|\theta\|^{k_1}\right) \left(1 + \|x\|_2^{\frac{2}{\zeta}}\right) \\
&\quad + 2w_\zeta(x)^2 K_2 \left(1 + \|\theta\|^{k_2}\right) \left(1 + \|x\|_2^{\frac{4}{\zeta}}\right) \\
&\leq K_1^2 \left(1 + \|\theta\|^{2k_1}\right) (C_3 w_\zeta(x)^{-2} w_\zeta(x)^2 + w_\zeta(x)^2) \\
&\quad + 4C(\hat{\Xi}_n^{-1}) K_1 \left(1 + \|\theta\|^{k_1}\right) (w_\zeta(x)^{2+\frac{\zeta}{2}} C_2 w_\zeta(x)^{-1} + w_\zeta(x)^{2+\frac{\zeta}{2}}) \\
&\quad + 2K_2 \left(1 + \|\theta\|^{k_2}\right) (C_3 w_\zeta(x)^{-2} w_\zeta(x)^2 + w_\zeta(x)^2) \\
&= K_1^2 \left(1 + \|\theta\|^{2k_1}\right) (C_3 + w_\zeta(x)^2) 4C(\hat{\Xi}_n^{-1}) K_1 \left(1 + \|\theta\|^{k_1}\right) (w_\zeta(x)^{1+\frac{\zeta}{2}} C_2 + w_\zeta(x)^{2+\frac{\zeta}{2}}) \\
&\quad + 2K_2 \left(1 + \|\theta\|^{k_2}\right) (C_3 + w_\zeta(x)^2).
\end{aligned}$$

Since  $\zeta > 0$  we have  $\sup_x w_\zeta(x)^{1+\zeta/2} = \sup_x w_\zeta(x)^{2+\zeta/2} = \sup_x w_\zeta(x)^2 = 1$  so using the upper bound above we obtain:

$$\begin{aligned}
\sup_x \mathcal{L}_{\text{NSM}}(\theta; x, \hat{\phi}_m) &\leq K_1^2 (C_3 + 1) \left(1 + \|\theta\|^{2k_1}\right) + 4(C_2 + 1) C(\hat{\Xi}_n^{-1}) K_1 \left(1 + \|\theta\|^{k_1}\right) \\
&\quad + 2(C_3 + 1) K_2 \left(1 + \|\theta\|^{k_2}\right) \\
&:= \gamma(\theta) < \infty.
\end{aligned}$$

Take  $k := \max\{2k_1, k_2\}$  then  $\sup_\theta |\gamma(\theta)| \lesssim (1 + \|\theta\|^k)$ . Moreover, since  $\pi(\theta)$  has infinitely many moments, we have that:  $\int_\Theta \pi(\theta) \gamma(\theta) d\theta < \infty$ . Moreover, by assumption for  $\|\theta\| \geq R$ ,  $\pi(\theta) \leq C \exp(-c\|\theta\|)$  hence:

$$\pi(\theta) \gamma(\theta) \lesssim (1 + \|\theta\|^k) C \exp(-c\|\theta\|) < \infty.$$

On the ball  $\{\theta : \|\theta\| \leq R\}$  we have that  $\gamma(\theta) \lesssim (1 + R^k)$  and  $\pi(\theta)$  is finite since it is a density hence  $\sup_\theta \gamma(\theta) \pi(\theta) < \infty$ . The result follows from Proposition B.1. of Altamirano et al. (2023).  $\square$

#### A.4.2 Proof of Proposition 2 (robustness for Gaussian Mixture-density Networks)

*Proof.* For simplicity, we drop the dependence on  $\theta$  and  $\hat{\phi}_m$  and denote  $\vartheta_k := \vartheta_k(\theta; \hat{\phi}_m)$  and  $\Omega_k := \Omega_k(\theta; \hat{\phi}_m)$ . Let  $f_k(x) := \mathcal{N}(x; \vartheta_k, \Omega_k)$  denote the  $k$ -th Gaussian density. Then the score of each density is  $\nabla_x \log f_k(x) = -\Omega_k^{-1}(x - \vartheta_k)$  and

$$\|\nabla_x \log f_k(x)\|_2 = \left\| -\Omega_k^{-1}(x - \vartheta_k) \right\|_2 \leq \left\| \Omega_k^{-1} \right\|_2 \|x - \vartheta_k\|_2 \leq \lambda_{\max}(\Omega_k^{-1}) (\|x\|_2 + \|\vartheta_k\|_2).$$

Since  $\Omega_k$  is symmetric positive-definite, it follows that  $\lambda_{\max}(\Omega_k^{-1}) = 1/\lambda_{\min}(\Omega_k)$  and by Assumption of Proposition 2 we have that for all  $k \in \{1, \dots, K\}$ ,  $\lambda_{\max}(\Omega_k^{-1}) = 1/\lambda_{\min}(\Omega_k) \leq 1/\lambda_{\min}$ . Hence, for the mixture, it follows that:

$$\begin{aligned}
\left\| \nabla_x \log q_{\hat{\phi}_m}(x|\theta) \right\|_2 &= \left\| \frac{\sum_{k=1}^K \omega_k(\theta; \hat{\phi}_m) \nabla_x f_k(x)}{\sum_{k=1}^K \omega_k(\theta; \hat{\phi}_m) f_k(x)} \right\|_2 = \left\| \sum_{k=1}^K \rho_k(x, \theta) \nabla_x \log f_k(x) \right\|_2 \\
&\leq \sum_{k=1}^K \rho_k(x, \theta) \|\nabla_x \log f_k(x)\|_2 \\
&\leq \frac{1}{\lambda_{\min}} (\|x\|_2 + \max_k \|\vartheta_k\|_2)
\end{aligned}$$

where  $\rho_k(x, \theta) := \omega_k(\theta; \hat{\phi}_m) f_k(x) / \sum_{j=1}^K \omega_j(\theta; \hat{\phi}_m) f_j(x)$ . Let  $h(\theta) := \frac{1}{\lambda_{\min}} (1 + \max_k \|\vartheta_k\|_2)$ , then:

$$\begin{aligned}
\left\| \nabla_x \log q_{\hat{\phi}_m}(x|\theta) \right\|_2 &\leq \frac{1}{\lambda_{\min}} \left( \|x\|_2 + \max_k \|\vartheta_k\|_2 \right) \leq \frac{1}{\lambda_{\min}} (1 + \|x\|_2) \left( 1 + \max_k \|\vartheta_k\|_2 \right) \\
&= h(\theta) (1 + \|x\|_2).
\end{aligned}$$

Thus, for any  $\zeta \leq 2$ , there exists  $\tilde{C} < \infty$  such that for  $\tilde{h}(\theta) := \tilde{C}h(\theta)$ , we have

$$\left\| \nabla_x \log q_{\hat{\phi}_m}(x|\theta) \right\|_2 \leq h(\theta) (1 + \|x\|_2) \leq \tilde{h}(\theta) \left( 1 + \|x\|_2^{\frac{2}{\zeta}} \right). \quad (26)$$

for all  $x \in \mathbb{R}^{d_x}$ . Furthermore, we have that  $\nabla_x^2 \log f_k(x) = -\Omega_k^{-1}$  hence standard operations yield:

$$\nabla_x^2 \log q_{\hat{\phi}_m}(x) = \sum_{k=1}^K \rho_k(x; \theta) \nabla_x^2 \log f_k(x) + \text{Cov}_\rho(\nabla_x \log f_k(x))$$

where  $\text{Cov}_\rho$  denotes the covariance under the weights  $\rho_k(x; \theta)$ . Therefore,

$$\begin{aligned} \left| \text{Tr} \nabla_x^2 \log q_{\hat{\phi}_m}(x|\theta) \right| &\leq \left| \sum_{k=1}^K \rho_k(x; \theta) \text{Tr} \Omega_k^{-1} \right| + \left| \text{Tr} \text{Cov}_\rho(\nabla_x \log f_k(x)) \right| \\ &\leq \sum_{k=1}^K \rho_k(x; \theta) \left| \text{Tr} \Omega_k^{-1} \right| + \text{Var}_\rho(\nabla_x \log f_k(x)) \\ &\leq \frac{d_x}{\lambda_{\min}} + \text{Var}_\rho(\nabla_x \log f_k(x)) \end{aligned}$$

where the first inequality follows from the fact that trace is a linear operation, the second follows from the fact that  $|\text{Tr} \text{Cov}_\rho(\nabla_x \log f_k)| \leq \sum_k \rho_k \|\nabla_x \log f_k(x)\|^2$  and the third follows from the fact that the trace is equal to the sum of its eigenvalues. From (26), we have that for any  $\zeta \leq 2$ :

$$\text{Var}_\rho(\nabla_x \log f_k(x)) \leq h(\theta)^2 (1 + \|x\|_2)^2 \leq 2h(\theta)^2 (1 + \|x\|_2^2) \leq 2\tilde{h}(\theta)^2 \left( 1 + \|x\|_2^{\frac{4}{\zeta}} \right).$$

Therefore  $\left| \text{Tr} \nabla_x^2 \log q_{\hat{\phi}_m}(x|\theta) \right| \leq (C_1 + 2\tilde{h}(\theta)^2)(1 + \|x\|_2^{4/\zeta})$  for  $C_1 := d_x/\lambda_{\min}$ . Since  $\tilde{h}(\theta) \propto 1/\lambda_{\min}(1 + \max_k \|\vartheta_k\|_2)$ , Assumption A4' holds since  $\max_k \|\vartheta_k(\theta)\|_2$  has polynomial growth by assumption.  $\square$

#### A.4.3 Proof of Proposition 3 (robustness for Masked Autoregressive Flows)

*Proof.* First we express the score and Hessian of  $q_{\hat{\phi}_m}(x|\theta)$  in terms of  $\mu_{\hat{\phi}_m,i}, \sigma_{\hat{\phi}_m,i}$  and their derivatives up to second order. Then we derive bounds for  $\mu_{\hat{\phi}_m,i}, \sigma_{\hat{\phi}_m,i}$  and their first two derivatives which we then substitute into the norm of the score and trace expressions to verify that their growth is in accordance with Assumption A4' for certain values of  $\zeta$ .

We want to show that there exists  $0 < K_1, K_2 < \infty$  and  $k_1, k_2 \geq 0$  such that  $\forall x \in \mathcal{X}$ :

$$\begin{aligned} \|\nabla_x \log q_{\hat{\phi}_m}(x|\theta)\|_2 &\leq K_1 \left( 1 + \|\theta\|^{k_1} \right) \left( 1 + \|x\|_2^{\frac{2}{\zeta}} \right) \\ |\text{Tr} \nabla_x^2 \log q_{\hat{\phi}_m}(x|\theta)| &\leq K_2 \left( 1 + \|\theta\|^{k_2} \right) \left( 1 + \|x\|_2^{\frac{4}{\zeta}} \right). \end{aligned}$$

From the definition of the normalising flow and the fact that  $p_z(z) = \mathcal{N}(0, I)$  we have that:

$$\log q_{\hat{\phi}_m}(x|\theta) = \sum_{i=1}^{d_x} \left[ \log p_z(z_i) - \log \sigma_{\hat{\phi}_m,i}(x_{<i}, \theta) \right] = \sum_{i=1}^{d_x} \left[ -\frac{1}{2} z_i^2 - \frac{1}{2} \log(2\pi) - \log \sigma_{\hat{\phi}_m,i}(x_{<i}, \theta) \right].$$

For each  $j = 1, \dots, d_x$  we have that:

$$\frac{\partial}{\partial x_j} \log q_{\hat{\phi}_m}(x|\theta) = \sum_{i=1}^{d_x} -z_i \frac{\partial z_i}{\partial x_j} - \frac{1}{\sigma_{\hat{\phi}_m,i}(x_{<i}, \theta)} \frac{\partial \sigma_{\hat{\phi}_m,i}(x_{<i}, \theta)}{\partial x_j} \quad (27)$$

and using the product and chain rule we further obtain:

$$\frac{\partial^2}{\partial x_j^2} \log q_{\hat{\phi}_m}(x|\theta) = \sum_{i=1}^{d_x} -z_i \frac{\partial^2 z_i}{\partial x_j^2} - \left( \frac{\partial z_i}{\partial x_j} \right)^2 - \frac{1}{\sigma_{\hat{\phi}_m,i}(x_{<i}, \theta)} \frac{\partial^2 \sigma_{\hat{\phi}_m,i}(x_{<i}, \theta)}{\partial x_j^2} - \frac{1}{\sigma_{\hat{\phi}_m,i}(x_{<i}, \theta)^2} \left( \frac{\partial \sigma_{\hat{\phi}_m,i}(x_{<i}, \theta)}{\partial x_j} \right)^2.$$

Therefore,

$$\left\| \nabla_x \log q_{\hat{\phi}_m}(x|\theta) \right\|_2 = \left\| \sum_{i=1}^{d_{\mathcal{X}}} -z_i \nabla_x z_i - \frac{1}{\sigma_{\hat{\phi}_{m,i}}(x_{<i}, \theta)} \nabla_x \sigma_{\hat{\phi}_{m,i}}(x_{<i}, \theta) \right\|_2, \quad (28)$$

$$\begin{aligned} \left| \text{Tr} \nabla_x^2 \log q_{\hat{\phi}_m}(x|\theta) \right| &= \sum_{j=1}^{d_{\mathcal{X}}} \left[ \sum_{i=1}^{d_{\mathcal{X}}} -z_i \frac{\partial^2 z_i}{\partial x_j^2} - \left( \frac{\partial z_i}{\partial x_j} \right)^2 - \frac{1}{\sigma_{\hat{\phi}_{m,i}}(x_{<i}, \theta)} \frac{\partial^2 \sigma_{\hat{\phi}_{m,i}}(x_{<i}, \theta)}{\partial x_j^2} \right. \\ &\quad \left. - \frac{1}{\sigma_{\hat{\phi}_{m,i}}(x_{<i}, \theta)^2} \left( \frac{\partial \sigma_{\hat{\phi}_{m,i}}(x_{<i}, \theta)}{\partial x_j} \right)^2 \right]. \end{aligned} \quad (29)$$

We now bound all individual terms in the expressions in (28) and (29). Since  $z_i = (x_i - \mu_{\hat{\phi}_{m,i}}(x_{<i}, \theta)) / \sigma_{\hat{\phi}_{m,i}}(x_{<i}, \theta)$  it follows that:

$$\frac{\partial z_i}{\partial x_j} = \begin{cases} \frac{1}{\sigma_{\hat{\phi}_{m,i}}(x_{<i}, \theta)} & \text{if } j = i \\ -\frac{1}{\sigma_{\hat{\phi}_{m,i}}^2} \frac{\partial \mu_{\hat{\phi}_{m,i}}}{\partial x_j} - \frac{x_i - \mu_{\hat{\phi}_{m,i}}}{\sigma_{\hat{\phi}_{m,i}}^2} \frac{\partial \sigma_{\hat{\phi}_{m,i}}}{\partial x_j} & \text{if } j < i \quad \text{and} \\ 0 & \text{if } j > i \end{cases} \quad (30)$$

$$\frac{\partial^2 z_i}{\partial x_j^2} = \begin{cases} \frac{1}{\sigma_{\hat{\phi}_{m,i}}^2} \frac{\partial \mu_{\hat{\phi}_{m,i}}}{\partial x_j} - \frac{1}{\sigma_{\hat{\phi}_{m,i}}^2} \frac{\partial^2 \mu_{\hat{\phi}_{m,i}}}{\partial x_j^2} - \frac{1}{\sigma_{\hat{\phi}_{m,i}}^2} \frac{\partial \sigma_{\hat{\phi}_{m,i}}}{\partial x_j} - \frac{x_i - \mu_{\hat{\phi}_{m,i}}}{\sigma_{\hat{\phi}_{m,i}}^2} \frac{\partial^2 \sigma_{\hat{\phi}_{m,i}}}{\partial x_j^2} & \text{if } j < i \\ 0 & \text{otherwise} \end{cases}. \quad (31)$$

Hence we need to bound terms involving  $\mu_{\hat{\phi}_{m,i}}$ ,  $\sigma_{\hat{\phi}_{m,i}}$  and their first and second derivatives. Since for each coupling layer, the networks computing  $\mu_{\hat{\phi}_{m,i}}$  and  $\sigma_{\hat{\phi}_{m,i}}$  are MLPs built from affine layers with tanh activations and an additional softplus at the final output for  $\sigma_{\hat{\phi}_{m,i}}$ ,  $\theta$  enters only in the first layer via:

$$h_1(x, \theta) = \tanh(W_1 x + \tilde{g}(\theta)), \quad \tilde{g}(\theta) = \tanh(V_0 \theta + b_0),$$

whereas subsequent layers take the form:

$$h_{l+1}(x, \theta) = \tanh(W_l h_l(x, \theta) + b_l), \quad \text{for } l = 2, \dots, L.$$

Since tanh is a bounded function, all intermediate layers are bounded. Hence, outputs  $\mu_{\hat{\phi}_{m,i}}$ ,  $\sigma_{\hat{\phi}_{m,i}}$  are affine functions of  $h_L$  and the scale is  $\sigma_{\hat{\phi}_{m,i}} = \text{softplus}(s_{\hat{\phi}_{m,i}})$ . Therefore, for  $k = 1, 2$ :

$$\left| \mu_{\hat{\phi}_{m,i}}(x_{<i}, \theta) \right| \leq C, \quad \left\| \frac{\partial^k \mu_{\hat{\phi}_{m,i}}}{\partial x_j^k} \right\| \leq C_k, \quad \text{for } j = 1, \dots, d_{\mathcal{X}} \quad (32)$$

and for some constants  $C, C_1, C_2 < \infty$  independent of  $\theta$ . For  $\sigma_{\hat{\phi}_{m,i}}$  we have that

$$s_{\hat{\phi}_{m,i}}(x_{<i}, \theta) = a_i^\top h_L(x_{<i}, \theta) + c_i, \quad \sigma_{\hat{\phi}_{m,i}}(x_{<i}, \theta) = \text{softplus}(s_{\hat{\phi}_{m,i}})$$

and since  $\|h_L\|_\infty \leq 1$  (since tanh is a bounded function) it follows that:

$$\left| s_{\hat{\phi}_{m,i}}(x_{<i}, \theta) \right| \leq \|a_i\|_1 + |c_i| := S_i. \quad (33)$$

Since  $\text{softplus}(t) := \log(1 + e^t)$  we have that  $\max\{0, t\} \leq \text{softplus}(t) \leq \max\{0, t\} + \log 2$  and since  $-S_i \leq s_{\hat{\phi}_{m,i}}(x_{<i}, \theta) \leq S_i$  from (33), it follows that

$$0 < \sigma_i^L := \text{softplus}(-S_i) \leq \sigma_{\hat{\phi}_{m,i}}(x_{<i}, \theta) \leq \text{softplus}(S_i) := \sigma_i^U < \infty. \quad (34)$$

Since the softplus function has globally bounded first and second derivatives, namely

$$\frac{\partial \text{softplus}(t)}{\partial t} = \frac{1}{1 + e^{-t}} \in (0, 1), \quad \frac{\partial^2 \text{softplus}(t)}{\partial t^2} = \frac{e^{-t}}{(1 + e^{-t})^2} \leq \frac{1}{4},$$

it follows by the chain rule that the first and second derivatives of  $\sigma_{\hat{\phi}_m, i}$  are also bounded, i.e.

$$\left\| \frac{\partial^k \sigma_{\hat{\phi}_m, i}}{\partial x_j^k} \right\| \leq \tilde{C}_k, \quad \text{for } k = 1, 2. \quad (35)$$

Applying the bounds from (32), (34), (35) in the expressions in (30) and (31) we have that for some constant  $C' < \infty$ :

$$|z_i| \leq \frac{|x_i| + C}{\sigma_i^L} \leq C'(1 + |x_i|), \quad \left| \frac{\partial z_i}{\partial x_j} \right| \leq \begin{cases} \frac{1}{\sigma_i^L} & \text{if } i = j \\ \frac{1}{\sigma_i^L} C + \frac{|x_i| + C}{(\sigma_i^L)^2} \tilde{C}_1 & \text{if } j < i \quad \text{and} \\ 0 & \text{if } j > i. \end{cases} \quad (36)$$

$$\left| \frac{\partial^2 z_i}{\partial x_j^2} \right| \leq \frac{1}{(\sigma_i^L)^2} C_1 + \frac{1}{(\sigma_i^L)^2} C_2 + \frac{1}{(\sigma_i^L)^2} \tilde{C}_1 + \frac{|x_i| + C}{(\sigma_i^L)^2} \tilde{C}_2. \quad (37)$$

Substituting (36) in (27), it follows that for each  $j = 1, \dots, d_{\mathcal{X}}$  there exist constants  $C_3, C_4 < \infty$  depending on  $C, C_1, \tilde{C}_1, \sigma_i^L$  such that:

$$\left| \frac{\partial}{\partial x_j} \log q_{\hat{\phi}_m} \right| \leq d_{\mathcal{X}} C_3 (1 + \|x\|_2) + d_{\mathcal{X}} C_4.$$

Setting  $C_5 := \max\{d_{\mathcal{X}} C_3, d_{\mathcal{X}} C_4\}$  it follows from (28) that:

$$\left\| \nabla_x \log q_{\hat{\phi}_m} (x|\theta) \right\|_2 = \left\| \sum_{i=1}^{d_{\mathcal{X}}} -z_i \frac{\partial z_i}{\partial x_j} - \frac{1}{\sigma_{\hat{\phi}_m, i}^L(x_{<i}, \theta)} \frac{\partial \sigma_{\hat{\phi}_m, i}(x_{<i}, \theta)}{\partial x_j} \right\|_2 \leq C_5 (1 + \|x\|_2^2). \quad (38)$$

Similarly, by substituting the bounds in (36), (37) into (29) we obtain:

$$\left| \text{Tr} \nabla_x^2 \log q_{\hat{\phi}_m} (x|\theta) \right| \leq C_6 (1 + \|x\|_2^2)$$

for some constant  $C_6 < \infty$  depending on  $d_{\mathcal{X}}, C', C_1, C_2, \tilde{C}_1, \tilde{C}_2, \sigma_i^L$ . To conclude, we have that:

$$\left\| \nabla_x \log q_{\hat{\phi}_m} (x|\theta) \right\|_2 \leq C_5 (1 + \|x\|_2^2), \quad \left| \text{Tr} \nabla_x^2 \log q_{\hat{\phi}_m} (x|\theta) \right| \leq d_{\mathcal{X}} C_6 (1 + \|x\|_2^2)$$

hence for any  $\zeta \leq 1$  there exist  $C_7, C_8 < \infty$  such that for any  $x \in \mathbb{R}^{d_{\mathcal{X}}}$ :

$$\left\| \nabla_x \log q_{\hat{\phi}_m} (x|\theta) \right\|_2 \leq C_7 \left( 1 + \|x\|_2^{\frac{2}{\zeta}} \right), \quad \left| \text{Tr} \nabla_x^2 \log q_{\hat{\phi}_m} (x|\theta) \right| \leq C_8 \left( 1 + \|x\|_2^{\frac{4}{\zeta}} \right).$$

and the statement holds by noting that  $C_7$ , and  $C_8$  are independent of  $\theta$  (hence polynomial functions of zero degree).  $\square$

#### A.4.4 Proof of Theorem 3

*Proof.* By Proposition 1 we have that  $p_{\text{NSM}}(\theta|x_{1:n}^o, \hat{\phi}_m) \propto \mathcal{N}(\theta; \mu_{n,m}, \Sigma_{n,m})$  with  $\mu_{n,m}, \Sigma_{n,m}$  as in (18) and (17). Similarly, we have that  $p_{\text{NSM}}(\theta|x_{1:n}^c, \hat{\phi}_m) \propto \mathcal{N}(\theta; \mu_{n,m}^c, \Sigma_{n,m}^c)$  where:

$$\begin{aligned} \left( \Sigma_{n,m}^c \right)^{-1} &:= \Sigma^{-1} + 2\beta n M_1(x_{1:n}^c) \quad \text{and} \\ \mu_{n,m}^c &:= \Sigma_{n,m}^c [\Sigma^{-1} \mu - 2\beta n M_2(x_{1:n}^c) - 2\beta n \ell_1(x_{1:n}^c)]. \end{aligned}$$

Let  $\mu_{n,m}^- := (\mu_{n,m}^c - \mu_{n,m})$ . Using the closed form of the KL divergence between Gaussian distributions (see e.g. Zhang et al., 2023), we hence have:

$$\text{PIF}_{\text{KL}}(x_j^c, \mathbb{P}_n, \mathcal{L}_{\text{NSM}}) = \underbrace{\frac{1}{2} \left( \text{Tr} \left( (\Sigma_{n,m}^c)^{-1} \Sigma_{n,m} \right) - d_{\Theta} \right)}_{(1)} + \underbrace{(\mu_{n,m}^-)^{\top} (\Sigma_{n,m}^c)^{-1} \mu_{n,m}^-}_{(2)} + \underbrace{\log \left( \frac{\det(\Sigma_{n,m}^c)}{\det(\Sigma_{n,m})} \right)}_{(3)}.$$

For the first term, we have that:

$$(1) = \text{Tr} \left( (\Sigma_{n,m}^c)^{-1} \Sigma_{n,m} \right) - d_\Theta \leq \text{Tr} \left( (\Sigma_{n,m}^c)^{-1} \right) \text{Tr} (\Sigma_{n,m}) \\ = \text{Tr} (\Sigma^{-1} + 2\beta n M_1(x_{1:n}^c)) \text{Tr} ((\Sigma^{-1} + 2\beta n M_1(x_{1:n}^o))^{-1})$$

where in the inequality we used the fact that  $\text{Tr}(AB) \leq \text{Tr}(A)\text{Tr}(B)$  for two PSD matrices  $A$  and  $B$  and that  $d_\Theta > 0$ . Since  $\Sigma^{-1} + 2\beta n M_1(x_{1:n}^o)$  does not depend on the contamination datum  $x_j^c$ , we write  $C_1 := \text{Tr} ((\Sigma^{-1} + 2\beta n M_1(x_{1:n}^o))^{-1})$  and we have:

$$(1) \leq \text{Tr} (\Sigma^{-1} + 2\beta n M_1(x_{1:n}^c)) C_1 = (\text{Tr}(\Sigma^{-1}) + \text{Tr}(2\beta n M_1(x_{1:n}^c))) C_1 \\ = \left( \text{Tr}(\Sigma^{-1}) + 2\beta \sum_{i \neq j}^n w(x_i^o)^2 \text{Tr} \left( \nabla_x T_{\hat{\phi}_m}(x_i^o) \nabla_x T_{\hat{\phi}_m}(x_i^o)^\top \right) \right. \\ \left. + 2\beta w(x_j^c)^2 \text{Tr} \left( \nabla_x T_{\hat{\phi}_m}(x_j^c) \nabla_x T_{\hat{\phi}_m}(x_j^c)^\top \right) \right) C_1.$$

The first two terms in the bracket do not depend on  $x_j^c$  so let

$$C_2 := \text{Tr}(\Sigma^{-1}) + 2\beta \sum_{i \neq j}^n w(x_i^o)^2 \text{Tr} \left( \nabla_x T_{\hat{\phi}_m}(x_i^o) \nabla_x T_{\hat{\phi}_m}(x_i^o)^\top \right).$$

Then by noting that  $\text{Tr} \left( \nabla_x T_{\hat{\phi}_m}(x) \nabla_x T_{\hat{\phi}_m}(x)^\top \right) = \|\nabla_x T_{\hat{\phi}_m}(x)\|_F^2$  we have:

$$(1) \leq \left( C_2 + 2\beta w(x_j^c)^2 \|\nabla_x T_{\hat{\phi}_m}(x_j^c)\|_F^2 \right) C_1 \leq \left( C_2 + 2\beta \sup_x w(x)^2 \|\nabla_x T_{\hat{\phi}_m}(x)\|_F^2 \right) C_1.$$

For the second term, since  $(\Sigma_{n,m}^c)^{-1}$  is symmetric we have (see e.g. [Horn and Johnson, 2012](#), Lemma 4.2.2):

$$(2) = (\mu_{n,m}^-)^\top \left( \Sigma_{n,m}^c \right)^{-1} \mu_{n,m}^- \leq \lambda_{\max} \left( (\Sigma_{n,m}^c)^{-1} \right) \|\mu_{n,m}^-\|_2^2$$

where  $\lambda_{\max} \left( (\Sigma_{n,m}^c)^{-1} \right)$  denotes the maximum eigenvalue of  $(\Sigma_{n,m}^c)^{-1}$ . Then, using Weyl's inequality ([Horn and Johnson, 2012](#), Theorem 4.3.1) we obtain:

$$\lambda_{\max}(\Sigma_{n,m}^c)^{-1}) = \lambda_{\max}(\Sigma^{-1} + 2\beta n M_1(x_{1:n}^c)) \leq \lambda_{\max}(\Sigma^{-1}) + \lambda_{\max}(2\beta n M_1(x_{1:n}^c)).$$

Since  $2\beta M_1(x_{1:n}^c)$  is PSD we have that  $\lambda_{\max}(2\beta M_1(x_{1:n}^c)) \leq \text{Tr}(2\beta M_1(x_{1:n}^c))$  (since the trace is equal to the sum of its eigenvalues). Hence, by letting

$$C_3 := \lambda_{\max}(\Sigma^{-1}) + 2\beta \sum_{i \neq j}^n w(x_i^o)^2 \nabla_x T_{\hat{\phi}_m}(x_i^o) \nabla_x T_{\hat{\phi}_m}(x_i^o)^\top$$

which does not depend on  $x_j^c$ , and using the same arguments as above we have:

$$\lambda_{\max}((\Sigma_{n,m}^c)^{-1}) \leq C_3 + 2\beta \sup_x w(x)^2 \left\| \nabla_x T_{\hat{\phi}_m}(x) \right\|_F^2 := C_4.$$

Substituting into (2) we obtain:

$$(2) \leq C_4 \left\| \mu_{n,m}^- \right\|_2^2 = C_4 \left\| \Sigma_{n,m}^c [\Sigma^{-1} \mu - 2\beta n M_2(x_{1:n}^c) - 2\beta n l_1(x_{1:n}^c)] \right. \\ \left. - \Sigma_{n,m} [\Sigma^{-1} \mu - 2\beta n M_2(x_{1:n}^o) - 2\beta n l_1(x_{1:n}^o)] \right\|_2^2.$$

Now let  $v^c := -2\beta[d(x_j^c) - d(x_j) + h(x_j^c) - h(x_j)]$  and  $A^c := 2\beta[M(x_j^c) - M(x_j)]$  where

$$h(x) := w(x)^2 \nabla_x T_{\hat{\phi}_m}(x) \nabla_x b_{\hat{\phi}_m}(x) \in \mathbb{R}^{d_\Theta}, \quad d(x) := \nabla_x \cdot (w(x)^2 \nabla_x T_{\hat{\phi}_m}(x)^\top)^\top \in \mathbb{R}^{d_\Theta}, \quad \text{and} \\ M(x) = w(x)^2 \nabla_x T_{\hat{\phi}_m}(x) \nabla_x T_{\hat{\phi}_m}(x)^\top \in \mathbb{R}^{d_\Theta \times d_\Theta}.$$

By re-arranging terms, we have:

$$\begin{aligned}
\|\mu_{n,m}^-\|_2 &= \left\| \Sigma_{n,m}^c [\Sigma^{-1}\mu - 2\beta n M_2(x_{1:n}^c) - 2\beta n l_1(x_{1:n}^c)] \right\|_2 \\
&\quad - \Sigma_{n,m} [\Sigma^{-1}\mu - 2\beta n M_2(x_{1:n}^o) - 2\beta n l_1(x_{1:n}^o)] \right\|_2 \\
&= \left\| \Sigma_{n,m}^c v^c - \Sigma_{n,m}^c A^c \mu_{n,m} \right\|_2 \\
&\leq \left\| \Sigma_{n,m}^c \right\|_2 \|v^c - A^c \mu_{n,m}\|_2.
\end{aligned}$$

Since  $(\Sigma_{n,m}^c)^{-1} = \Sigma^{-1} + 2\beta n M_1(x_{1:n}^c)$  and  $2\beta n M_1(x_{1:n}^c)$  is PSD we have  $(\Sigma_{n,m}^c)^{-1} \succeq \Sigma^{-1}$  and hence  $\Sigma \succeq \Sigma_{n,m}^c$ . For symmetric PSD matrices  $A, B$ ,  $A \succeq B$  implies  $\lambda_{\max}(A) \geq \lambda_{\max}(B)$  from Weyl's theorem, and  $\|A\|_2 = \lambda_{\max}(A)$  hence since  $\Sigma, \Sigma_{n,m}^c$  are symmetric PSD matrices:

$$\left\| \Sigma_{n,m}^c \right\|_2 = \lambda_{\max}(\Sigma_{n,m}^c) \leq \lambda_{\max}(\Sigma) = \|\Sigma\|_2.$$

Now consider the term  $\|v^c - A^c \mu_{n,m}\|_2$ . Since  $C_6 := \|\mu_{n,m}\|_2$  does not depend on  $x_j^c$  we have,

$$\|A^c \mu_{n,m}\|_2 \leq C_6 \|A^c\|_2 = C_6 2\beta \left\| M(x_j^c) - M(x_j) \right\|_2.$$

Next, we have

$$\begin{aligned}
\|v^c\|_2 &= \left\| -2\beta [d(x_j^c) - d(x_j) + h(x_j^c) - h(x_j)] \right\|_2 \leq 2\beta (\|d(x_j^c)\|_2 + \|d(x_j)\|_2 + \|h(x_j^c)\|_2 + \|h(x_j)\|_2) \\
&\leq C_5 + 2\beta (\|d(x_j^c)\|_2 + \|h(x_j^c)\|_2)
\end{aligned}$$

where the first inequality follows from the triangle inequality and the second inequality follows from defining  $C_5 := 2\beta(\|d(x_j)\|_2 + \|h(x_j)\|_2)$ , independent of  $x_j^c$ . Now,

$$\begin{aligned}
\|h(x_j^c)\|_2 &= w(x_j^c)^2 \left\| \nabla_x T_{\hat{\phi}_m}(x_j^c) \nabla_x b_{\hat{\phi}_m}(x_j^c) \right\|_2 \leq w(x_j^c)^2 \left\| \nabla_x T_{\hat{\phi}_m}(x_j^c) \right\|_2 \left\| \nabla_x b_{\hat{\phi}_m}(x_j^c) \right\|_2 \\
&\leq w(x_j^c)^2 \left\| \nabla_x T_{\hat{\phi}_m}(x_j^c) \right\|_F \left\| \nabla_x b_{\hat{\phi}_m}(x_j^c) \right\|_2.
\end{aligned}$$

On the other hand, for  $k \in \{1, \dots, d_\Theta\}$ , the  $k$ -th entry of  $d(x)$  has the form:

$$(d(x))_k = \sum_{j=1}^{d_\mathcal{X}} \frac{\partial}{\partial x_j} (w(x)^2 (\nabla_x T_{\hat{\phi}_m}(x))_{kj}) = \nabla w(x)^2 \cdot (\nabla_x T_{\hat{\phi}_m}(x))_{k,:}^\top + w(x)^2 \text{Tr}(\nabla_x^2(T_{\hat{\phi}_m}(x))_k).$$

Let  $d_1(x) \in \mathbb{R}^{d_\Theta}$  be such that  $(d_1(x))_k := \nabla w(x)^2 \cdot (\nabla_x T_{\hat{\phi}_m}(x))_{k,:}^\top$  and  $d_2(x) \in \mathbb{R}^{d_\Theta}$  be such that  $(d_2(x))_k := w(x)^2 \text{Tr}(\nabla_x^2(T_{\hat{\phi}_m}(x))_k)$  for  $k \in \{1, \dots, d_\Theta\}$ . Then  $d(x) = d_1(x) + d_2(x)$ . By the triangle inequality it follows that  $\|d(x_j^c)\|_2 \leq \|d_1(x_j^c)\|_2 + \|d_2(x_j^c)\|_2$ . By the Cauchy-Schwartz inequality, we have:

$$\begin{aligned}
\|d_1(x_j^c)\|_2 &= \left( \sum_{k=1}^{d_\Theta} (d_1(x_j^c))_k^2 \right)^{\frac{1}{2}} \leq \left\| \nabla w(x_j^c)^2 \right\|_2 \left( \sum_{k=1}^{d_\Theta} \left\| (\nabla_x T_{\hat{\phi}_m}(x))_{k,:} \right\|_2^2 \right)^{\frac{1}{2}} \\
&= \left\| \nabla w(x_j^c)^2 \right\|_2 \left\| \nabla_x T_{\hat{\phi}_m}(x_j^c) \right\|_F.
\end{aligned}$$

Similarly, for the second term, we have,

$$\begin{aligned}
\|d_2(x_j^c)\|_2 &= \left( \sum_{k=1}^{d_\Theta} (w(x_j^c)^2 \text{Tr}(\nabla_x^2(T_{\hat{\phi}_m}(x_j^c))_k))^2 \right)^{\frac{1}{2}} \leq w(x_j^c)^2 \sqrt{\sum_{k=1}^{d_\Theta} d_\mathcal{X} \left\| \nabla_x^2(T_{\hat{\phi}_m}(x_j^c))_k \right\|_F^2} \\
&= w(x_j^c)^2 \sqrt{d_\mathcal{X}} \left\| \nabla_x^2 T_{\hat{\phi}_m}(x_j^c) \right\|_F.
\end{aligned}$$

Putting these together, we obtain an upper bound for  $\|d(x_j^c)\|_2$  as follows:

$$\|d(x_j^c)\|_2 \leq \|\nabla w(x_j^c)^2\|_2 \|\nabla_x T_{\hat{\phi}_m}(x_j^c)\|_F + \sqrt{d_{\mathcal{X}}} w(x_j^c)^2 \|\nabla_x^2 T_{\hat{\phi}_m}(x_j^c)\|_F.$$

And therefore, by defining  $C_7 := \|\Sigma\|_2^2$ ,  $C_8 := 4\beta C_6$  and  $C_9 := d_{\mathcal{X}}$  we obtain:

$$\begin{aligned} (2) &\leq C_4 \|\mu_{n,m}^-\|_2^2 \leq \|\Sigma_{n,m}^c\|_2^2 \|v^c - A^c \mu_{n,m}\|_2^2 \\ &\leq \|\Sigma\|_2^2 (w(x_j^c)^2 \|\nabla_x T_{\hat{\phi}_m}(x_j^c)\|_F \|\nabla_x b_{\hat{\phi}_m}(x_j^c)\|_2 + \|\nabla w(x_j^c)^2\|_2 \|\nabla_x T_{\hat{\phi}_m}(x_j^c)\|_F \\ &\quad + \sqrt{d_{\mathcal{X}}} w(x_j^c)^2 \|\nabla_x^2 T_{\hat{\phi}_m}(x_j^c)\|_F + C_6 2\beta \|M(x_j^c) - M(x_j)\|_2^2) \\ &\leq C_7 \left( \sup_x w(x)^2 \|\nabla_x T_{\hat{\phi}_m}(x)\|_F \|\nabla_x b_{\hat{\phi}_m}(x)\|_2 + \sup_x \|\nabla w(x)^2\|_2 \|\nabla_x T_{\hat{\phi}_m}(x)\|_F \right. \\ &\quad \left. + C_9 \sup_x w(x)^2 \|\nabla_x^2 T_{\hat{\phi}_m}(x)\|_F + C_8 \sup_x w(x)^2 \|\nabla_x T_{\hat{\phi}_m}(x)\|_F^2 \right)^2 \end{aligned}$$

Finally, for the third term, we have:

$$\begin{aligned} (3) &= \log \left( \frac{\det(\Sigma_n^c)}{\det(\Sigma_{n,m}^c)} \right) = \log \left( \frac{\det((\Sigma^{-1} + 2\beta n M_1(x_{1:n}^c))^{-1})}{\det((\Sigma^{-1} + 2\beta n M_1(x_{1:n}^o))^{-1})} \right), \quad \text{and} \\ (\Sigma_{n,m}^c)^{-1} &= \underbrace{\Sigma_{n,m}^{-1} - 2\beta n M(x_j)}_{:=C(x_{1:n}^o)} + \underbrace{2\beta n M(x_j^c)}_{:=C(x_j^c)} \end{aligned}$$

where  $C(x_{1:n}^o) = \Sigma^{-1} + 2\beta n M_1(x_{1:n}^o) - 2\beta n M(x_j) = \Sigma^{-1} + 2\beta \sum_{i=1, i \neq m}^n w(x_i^o)^2 \nabla_x T_{\hat{\phi}_m}(x_i^o) \nabla_x T_{\hat{\phi}_m}(x_i^o)^\top$ . Since  $\Sigma^{-1}$  is positive definite and  $M(x)$  is positive semi-definite for all  $x$ , then  $C(x_{1:n}^o)$  is the sum of a positive semi-definite and a positive definite matrix and is hence positive definite. Moreover,  $C(x_j^c) := 2\beta n M(x_j^c)$  and is positive semi-definite. Let  $C(x_j) := 2\beta n M(x_j)$  then

$$\Sigma_{n,m}^{-1} = C(x_{1:n}^o) + C(x_j) = C(x_{1:n}^o)^{1/2} (I + C(x_{1:n}^o)^{-1/2} C(x_j) C(x_{1:n}^o)^{-1/2}) C(x_{1:n}^o)^{1/2}$$

and hence,

$$\begin{aligned} \det(\Sigma_{n,m}^{-1}) &= \det(C(x_{1:n}^o)^{1/2}) \det(I + C(x_{1:n}^o)^{-1/2} C(x_j) C(x_{1:n}^o)^{-1/2}) \det(C(x_{1:n}^o)^{1/2}) \\ &= \det(C(x_{1:n}^o)) \det(I + C(x_{1:n}^o)^{-1/2} C(x_j) C(x_{1:n}^o)^{-1/2}). \end{aligned}$$

Therefore,

$$\begin{aligned} (3) &= \log \left( \frac{\det(\Sigma_{n,m}^{-1})}{\det(C(x_{1:n}^o) + C(x_j^c))} \right) = \log \left( \det(I + C(x_{1:n}^o)^{-1/2} C(x_j) C(x_{1:n}^o)^{-1/2}) \frac{\det(C(x_{1:n}^o))}{\det(C(x_{1:n}^o) + C(x_j^c))} \right) \\ &= \log \left( C_{10} \frac{\det(C(x_{1:n}^o))}{\det(C(x_{1:n}^o) + C(x_j^c))} \right) \end{aligned}$$

where we defined  $C_{10} := \det(I + C(x_{1:n}^o)^{-1/2} C(x_j) C(x_{1:n}^o)^{-1/2})$  as it does not depend on the contamination. Finally,  $\det(C(x_{1:n}^o)) > 0$  since it is the sum of two matrices, including a PD one ( $\Sigma^{-1}$ ), hence since  $C(x_{1:n}^o) + C(x_j^c) \succeq C(x_{1:n}^o)$  we have that  $\det(C(x_{1:n}^o) + C(x_j^c)) \geq \det(C(x_{1:n}^o))$  by monotonicity of the determinant and hence:

$$\frac{\det(C(x_{1:n}^o))}{\det(C(x_{1:n}^o) + C(x_j^c))} \leq 1$$

and (3)  $\leq \log C_{10} := C_{11}$ . Therefore, under the assumptions of the Theorem, we have that:

$$\sup_{x_j^c \in \mathbb{R}^{d_{\mathcal{X}}}} \text{PIF}_{\text{KL}}(x_j^c, \mathbb{P}_n, \mathcal{L}_{\text{NSM}}) \leq \frac{1}{2} (C_2 + 2\beta C^2) C_1 + C_7 (C^2 + C' + C_9 C^2 + C_8 C^2)^2 + C_{11} < \infty.$$

□

#### A.4.5 Connection between Assumptions A4 and A5

In this section, we prove the following Lemma which shows that under some simple additional conditions robustness in the  $\text{PIF}_{\text{KL}}$  sense yields robustness in the  $\text{PIF}_{\Delta}$  sense for NSM-Bayes-conj.

**Lemma 1.** *Suppose Assumptions A1, A3 and A5 hold and additionally that there exist  $\tilde{C}_1, \tilde{C}_2 < \infty$  such that  $\|\nabla_x b_{\hat{\phi}_m}(x)\|_2 \leq \tilde{C}_1 \min\{w(x)^{-1}, \|\nabla_x w(x)^2\|_2^{-1}\}$ ,  $\|\nabla_x^2 b_{\hat{\phi}_m}(x)\|_F \leq \tilde{C}_2 w(x)^{-2}$ . Then, NSM-Bayes-conj is globally-bias-robust:  $\sup_{\theta \in \Theta, x^c \in \mathcal{X}} \text{PIF}(x^c, \theta, \mathbb{P}_n, \mathcal{L}_{\text{NSM}}) < \infty$ .*

*Proof.* From Assumption A3 we have that  $q_{\hat{\phi}_m}(x|\theta) \propto \exp(T_{\hat{\phi}_m}(x)^\top \theta + b_{\hat{\phi}_m}(x))$ , hence  $\nabla_x \log q_{\hat{\phi}_m}(x|\theta) = (\nabla_x T_{\hat{\phi}_m}(x))^\top \theta + \nabla_x b_{\hat{\phi}_m}(x)$  and under the assumptions:

$$\|\nabla_x \log q_{\hat{\phi}_m}(x|\theta)\|_2 \leq \|(\nabla_x T_{\hat{\phi}_m}(x))^\top \theta\|_2 + \|\nabla_x b_{\hat{\phi}_m}(x)\|_2 \leq (C\|\theta\|_2 + \tilde{C}_1) w(x)^{-1}.$$

and simultaneously (from the second bound of Assumption A5),

$$\|\nabla_x \log q_{\hat{\phi}_m}(x|\theta)\|_2 \leq \|(\nabla_x T_{\hat{\phi}_m}(x))^\top \theta\|_2 + \|\nabla_x b_{\hat{\phi}_m}(x)\|_2 \leq (C'\|\theta\|_2 + \tilde{C}_1) \|\nabla_x w(x)^2\|_2^{-1}.$$

Hence choosing  $C_3 := \max\{C, C'\}$  we have that

$$\|\nabla_x \log q_{\hat{\phi}_m}(x|\theta)\|_2 \leq (C_3\|\theta\|_2 + \tilde{C}_1) \min\{w(x)^{-1}, \|\nabla_x w(x)^2\|_2^{-1}\}.$$

Similarly,

$$\begin{aligned} |\text{Tr} \nabla_x^2 \log q_{\hat{\phi}_m}(x|\theta)| &= \left| \text{Tr} \left( \nabla_x^2 T_{\hat{\phi}_m}(x)^\top \theta + \nabla_x^2 b_{\hat{\phi}_m}(x) \right) \right| \leq \|\nabla_x^2 T_{\hat{\phi}_m}(x)\|_F \|\theta\|_2 + \|\nabla_x^2 b_{\hat{\phi}_m}(x)\|_F \\ &\leq C^2 w(x)^{-2} \|\theta\|_2 + \tilde{C}_2 w(x)^{-2} \\ &= (C^2\|\theta\|_2 + \tilde{C}_2) w(x)^{-2}. \end{aligned}$$

Take  $f(\theta) := C_3\|\theta\|_2 + \tilde{C}_1$  and  $g(\theta) := C^2\|\theta\|_2 + \tilde{C}_2$ . Recall that for NSM-Bayes-conj we select  $\pi(\theta) \propto \mathcal{N}(\theta; \mu, \Sigma)$ . Since both  $f, g$  have linear growth in  $\theta$  and  $\pi$  has finite second moments it follows that  $f \in L^2(\pi), g \in L^1(\pi)$ . Moreover, since  $\pi$  has exponential decay in  $\theta$  and  $f$  and  $g$  have linear growth in  $\theta$  it follows that  $\sup_{\theta \in \Theta} (f(\theta)^2 + f(\theta) + g(\theta)) \pi(\theta) < \infty$ . Therefore, Assumption A4 holds and global-bias robustness follows from Theorem 2.  $\square$

## B Experimental details and additional results

Section B.1 provides further details on the algorithm we use to tune the learning rate in non-conjugate GBI methods such as NSM-Bayes. Implementation details for our methods and the baselines are in Section B.2 and Section B.3, respectively. Section B.4 contains the additional experiments and results from Section 5. In Section B.5, we analyse of the performance of certain baseline methods under increased simulation budget.

### B.1 Setting the learning rate for non-conjugate GBI posteriors

The Syring and Martin (2019) method for tuning the learning rate outlined in Algorithm 1 algorithm requires the posterior (mean and covariance) to be computed  $T \times B$  times, where  $B$  is the number of bootstrap samples and  $T$  is the number of stochastic steps. This is straightforward for NSM-Bayes-conj where the posterior is conjugate. However, for most GBI methods such as NSM-Bayes, running MCMC hundreds of times to tune  $\beta$  can be infeasible. Therefore, we first run MCMC once at an initial value of  $\beta$ , and use importance sampling (IS) to estimate the posterior for each bootstrapped sample. We also monitor the effective sample size (ESS) of the importance weights at each step and re-run MCMC with the current value of  $\beta$  if the ESS falls below 30%. The full algorithm is outlined in Algorithm 2.

---

**Algorithm 2** Learning-rate calibration for GBI methods via bootstrap re-weighting

---

**Require:** Data  $x_{1:n}^o$ , initial  $\beta_0$ , iterations  $T$ , bootstraps  $B$ , MCMC draws  $M$ , step-sizes  $\{\kappa_t\}$ , target  $1 - \alpha$ , ESS threshold  $\text{ESS}_{\min}$

**Ensure:** Calibrated learning rate  $\beta^*$

- 1: Compute  $\hat{\theta}_n = \arg \min_{\theta} \mathcal{L}(\theta; x_{1:n}^o)$  using gradient-based solvers
- 2: Initialise  $\beta \leftarrow \beta_0$ ; draw  $\{\theta^{(i)}\}_{i=1}^M \sim \pi_{\mathcal{L}}^{\beta}(\theta | x_{1:n}^o)$  via MCMC
- 3: Cache per-observation losses  $\mathcal{L}_{ij} \leftarrow \mathcal{L}(\theta^{(i)}; x_j^o)$  for all  $i = 1:M, j = 1:n$
- 4: **for**  $t = 1$  **to**  $T$  **do**
- 5:     Draw bootstrap counts  $N_b \sim \text{Multinomial}\left(n; \frac{1}{n}, \dots, \frac{1}{n}\right)$  for  $b = 1:B$
- 6:     **for**  $b = 1$  **to**  $B$  **do**
- 7:         Compute self-normalised IS weights  $\{W_{b,i}(\beta)\}_{i=1}^M$  using cached  $\mathcal{L}_{ij}$  and counts  $N_b$
- 8:         Compute weighted mean/covariance  $(\mu_b^{(\beta)}, \Sigma_b^{(\beta)})$  from  $\{(\theta^{(i)}, W_{b,i}(\beta))\}_{i=1}^M$
- 9:         Compute  $D_{b,i}^2 = (\theta^{(i)} - \hat{\mu}_{\beta_t}^{(b)})^\top (\Sigma_{\beta_t}^{(b)})^{-1} (\theta^{(i)} - \hat{\mu}_{\beta_t}^{(b)})$  and
- 10:         Form the credible region:  $C_{\alpha, \beta_t}(x_{1:n}^{*(b)}) = \{\theta : D_{b,i}^2 \leq \tau_b(\beta_t)\}$  for threshold  $\tau_b(\beta)$   
(weighted  $(1 - \alpha)$ -quantile of  $\{D_{b,i}^2\}_{i=1}^M$  under weights  $W_{b,i}(\beta_t)$ )
- 11:         Set indicator  $\mathbb{I}_b(\beta) \leftarrow \mathbf{1}\{(\hat{\theta}_n - \mu_b^{(\beta)})^\top (\Sigma_b^{(\beta)})^{-1} (\hat{\theta}_n - \mu_b^{(\beta)}) \leq \tau_b(\beta)\}$
- 12:     **end for**
- 13:     Estimate coverage:  $\hat{c}(\beta) \leftarrow \frac{1}{B} \sum_{b=1}^B \mathbb{I}_b(\beta)$
- 14:     Update  $\beta \leftarrow \beta + \kappa_t(\hat{c}(\beta) - (1 - \alpha))$
- 15:     **if** mean ESS across bootstraps  $< \text{ESS}_{\min}$  **then**
- 16:         Re-run MCMC at current  $\beta$  to obtain  $\{\theta^{(i)}\}_{i=1}^M$  and refresh cache  $\mathcal{L}_{ij}$
- 17:     **end if**
- 18: **end for**
- 19: **return**  $\beta^* \leftarrow \beta$

---

**Closed-form estimation of  $\hat{\theta}_n$  for NSM-Bayes-conj.** In the case where  $q_\phi$  is an energy-based model satisfying **A3**, we can solve  $\hat{\theta}_n = \arg \min_{\theta} \mathcal{L}_{\text{NSM}}(\theta; x_{1:n}^o, \hat{\phi}_m)$  in closed-form as the objective is quadratic in  $\theta$ . Recall the loss expression:

$$\begin{aligned} \mathcal{L}_{\text{NSM}}(\theta; x_{1:n}^o, \hat{\phi}_m) &= \theta^\top A_n \theta + 2\theta^\top B_n + C_n, \quad \text{where} \\ A_n &= \frac{1}{n} \sum_{i=1}^n w(x_i^o)^2 \nabla_x T_{\hat{\phi}_m}(x_i^o) \nabla_x T_{\hat{\phi}_m}(x_i^o)^\top, \\ B_n &= \frac{1}{n} \sum_{i=1}^n \left[ w(x_i^o)^2 \nabla_x T_{\hat{\phi}_m}(x_i^o) \nabla_x b_{\hat{\phi}_m}(x_i^o) + \nabla_x \cdot (w(x_i^o)^2 \nabla_x T_{\hat{\phi}_m}(x_i^o)^\top)^\top \right], \end{aligned}$$

and  $C_n$  does not depend on  $\theta$ . If  $A_n$  is positive definite, the minimiser of the optimisation problem is  $\hat{\theta}_n = -A_n^{-1}B_n$ . However, in practice, especially for low-dimensional data, the matrix  $A_n$  can be severely ill-conditioned or nearly singular. To ensure numerical stability, we compute a ridge-stabilised estimator:

$$\hat{\theta}_0^{(\lambda)} := \arg \min_{\theta} \left\{ \mathcal{L}_{\text{NSM}}(\theta; x_{1:n}^o, \hat{\phi}_m) + \frac{\lambda}{2} \|\theta\|_2^2 \right\} = -(A_n + \lambda I_{d_\Theta})^{-1} B_n.$$

For all the experiments, we set the ridge parameter as  $\lambda = 10^{-2} \text{Tr}(A_n)/d_\Theta + 10^{-12}$ . In principle, one could use an adaptive scheme which would compute eigenvalues of  $A_n$  and then set  $\lambda$  based on a target condition number  $\kappa_{\text{target}}$ , for example,  $\lambda \geq \lambda_{\max}(A_n) - \kappa_{\text{target}}\lambda_{\min}(A_n)/(\kappa_{\text{target}} - 1)$ .

**Selecting  $\beta$  for ACE and GBI-SR.** Since neither Gao et al. (2023) or Pacchiardi et al. (2024) provide a method to select  $\beta$  for their methods, we use an approach similar to that described in

---

**Algorithm 3** Learning-rate calibration for ACE and GBI-SR

---

**Require:** Data  $x_{1:n}^o$ , bootstraps  $B$ , iterations  $T$ , learning rates in descending order  $\beta_{\text{list}}$ , MCMC draws  $M$ .  
 $\hat{\theta}_n \leftarrow \arg \min_{\theta} \mathcal{L}(\theta; x_{1:n}^o)$ ,  $\beta^* \leftarrow \text{None}$ ,  $\Delta^* \leftarrow +\infty$   
**for**  $\beta \in \beta_{\text{list}}$  **do**  
    Draw  $B$  bootstraps datasets  $x_{1:n}^{\star(b)}$  and obtain  $M$  posterior draw from each  
    Estimate coverage  $\hat{c}(\beta)$  using Algorithm 1  
    **if**  $|\hat{c}(\beta) - (1 - \alpha)| \leq \Delta^*$  **then**  $\Delta^* \leftarrow |\hat{c}(\beta) - (1 - \alpha)|$ ,  $\beta^* \leftarrow \beta$  **end if**  
**end for**  
**return**  $\beta^*$

---

Syring and Martin (2019) that we use for our methods. As a direct application of Algorithm 1 or Algorithm 2 to ACE and GBI-SR would require a substantially larger number of simulations than the fixed budget used in our experiments, we employ the method outlined in Algorithm 3. We set  $T = 200$  and  $B = 20$  for the both methods and set  $M = N_{\text{post}}$  for ACE, while for GBI-SR we select according to available simulation budget. We set  $\beta_{\text{list}} = \{1, 10, 100, 1000, 10000\}$  and  $\beta_{\text{list}} = \{1, 10, 100\}$  for ACE and GBI-SR, respectively. The grid of  $\beta$  values is less for GBI-SR due to limited simulation budget and numerical issues encountered for  $\beta = 1000, 10000$ . As the SIR model is non-differentiable, estimating  $\hat{\theta}_n$  using gradient-based methods is infeasible for GBI-SR. We therefore replace  $\hat{\theta}_n$  with the posterior mean obtained using the initial value  $\beta_0 = 1$ , which requires additional simulation.

## B.2 Implementation details

For all the experiments with NSM-Bayes-conj, we parameterise the exponential family density estimator components  $T_\phi$  and  $b_\phi$  using fully connected two-layer multilayer perceptrons with a single hidden layer of width 128, a tanh activation function, and linear output heads. Since tanh is bounded, the resulting  $T_\phi(x)$  and  $b_\phi(x)$  are bounded in  $x$ , which ensures that  $q_\phi(x|\theta)$  is normalisable. All linear layers are initialised with Xavier/Glorot uniform weights, and biases are set to 0.01 to avoid near-zero initial activations. Following common practice, we standardise the simulated data to be zero-mean and identity covariance before training, and use a fixed learning rate of  $5 \times 10^{-4}$ , weight decay  $10^{-5}$ , batch size 128, and a maximum of 1000 epochs. The training dataset is randomly split into 80% training and 20% validation subsets, with the training set shuffled each epoch. We apply early stopping with patience 20 based on the validation loss, saving the model parameters with the best validation performance and restoring them at the end of training. For all the baseline methods, we use the default setting of the original code unless stated otherwise. This includes the MCMC sampler, the neural network architecture, and the associated hyperparameters; see Section B.3 for more details.

For our methods in Section 5, we select the learning rate  $\beta$  using the procedure described in Section B.1 with  $\alpha = 0.05$ , which corresponds to 95% coverage. We set the number of bootstrap samples to  $B = 100$ , the number of stochastic approximation steps to  $T = 20$ , and the adaptive step-size to  $\kappa_t = 10/(t + 10)$  in all the experiments. We use a log-transform for  $\beta$  and set the initial learning rate  $\beta_0$  for NSM-Bayes to 1.0,  $10^{-6}$ , and 0.01 for g-and-k, SIR and radio propagation models. The corresponding values for NSM-Bayes-conj are 0.1, 0.01, and 0.01. The learning rate is clamped at  $\beta_0/100$  during the stochastic approximation. For the other GBI methods (ACE and GBI-SR), we select  $\beta$  using a strategy inspired by the procedure in Section B.1. We do not apply the exact same procedure, as it would require significantly more simulations for both ACE and GBI-SR than the assigned budget, making the comparison unfair. Instead of the stochastic approximation steps, we use a grid of  $\beta$  values; see Section B.3.

**Performance metrics.** We use the MMD<sup>2</sup> as one of the performance metric. Given a reproducing kernel, the MMD<sup>2</sup> between distributions  $\mathbb{Q}_1, \mathbb{Q}_2$  is:

$$\text{MMD}^2(\mathbb{Q}_1, \mathbb{Q}_2) = \mathbb{E}_{Y, Y' \sim \mathbb{Q}_1} [k(Y, Y')] - 2\mathbb{E}_{Y \sim \mathbb{Q}_1, Y' \sim \mathbb{Q}_2} [k(Y, Y')] + \mathbb{E}_{Y, Y' \sim \mathbb{Q}_2} [k(Y, Y')].$$

We estimate this quantity using independent samples  $y_{1:n_1} \sim \mathbb{Q}_1, \tilde{y}_{1:n_2} \sim \mathbb{Q}_2$ :

$$\text{MMD}^2(y_{1:n_1}, \tilde{y}_{1:n_2}) := \frac{1}{n_1^2} \sum_{i,j=1}^{n_1} k(y_i, y_j) - \frac{2}{n_1 n_2} \sum_{i=1}^{n_1} \sum_{j=1}^{n_2} k(y_i, \tilde{y}_j) + \frac{1}{n_2^2} \sum_{i,j=1}^{n_2} k(\tilde{y}_i, \tilde{y}_j)$$

Throughout, we use a Gaussian kernel defined as  $k(y, y') = \exp(-\|y - y'\|_2^2/2l^2)$  for  $\text{MMD}_{\text{ref}}^2$  and wherever MMD is used in the baseline methods. Thus,  $\text{MMD}_{\text{ref}}^2 := \text{MMD}^2(\tilde{\theta}_{1:N_{\text{post}}}, \theta_{1:N_{\text{post}}})$ , where  $\tilde{\theta}_{1:N_{\text{post}}}$  are samples from the reference NLE posterior. The lengthscale  $l$  is estimated using the median heuristic  $l = \sqrt{\text{median}(\|x_i - x_j\|^2/2), i, j \in \{1, \dots, n\}}$ . MSE is computed in closed-form for NSM-Bayes as  $\text{MSE} = \|\mu_{n,m} - \theta^*\|_2^2 + \text{tr}(\Sigma_{n,m})$ , while for all the other methods, it is estimated using Monte Carlo samples from the posterior.

### B.3 Description of the baseline methods

**RSNLE (Kelly et al., 2024).** This method considers model misspecification in the space of summary statistics  $s \in \mathcal{S} \subseteq \mathbb{R}^{d_s}$  defined by a summary function  $s : \mathcal{X}^n \rightarrow \mathcal{S}$ . The model is said to be misspecified in the summary space if there exists no  $\theta \in \Theta$  such that  $\mathbb{E}_{X_{1:n} \sim \mathbb{P}_\theta} [s(X_{1:n})] = \mathbb{E}_{X_{1:n}^o \sim \mathbb{P}_0} [s(X_{1:n}^o)]$ . To address this issue, RSNLE introduces an auxiliary variable  $\Gamma \in \mathbb{R}^{d_s}$  that explicitly captures the discrepancy between the observed summary statistics  $s(x_{1:n}^o)$  and the simulated statistics  $s(x_{1:n})$ . Incorporating this discrepancy into the sequential NLE method consisting of  $R$  rounds yields the augmented posterior:

$$\pi_{\text{RSNLE}}(\theta, \Gamma | s(x_{1:n}^o), \hat{\phi}_m^R) \propto q_{\hat{\phi}_m^R}(s(x_{1:n}^o) - \Gamma | \theta) \pi(\theta) \pi^R(\Gamma | x_{1:n}^o).$$

The first round involves standard NLE training, yielding the estimator  $\hat{q}_{\phi_m^1}$ . At this stage, an independent Laplace prior is placed on each component of the discrepancy variable  $\Gamma$ . For subsequent rounds, the neural likelihood is retrained using parameters drawn from the posterior of the previous round, resulting in an updated estimator  $\hat{q}_{\phi_m^{r+1}}$ ,  $r = 1, \dots, R-1$ . The discrepancy prior is updated according to  $\pi^r(\gamma_i | x_{1:n}^o) = \text{Laplace}(0, |0.3 \tilde{s}_i^r(x_{1:n}^o)|)$ , where  $\tilde{s}_i^r$  denotes the standardized  $i$ -th summary statistic, with mean and standard deviation computed over the accumulated simulated data  $\{\{x_{1:n,i}^{(r')}\}_{i=1}^m\}_{r'=0}^r$ . Following the original implementation, we use a RealNVP normalizing flow for  $q_\phi$  and the NUTS sampler to obtain posterior samples. In the g-and-k experiments, we use the quantile based summary statistics:  $s_1 = q_{50}, s_2 = q_{75} - q_{25}, s_3 = (q_{90} + q_{10} - 2q_{50})/(q_{90} - q_{10}), s_4 = (q_{90} - q_{10})/(q_{75} - q_{25})$ , which we verify to be informative. As this is a statistics-based method, we need to simulate  $n$  iid samples of  $x$  per sample of  $\theta$  in order to compute  $s(x_{1:n})$ . We therefore adjust the number of prior samples for RSNLE such that the total simulation budget is  $m$ ; see Table 2 for the specific values. As RSNLE uses the observed data in each round, it is not amortised.

**NPE-RS (Huang et al., 2023).** This method also considers model misspecification in the space of summary statistics, and aims to learn a summary network  $s_\psi : \mathbb{R}^{n \times d_x} \rightarrow \mathbb{R}^k$ , with learnable parameter  $\psi \in \Psi$ , jointly with the posterior network  $q_\phi$  such that  $s_\psi(x_{1:n})$  is in the vicinity of  $s_\psi(x_{1:n}^o)$ . To do that, NPE-RS penalises an NPE objective with the MMD<sup>2</sup> between summary statistics of simulated data and observed data:

$$\hat{\phi}_m^\lambda := \arg \min_{\phi \in \Phi} -\frac{1}{m} \sum_{i=1}^m \log q_\phi(\theta_i | s_\psi(x_{1:n,i})) + \lambda \sum_{i=1}^m \text{MMD}^2(s_\psi(x_{1:n,i}), s_\psi(x_{1:n}^o)).$$

The hyperparameter  $\lambda > 0$  controls the relative weight of the penalisation term in the optimisation. Once trained, the NPE-RS posterior  $\pi_{\text{NPE-RS}}(\theta | x_{1:n}^o, \hat{\phi}_m^\lambda, \hat{\psi}_m^\lambda) = q_{\hat{\phi}_m^\lambda}(\theta | s_{\hat{\psi}_m^\lambda}(x_{1:n}^o))$  is obtained

by a simple forward pass. Following the original implementation, we use an MAF for the inference network and set  $\lambda = 1$ . We use a deep set architecture (Zaheer et al., 2017) for the summary network with 20 dimensional output. Similar to RSNLE, we adjust the number of prior samples used for NPE-RS in order to keep the total simulation budget fixed to  $m$ . Note that NPE-RS is also not amortised as it uses  $x_{1:n}^o$  during training.

**NPL-MMD (Dellaporta et al., 2022).** NPL-MMD employs the Bayesian nonparametric learning approach with an MMD-based loss. Instead of using a prior on the parameters, this method sets a Dirichlet process (DP) prior on the true data-generating process  $\mathbb{P}_0 \in \mathcal{P}(\mathcal{X})$ , with two prior hyperparameters: a concentration parameter  $\alpha \geq 0$  and a centring measure  $\mathbb{F} \in \mathcal{P}(\mathcal{X})$ . The posterior conditioned on  $x_{1:n}^o \sim \mathbb{P}_0$  is also Dirichlet process due to conjugacy. Following the original paper, we set the concentration parameter to  $\alpha = 0$ , leading to a non-informative prior. In this case, (approximate) samples from the posterior are obtained through:

$$\mathbb{P}_j \mid x_{1:n}^o \sim \text{DP-Posterior} \Leftrightarrow \mathbb{P}_j = \sum_{i=1}^n w_{j,i} \delta_{x_i^o}, \quad w_{j,1:n} \sim \text{Dir}(1, \dots, 1).$$

Given a draw  $\mathbb{P}_j$  from the DP posterior, a posterior sample in parameter space is obtained by solving  $\hat{\theta}_j = \arg \min_{\theta \in \Theta} \text{MMD}^2(\tilde{x}_{1:n'}, x_{1:n}) \approx \arg \min_{\theta \in \Theta} \text{MMD}^2(\mathbb{P}_j, \mathbb{P}_\theta)$ . Thus, NPL-MMD is not amortised as it needs to be rerun from scratch for each new  $x_{1:n}^o$ . Each posterior draw requires  $n' \times N_{\text{step}}$  simulator evaluations, where  $N_{\text{step}}$  denotes the number of optimization iterations; see Table 2 for the exact values used in order to keep the simulation budget the same.

**ACE (Gao et al., 2023).** ACE trains a neural network  $\text{NN}_\phi$  to approximate the loss function in GBI. Specifically they learn the MMD between each simulated dataset  $x_{1:n,i}$ ,  $i = 1, \dots, m$ , and a target dataset  $x'_{1:n,j}$ ,  $j = 1, \dots, m'$ . The target dataset consists of (i)  $m$  simulated datasets, (ii)  $m_{\text{aug}} = 100$  noise augmented samples, and (iii)  $K$  independent observation datasets  $x_{1:n,1}^o, \dots, x_{1:n,K}^o$ , such that  $m' := m + m_{\text{aug}} + K$  is the total number of target samples. Then, the neural network is trained by solving:

$$\hat{\phi}_{m'} := \arg \min_{\phi \in \Phi} \frac{1}{mm'} \sum_{i=1}^m \sum_{j=1}^{m'} \text{NN}_\phi(\theta_i, x'_{1:n,j}) - \text{MMD}^2(x_{1:n,i}, x'_{1:n,j})^2.$$

Once trained, the ACE posterior  $\pi_{\text{ACE}}(\theta \mid x_{1:n,k}^o, \hat{\phi}_{m'}) \propto \exp(-\beta \text{NN}_{\hat{\phi}_{m'}}(\theta, x_{1:n,k}^o))\pi(\theta)$  can be obtained via MCMC, making it partially amortised. As the loss computation is amortised, implementing Algorithm 3 for ACE does not require additional simulations.

**GBI-SR (Pacchiardi et al., 2024).** GBI-SR is a GBI method for simulators based on scoring rules. The original paper considers an energy score and a kernel score, with the latter giving a generalised posterior equivalent to MMD-Bayes (Chérif-Abdellatif and Alquier, 2020). In this paper, we only consider the kernel score, which gives robustness guarantees with a bounded kernel. In contrast, the energy score does not in fact lead to robustness beyond trivial settings (e.g. bounded domains) where even standard Bayesian posteriors are robust. Using the kernel score  $\hat{S}(\mathbb{P}_\theta, x_i^o)$ , the GBI-SR posterior is  $\pi_{\text{GBI-SR}}(\theta \mid x_{1:n}^o) \propto \exp(-\beta \sum_{i=1}^n \hat{S}(\mathbb{P}_\theta, x_i^o))\pi(\theta)$ , where

$$\hat{S}(\mathbb{P}_\theta, x_i^o) = \frac{1}{n'(n'-1)} \sum_{j,k=1, j \neq k}^{n'} k(x_j, x_k) - \frac{2}{n'} \sum_{j=1}^{n'} k(x_j, x_i^o), \quad x_{1:n}^o \sim \mathbb{P}_\theta.$$

For differentiable simulators, as is the case with the g-and-k distribution, they propose using stochastic gradient MCMC, specifically adaptive stochastic gradient Langevin dynamics (adS-GLD) (Jones and Leimkuhler, 2011). For non-differentiable simulators such as the SIR and the radio propagation model where gradients cannot be computed, we use the pseudo-marginal MCMC (Andrieu and Roberts, 2009), as per their recommendation. As the kernel score computation requires the observed data, GBI-SR is not amortised. Obtaining one posterior sample in GBI-SR requires  $n'$  simulation. Assuming  $N_{\text{warm}}$  warm-up steps in MCMC and total  $N_{\text{post}}$

Table 2: Simulation budget formulas, parameter configurations, and total forward simulations for all methods on the g-and-k and SIR, and Turin simulators.

Method	Formula	Value	Budget
<b>g-and-k</b>			
Our methods	$m$	$m = 100,000$	100,000
RSNLE	$Rmn$	$R = 2, m = 500, n = 100$	100,000
NPE-RS	$mn$	$m = 1000, n = 100$	100,000
NPL-MMD	$N_{\text{post}} n' N_{\text{step}}$	$N_{\text{post}} = 500, n' = 20, N_{\text{step}} = 10$	100,000
ACE	$mn$	$m = 1000, n = 100$	100,000
GBI-SR	$Tn'_b +  \beta_{\text{list}}  B M n'_b + (N_{\text{warm}} + N_{\text{post}}) n'$	$T = 200, n'_b = 7,  \beta_{\text{list}}  = 3, B = 20 M = 200, N_{\text{warm}} = N_{\text{post}} = 500, n' = 15$	100,400
<b>SIR / Turin</b>			
Our methods	-	$m = 50,000$	50,000
ACE	-	$m = 500, n = 100$	50,000
GBI-SR (only SIR)	$N_{\text{post},\hat{\theta}} n'_b +  \beta_{\text{list}}  B M n'_b + (N_{\text{warm}} + N_{\text{post}}) n'$	$N_{\text{post},\hat{\theta}} = 200, n'_b = 4, M = 172, n' = 8$ (others same as g-and-k)	50,080

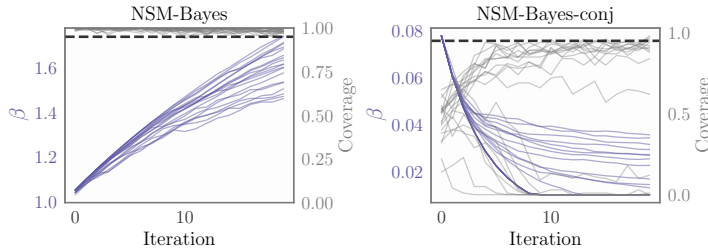


Figure 7: Trace plots obtained across the 20 runs during the stochastic approximation of the learning rate in the g-and-k experiment.

Table 3: Training and inference times for different methods in the SIR experiment with undercounting contamination model.

	Training time [s]	Inference time [s]
NLE	92 (12)	63 (71)
ACE	545 (39)	390 (6)
GBI-SR	-	92 (2)
NSM-Bayes	92 (12)	167 (1)
NSM-Bayes-conj	1312 (117)	19 (0.1)

posterior samples, GBI-SR requires  $n'(N_{\text{warm}} + N_{\text{post}})$  simulations. Additionally, simulation budget is spent on in computing  $\hat{\theta}_n$  and tuning the learning rate using Algorithm 3; see Table 2 for the exact values used in our experiments.  $M$  denotes the number of posterior draws for the bootstrap samples as before,  $n'_b$  denotes  $n'$  in the bootstrap setting, and  $N_{\text{post},\hat{\theta}}$  denotes the number of posterior samples used to estimate  $\hat{\theta}_n$  for non-differentiable simulators.

## B.4 Additional results

We now present additional results from our experiments in Section 5.

### B.4.1 The g-and-k simulator

**Calibrating  $\beta$  for g-and-k distribution.** In Figure 7, we show the trace plots from estimating the learning rate  $\beta$  for NSM-Bayes and NSM-Bayes-conj using the method described in Section B.1. We observe that the starting value  $\beta_0$  for NSM-Bayes was low, which resulted in 100% coverage. As the stochastic steps proceed,  $\beta$  keeps increasing until the coverage drops towards the target of 95%. For NSM-Bayes-conj, the reverse occurs: starting value of  $\beta$  is too high, leading to near 50% coverage. So the  $\beta$  value increases over the iterations, until they reach 95% coverage, after which the values stabilise. In some of the runs for NSM-Bayes-conj, the coverage is much lower. This occurs when the matrix inversion in the closed-form expression for  $\hat{\theta}_n$  becomes numerically unstable, leading to  $\hat{\theta}_n$  being far from the true parameter value  $\theta^*$ .

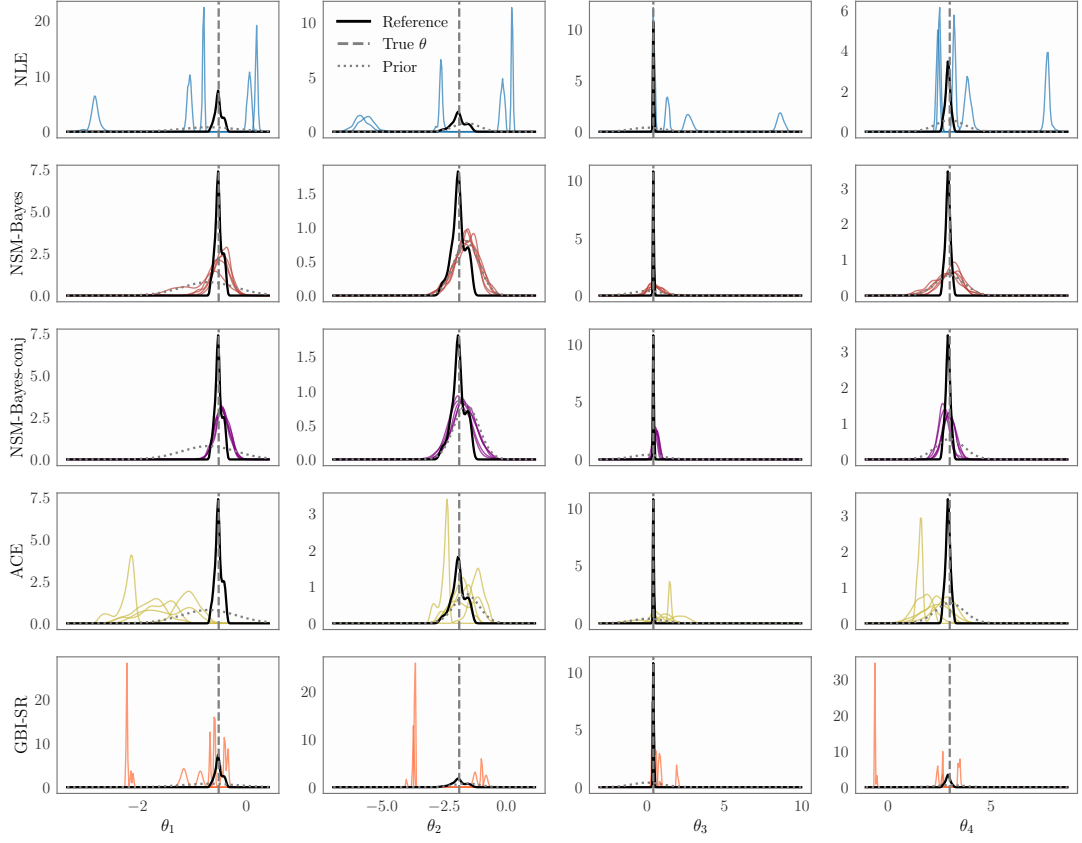


Figure 8: Kernel density estimates of the marginal posterior plots of NLE (■), NSM-Bayes (■), NSM-Bayes-conj (■), ACE (■), and GBI-SR (■) in the SIR undercounting experiment.

#### B.4.2 The SIR simulator

The marginal posterior plots from the SIR undercounting experiment in the main text are shown in Figure 8. Here, NLE catastrophically fails, yielding very confident but heavily biased posteriors. In contrast, NSM-Bayes and NSM-conj posteriors are accurately concentrating around the true  $\theta$ . ACE and GBI-SR do not perform well in this case, mainly because the simulation budget is not large enough for them. We report the training and inference times in Table 3. In this higher dimensional case, NSM-Bayes-conj takes 19 seconds to calibrate  $\beta$ . Its training time is also large, as the network keeps training for all 1000 epochs. The validation loss keeps going down and so the stopping criterion does not get activated.

**Varying learning rate  $\beta$ .** In Figure 9, we analyse the behaviour of NSM-Bayes-conj as the learning rate  $\beta$  varies. The learning rate  $\beta$  controls the coverage of the GBI posterior. As  $\beta$  increases, the posterior gets concentrated around the loss minimising parameter estimate  $\hat{\theta}_n$ . When  $\beta$  is low, the posterior becomes less impacted by the NSM loss and resembles the prior.

**Ablation study.** We now analyse the impact of our choice of robust mean (i.e. median)  $\hat{\nu}_n$  and robust covariance  $\hat{\Xi}_n$  estimators on the performance of NSM-Bayes-conj. To that end, we replace them with their non-robust, sample-based estimators, i.e., sample mean and sample covariance in the SIR undercounting experiment. The performance metrics are reported in Table 4. We observe that the performance degrades across both metrics when choosing the non-robust

Table 4: Ablation study on NSM-Bayes-conj method involving the estimators used in the IMQ weight function  $w(x)$ .

	MSE	$MMD_{ref}^2$
Robust $\hat{\nu}_n$ , $\hat{\Xi}_n$	<b>0.42</b> (0.05)	<b>0.26</b> (0.06)
Sample $\hat{\nu}_n$ , $\hat{\Xi}_n$	2.27 (0.00)	0.41 (0.04)

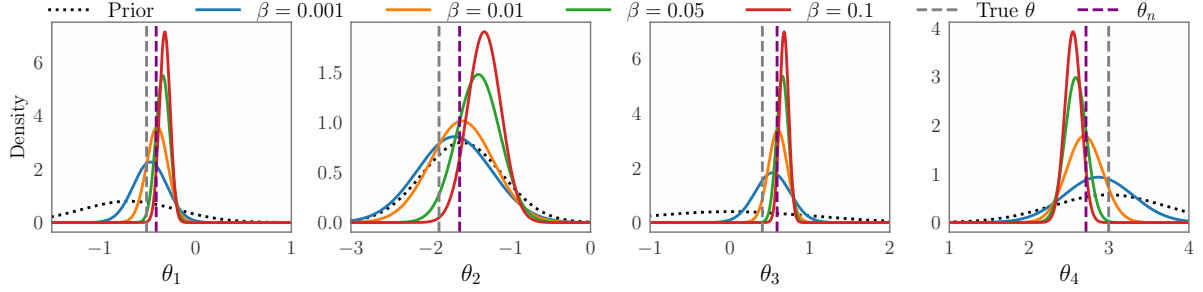


Figure 9: Varying the learning rate  $\beta$  for NSM-Bayes-conj in the SIR undercounting experiment.

Table 5: Inference times for the radio propagation example shown in Figure 5.

	NLE	ACE	NSM-Bayes	NSM-Bayes-conj
Inference time [s]	13.7	589.0	198.3	19.8

estimators for  $\nu$  and  $\Xi$  in the IMQ weight function.

#### B.4.3 The radio propagation simulator

Finally, the inference times for all the methods in the radio propagation experiment are reported in Table 5. Note that the MCMC in NLE is much faster in this case due to the conditional density being a mixture density network instead of the normalising flow. NSM-Bayes takes longer in this case due to repeated MCMC needed during learning rate tuning, as the effective sample size of the importance sample kept going below 30%. When the data-dimension is higher, tuning  $\beta$  takes longer in NSM-Bayes-conj.

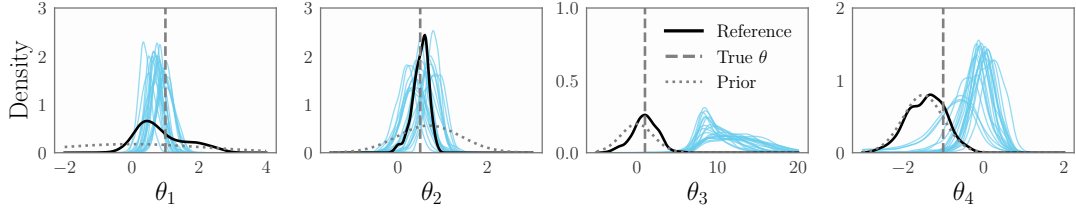
#### B.5 Analysis of baseline methods

**NPL-MMD.** This method places a non-informative Dirichlet process prior on the data-generating measure, whereas all the other methods place a prior on the parameter space, which is informative in the g-and-k experiment. Thus, forcing NPL-MMD to have the same simulation budget as the other methods is somewhat unfair to it, considering it needs to learn the posterior without knowledge of the prior. As shown in Figure 10(a), increasing the budget substantially improves accuracy, particularly for  $\theta_1$  and  $\theta_2$ , with  $\theta_4$  also moving closer to the true value. However, the posterior for  $\theta_3$  remains biased and an even much larger budget would likely be required to improve on this.

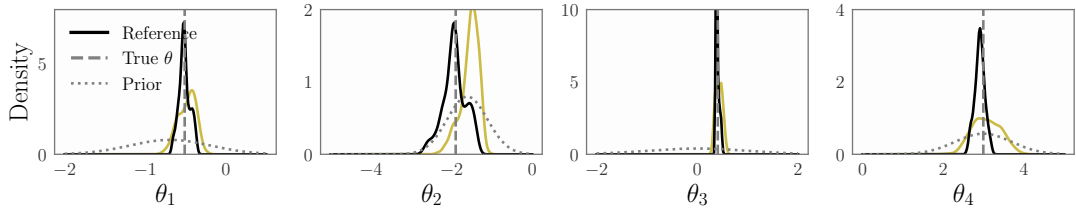
**ACE.** Although ACE achieves competitive performance in the g-and-k and the radio propagation experiments, it fails to yield robust posteriors in the SIR experiment. This is primarily due to the limited simulation budget, which leads to a poor approximation of the loss function with the neural network. Doubling the simulation budget to  $m = 10^5$  substantially improves its performance, as shown in Figure 10(b). This indicates that NSM-Bayes and NSM-Bayes-conj are more sample-efficient than ACE, requiring less simulation budget to achieve similar performance.

**GBI-SR.** While stochastic gradient MCMC could be used for the g-and-k experiment, the non-differentiability of the SIR simulator forced us to use pseudo-marginal MCMC. Given the slower convergence and poorer mixing of pseudo-marginal MCMC (Pacchiardi et al., 2024), 500 posterior samples were insufficient for adequate mixing. We therefore increase the simulation budget for GBI-SR to more than  $4\times$  the original budget and draw 10,000 posterior samples. This leads to a substantial improvement in its performance, as shown in Figure 10(c). Once

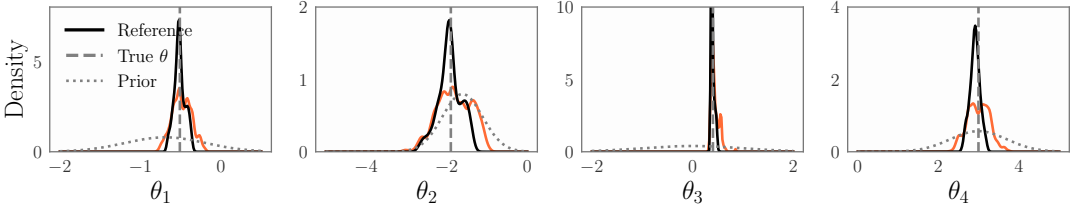
again, this shows that NSM-Bayes and NSM-Bayes-conj are more sample-efficient (in terms of the number of simulations).



(a) Marginal NPL-MMD (■) posterior for the g-and-k model using 500 posterior samples. We set  $n' = 2^9$ ,  $N_{\text{step}} = 1000$ , and step size to 0.1, leading to a total simulation budget of  $2.56 \times 10^7$ .



(b) Marginal ACE (■) posterior for the SIR undercounting experiment. We set  $m = 1000$  with fixed  $\beta = 100$ , resulting in a simulation budget of 100,000, which is twice the budget used in Section 5.2.



(c) Marginal GBI-SR (■) posterior for the SIR undercounting experiment. We set  $N_{\text{post}} = 10,000$ ,  $N_{\text{warmup}} = 1000$ ,  $n' = 200$ , and fix  $\beta = 1$ , such that total simulation budget is  $2.2 \times 10^6$ .

Figure 10: Performance of NPL-MMD, ACE and GBI-SR under increased simulation budget.

**RSNLE.** Finally, we investigate the poor performance of RSNLE in estimating the  $\theta_3$  parameter of the g-and-k distribution. To that end, we look at the scatter plot of the third and fourth simulated statistics (■),  $s_3$  and  $s_4$ , used for RSNLE in Figure 11. We also plot the observed statistics from the 20 runs of the g-and-k experiment (■), and the statistic corresponding to the uncorrupted data (■) obtained from  $\theta^*$  with  $\epsilon = 0$ . We see that the outliers cause a shift in both the observed  $s_3$  and  $s_4$ . Note that while the observed  $s_4$  go out of the simulated statistics distribution, this does not happen for  $s_3$ . Thus, the simulator can produce statistics that match the observed  $s_3$ , and so the posterior RSNLE yields for  $\theta_3$  (which is determined by  $s_3$ ) becomes biased. This points to a failure mode of RSNLE, wherein contamination in the data biases the observed statistic away from the uncorrupted statistic, but still within the training distribution that RSNLE sees.

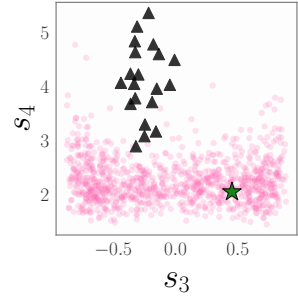


Figure 11: Analysing summary statistics in RSNLE.